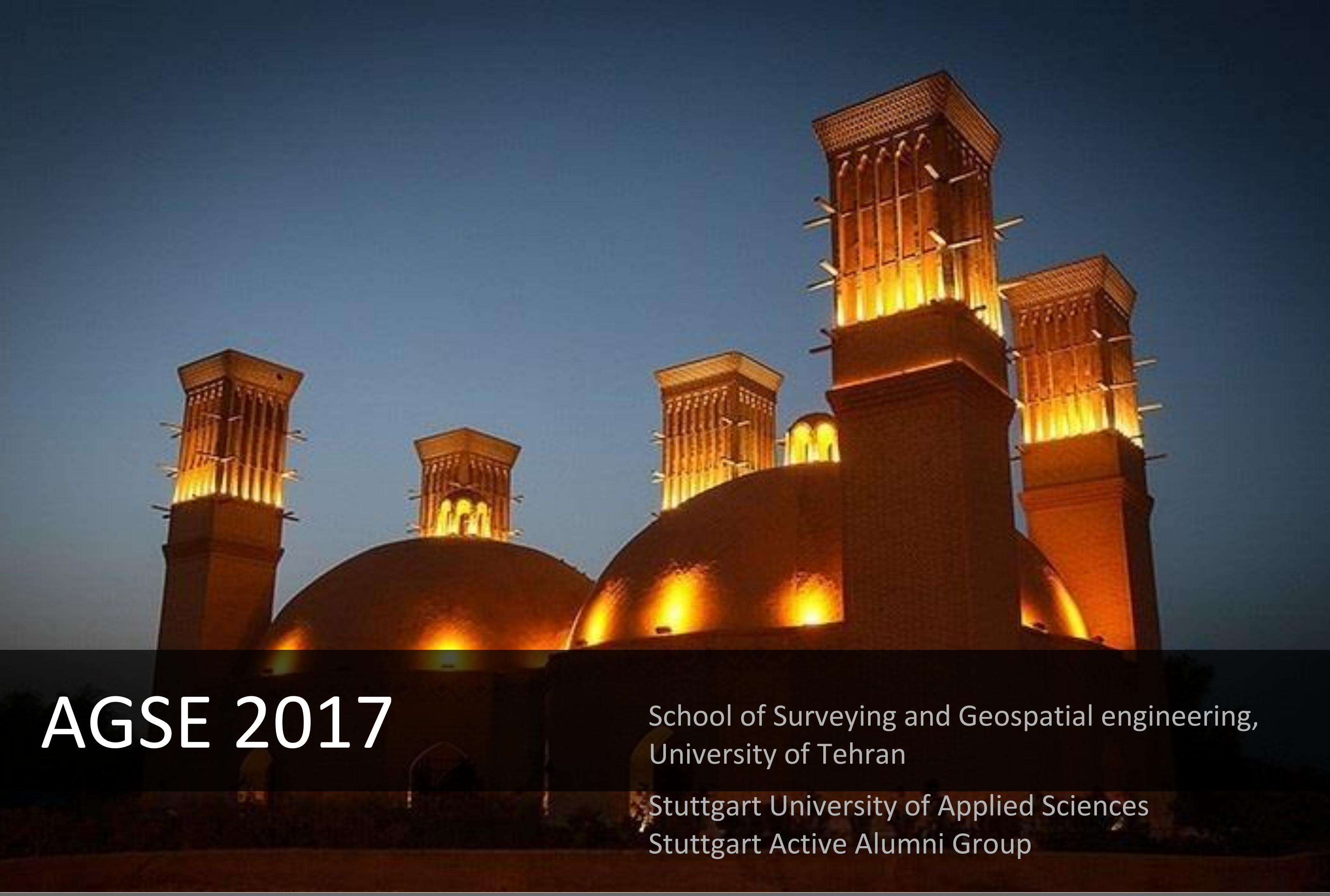

AGSE 2017

School of Surveying and Geospatial engineering,
University of Tehran

Stuttgart University of Applied Sciences
Stuttgart Active Alumni Group

Hossein Arefi, Franz-Josef Behr, Fatemeh Alidoost

Geoinformation – Supporting Crisis and Disaster Management

Applied Geoinformatics for Society and Environment

Eighth International Summer School and Conference

A G S E P u b l i s h i n g

Geoinformation – Supporting Crisis and Disaster Management

Applied Geoinformatics for Society and Environment

AGSE 2017

Hossein Arefi, Franz-Josef Behr, Fatemeh Alidoost
(Editors)

Publications of AGSE
Karlsruhe, Germany

2018

ISBN 978-3-943321-15-9

AGSE Publishing, http://applied-geoinformatics.org/publications

ISBN 978-3-943321-15-9

Conference Web Site: http://applied-geoinformatics.org/

Typesetting: Muhammad Yahya, Shams Uddin Al Azad M.Sc.

Cover photo: By Tasnim News Agency [CC BY 4.0 (http://creativecommons.org/licenses/by/4.0)], via Wikimedia Commons [2011-07-04] [accessed 2018-01-17]

Editors:

Dr. Hossein Arefi, School of Surveying and Geospatial Engineering, University of Tehran, Iran
Prof. Dr. Franz-Josef Behr, Stuttgart University of Applied Sciences, Germany, Alumni Representative
Fatemeh Alidoost, M. Sc., School of Surveying and Geospatial Engineering, University of Tehran, Iran

International Organizing Committee

Local Organizing Committee:

Advisory Board

Acknowledgment

The conference was supported by the German Academic Exchange Service (DAAD, http://www.daad.de/en/) financed by means of the Federal Ministry for Economic Cooperation and Development (BMZ), the University of Tehran, the Stuttgart University of Applied Sciences, Germany, and the Knödler-Decker Foundation, Stuttgart, Germany.

The support of Uddin Al Azad M.Sc. during proof-reading is also greatly acknowledged.

Table of Contents

Preface

The 8th International Summer School of Applied Geoinformatics for Society and Environment (AGSE2017), which was co-organized by University of Applied Sciences Stuttgart, University of Tehran, German Academic Exchange Service (DAAD), and International Society for Photogrammetry and Remote Sensing (ISPRS) held at the Kish International Campus University of Tehran, Kish Island from April 29 to May 04, 2017.

The overall goal of this conference was to take into account the current state-of-the-art in Geosciences related disciplines such as photogrammetry, remote sensing, and geo-information topics to a wide range of application areas, with significant focus on "Crisis and Disaster Management".

During this summer school different practical and educational workshops have been conducted by outstanding and internationally known researchers on different fields of geospatial data acquisition, analysis and application. Generally, about 23 articles and works in progress and about 11 workshops were presented during five days. The scope of the presentations covered the latest science and technology developments as well as recent applications and research activities for crisis and disaster management, risk assessments, monitoring natural and man-made disasters, based on earth observation or ground based techniques as well as the other contribution of geoinformatics, remote sensing, and planning to preparation, response, recovery, and mitigation of disasters.

The overall success of AGSE2017 summer school was demonstrated by the impressive attendance, with more than 50 participants from universities and research organizations, but also from application oriented institutions, primarily from Iran but also from twelve other nations such as Germany, France, The Netherlands, Colombia, Kenya, Bangladesh, Ethiopia, Sri Lanka, India, Nigeria, Nepal, and Tanzania.

With the particular focus of the summer school on "Crisis and Disaster Management" the thematic extents of this edition aimed at contributions of Geoinformatics, Remote Sensing, and Planning to preparation, response, recovery, and mitigation of disasters. An overview of the presented subjects can be summarized as follows:

- Collaborative Geographic Information Systems for Disaster Management
- Flood Risk Modeling and Mapping
- Building Resilience against Disasters
- Software-neutral best practices
- GIS for Disaster Management Research Agenda
- E-Learning to support Disaster Management
- Psycho-Social Implications of Disaster Management and Volunteering
- Contribution of Remote Sensing Approaches
- Contribution of Spatial Data Infrastructures
- Alerting people
- Disaster Management Approaches on regional and national levels
- Using UAVs for data collection
- Data sources and rapid web based data provision

- Crowed-based Data collection using OpenDataKit and KoboCollect
- Deep Learning for Emergency Response
- 3D Data for detailed Infrastructure information

Finally, it can be stated that AGSE2017 summer school has been a very interesting and vivid conference with a broad range of high level presentations and workshops of very good scientific quality which it could bring both a professionally rewarding and personally memorable experience for all of its participants. I would like to thank the Stuttgart University of Applied Sciences, Germany for giving the University of Tehran an opportunity to host this year's Applied Geoinformatics for Society and Environment (AGSE2017) conference and summer school.

On behalf of the editors

Dr. Hossein Arefi

09 June 2017

Application of Deep Learning for Emergency Response and Disaster Management

Fatemeh Alidoost, Hossein Arefi*

School of Surveying and Geospatial Engineering, College of Engineering, University of Tehran, Tehran, Iran - (falidoost, hossein.arefi)@ut.ac.ir

ABSTRACT:

Each year, natural crisis and disasters such as earthquakes, landslides, flood and typhoon impact broad areas of the world especially residential areas and man-made structures like buildings. In order to decrease the negative impacts of such events, accessibility to (near) real time and accurate geospatial information of degraded areas is so vital at early stages. In this study, the application of deep learning algorithms is introduced to detect affected areas such as buildings. Also, a modern structure including the combination of the acquired images by Unmanned Aerial vehicles (UAVs) and deep learning algorithms is proposed for (near) real time disaster mapping. This structure is called DeepEye which it is utilized the Convolutional Neural Networks (CNNs) to fast analysis and automatic interpretation of UAV images in order to calculate accurate locations as well as the percentage of degraded areas. The DeepEye structure could be critically useful to extract a lot of information from acquired images over degraded areas in a short period of time in emergency response and disaster management applications.

1 Introduction

In recent years, natural and man-made disasters have been increased due to global climate change, infrastructure vulnerability, unplanned urbanization, and population growth. In order to manage these situations more effectively, real-time acquisition of geospatial information and rapid mapping of degraded areas as well as the fast analysis of these information plays an important role to decrease their negative social and economic impacts. As shown in Figure 1, due to high impact of global disasters in economy, society and human lives, the demands for a rapid emergency response system has been increased recently. This system need to be not only fast and more accurate to generate the spatial information but also be more intelligent to detect the type of the disasters and the amount of damages over the large scale areas.

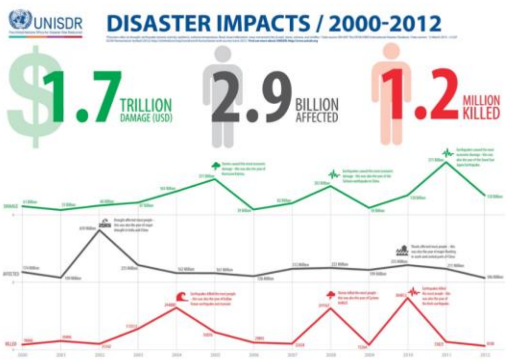

Figure 1: Disaster impacts from 2002 to 2012, prepared by the United Nations Office of Disaster Risk Reduction [1]

Since the Unmanned Aerial vehicles (UAVs) are fast, robust, autonomous, and low cost systems to acquire very high resolution images, they are critically useful to extract a lot of information from degraded areas in a short period. However, the acquired data by UAVs need to be processed and interpreted by real-time/near real-time algorithms in order to have an online emergency response system efficiently. In order to overcome this shortcoming (i.e. the post processing and offline analyzing needs of UAV images in order to extract information from images), this study is aiming at introducing the power of deep learning algorithms as the advanced computer vision approaches, to have a (near) real time disaster detection system based on UAVs data which can be effectively used in emergency response and disaster management applications. This structure is called DeepEye (Figure 2). In this structure, a Convolutional Neural Network (CNN) is firstly trained based on an off-line-generated library including aerial images of different disasters in various classes. Next, the well-trained CNN is fed into the UAV's processing unit. In the flight time, the CNN can analyze the captured images, by the installed camera on the UAV, very fast without any significant preprocessing and the disaster parameters such as the type, locations as well as the percentage of damages can be extracted. These information are transferred to the ground station and could be used to make decisions better regarding the relief actions.

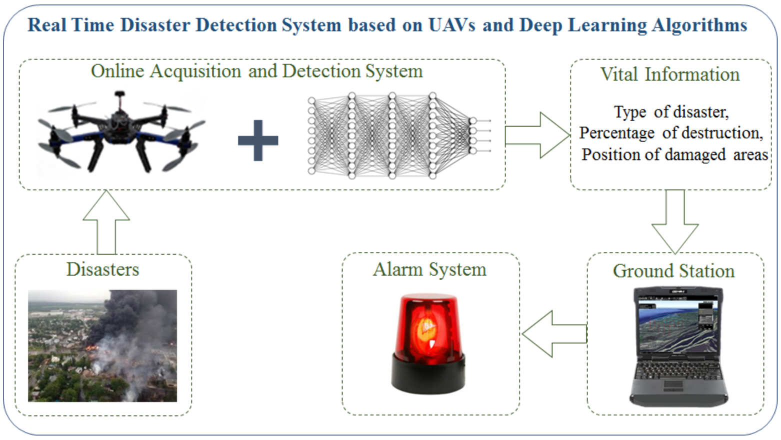

Figure 2: DeepEye: A (near) real time disaster detection system based on UAVs and deep learning algorithms

2 Deep Learning and Convolutional Neural Networks

Deep learning (DL) is a subfield of machine learning and Artificial Neural Network (ANN) based on hierarchical learning representations of data using a deep structure composed of multiple different layers with linear or non-linear transformations [2], [3-5] and it is currently used in many applications including automatic speech recognition [6], object recognition [7], object detection [8, 9], image classification [10, 11], bioinformatics [12]. Convolutional Neural Network (CNN) is a type of the deep learning techniques which is inspired by biological processes [13] and contains more hidden layers of small neuron collections which look at small portions of the input layer, called receptive fields [14] (Figure 3). As shown in Figure 3, a common structure of CNN includes input layer, hidden layers and output layer. The input layer is an image matrix with optional dimension and the output layer is a fixed length vector of highly distinguishable CNN features. The hidden layers include the convolutional layers, sampling layers (pooling layers) and the fully connected layers [15, 16]. The convolutional layers are composed of filters with different sizes which are applied to the local patches of the input image in order to extract features automatically. The sampling layer is a non-linear down sampling function such as maximum pooling that progressively reduces the spatial size of the input layer. The fully connected layer is the final layer of the network with high-level features and each neuron of this layer is connected to exactly one of the previous feature map [15].

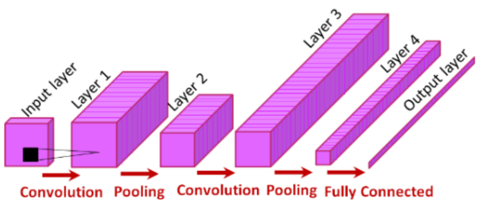

Figure 3: The CNN architecture including the convolutional, pooling and fully connected layers

3 Application of Deep Learning for Disaster Detection

Most common natural disasters are earthquakes, forestry fire, flood, drought and landslide which cause to damage man-made structures such as buildings and roads. Detection of affected and degraded areas is a vital issue at early stage in order to mitigate the negative effects of disastrous events and manage them. For large scale outdoor environments, a vision-based disaster detection system using deep learning algorithms could be employed to detect and extract the degraded areas from optical aerial images almost in real time.

4 Building Damage Assessment

In order to assess damages of buildings in an area of undergoing a catastrophe, such as an earthquake or a typhoon, [17] fed the only post-event data to multiple CNNs to extract rich features. For this, a semantic segmentation algorithm is utilized to classify the image pixels into two damaged and non-damaged parts. In another study by [18], the combination of both CNN and 3D point cloud features is used for image classification and to detect the damaged areas from multi-view oblique images (Figure 4).

Figure 4: Super-pixels of UAV images, that were voted as damages based on the classified CNN features by the Support Vector Machine (SVM) classifier, are highlighted as red polygons in the subset of UAV images of Kathmandu (left-top), Mirabello (left-bottom) and L'Aquila (right) [18]

5 Drought Prediction

Deep learning algorithms can improve the disaster prediction technologies such as drought prediction systems. In order to predict the drought time series, a Deep Belief Networks (DBN) can be used to calculate different drought indexes such as Standardized Precipitation Index (SPI) with higher precision than other neural network methods [19].

6 Landslide Detection

In order to capture more distinct features hidden in landslide images a Deep Auto Encoder Network Model (DAE) with wavelet coefficient can be applied on optical remote sensing images. In comparison to usual Artificial Neural Network (ANN), the image classification based on the deep learning algorithms has higher capability for landslide recognition [20]. Moreover, the patch-wise object detection techniques based on CNNs can be utilized for automatic disaster detection such as flood and landslide. The accuracy of landslide detection by the CNN is calculated based on the precision of 0.93, recall of 0.94 and f-measure of 0.93 (Figure 5) [21].

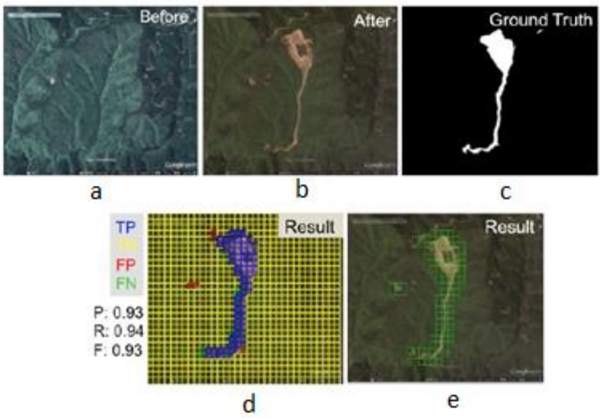

Figure 5: Result of landslide detection by the CNN: Pre-disaster aerial image (a), Post-disaster aerial image (b), Ground truth (c), Accuracy of disaster detection output (d), Disaster detection output for operator usage (e) [21]

7 Fire Detection

Since the CNNs have shown very well results in the area of category classification as well as object detection, by application of CNNs, fire and smoke can be detected from raw RGB images with the accuracy of 97.9% [22]. A fire detector system could be developed based on deep learning algorithms and can be implemented on UAVs in forestry applications. To improve the accuracy of the CNN, the combination of a local patch Nonlinear Neural network (NN) fire classifier and a CNN based classifier are trained to detect the image patches including smoke and fire in forestry areas [23]. As shown in Figure 6, the combination of the CNN and NN classifiers can detect fires in different images with more accuracy.

Figure 6: Detections results of different classifiers, from top to bottom, SVM algorithm, CNN algorithm, and CNN and NN algorithms [23]

8 Building Detection

Building detection from aerial images is of great practical interest for a number of applications especially for change detection and disaster assessments. In order to distinguish building from non-building objects using CNNs, a multi-scale saliency computation can be employed to extract the built up areas. Then, a CNN is used to classify the extracted regions [24]. To improve the result of building detection based on CNNs, additional information such as building footprint data can be used in training process [25]. The combination of CNN and Markov Random Field (MRF) models can be used to develop an automated building detection framework to extract building areas from very high resolution images [26]. The combination of spectral (RGB images) and geometrical (Digital Surface Models) information can be employed in a CNN based building recognition approach [27] (Figure 7).

Figure 7: The Final results of buildings' roofs detection and recognition based on the combination of RGB images and DSMs [27]

9 Conclusion

In order to efficiently manage the numerous tragic and hazardous natural disasters, it is useful to develop the automatic disaster detection systems based on advanced computer vision approaches such as deep learning algorithms. This study is aiming at introducing the different applications of the modern powerful deep learning algorithms for disaster detection from optical remote sensing data. In order to feed the accurate and fast spatial information into deep learning models and therefore for a (near) real time assessment and disaster management, a UAV-based rapid mapping system, which it is called DeepEye structure, can be developed for emergency responses. In this system, the acquired video or image data by low cost sensors, mounted on a UAV, are processed by deep learning algorithms such as CNNs automatically and in a (near) real time framework to detect the presence of a disaster such as fire, flood, or landslide, to assess the amount of structural damages in buildings or even to predict the disasters such as drought and flood.

References

[1] http://geoawesomeness.com/drones-fly-rescue/

[2] Bengio, Y., 2009. Learning Deep Architectures for AI. Foundations and Trends in Machine Learning, 2(1), pp. 1–127.

[3] Deng, L., Yu, D., 2014. Deep Learning: Methods and Applications. Foundations and Trends in Signal Processing, 7 (3-4), pp. 1–199.

[4] Schmidhuber, J., 2015. Deep Learning in Neural Networks: An Overview. Neural Networks, Vol. 61, pp. 85–117.

[5] Bengio, Y., LeCun, Y., Hinton, G., 2015. Deep Learning. Nature, Vol. 521, pp. 436–444.

[6] Yu, D., Deng, L., 2015. A Deep Learning Approach, Springer-Verlag London.

[7] Zuo, Z., Wang, G., 2014. Learning Discriminative Hierarchical Features for Object Recognition, IEEE Signal Processing Letters, 21(9).

[8] Zhang, Y., Sohn, K., Villegas, R., Pan, G., Lee, H., 2015. Improving object detection with deep convolutional networks via Bayesian optimization and structured prediction. In: IEEE Conference on Computer Vision and Pattern Recognition (CVPR), Boston, MA.

[9] Girshick, R., Donahue, J., Darrell, T., Malik, J., 2015. Region-based convolutional networks for accurate object detection and semantic segmentation. IEEE Transactions on Pattern Analysis and Machine Intelligence, 38(1), pp. 142-158.

[10] Tuia, D., Flamary, R., Courty, N., 2016. Multiclass feature learning for hyperspectral image classification: sparse and hierarchical solutions. ISPRS Journal of Photogrammetry and Remote Sensing, Vol. 105, pp. 272-285.

[11] Chen, Y., Zhao, X., Jia, X., 2015. Spectral–Spatial Classification of Hyperspectral Data Based on Deep Belief Network. IEEE Journal of Selected Topics in Applied Earth Observations and Remote Sensing, 8(6), pp. 2381-2392.

[12] Chicco, D., Sadowski, P., Baldi, P., 2014. Deep autoencoder neural networks for gene ontology annotation predictions. Proceedings of the 5th ACM Conference on Bioinformatics, Computational Biology, and Health Informatics, pp. 533-540, NY, USA.

[13] Convolutional Neural Networks (LeNet) – DeepLearning 0.1 documentation. DeepLearning 0.1. LISA Lab. Retrieved 31 August 2013.

[14] Palade, V., Howlett, R.J., Jain, L., 2003. Knowledge-Based Intelligent Information and Engineering Systems. Chapter: A Convolutional Neural Network VLSI for Image Recognition Using Merged/Mixed Analog-Digital Architecture. Korekado, K., Morie, T., Nomura, O., Ando, H., Nakano, T., Matsugu, M., Iwata, A., Vol. 2774, pp. 169–176, Springer Berlin Heidelberg.

[15] Phung, S. L., Bouzerdoum, A., 2009. MATLAB Library for Convolutional Neural Networks, Technical Report, Visual and Audio Signal Processing Lab, University of Wollongong.

[16] Liu, T., Fang, S., Zhao, Y., Wang, P., Zhang, J., 2015. Implementation of training convolutional neural networks, Computer Vision and Pattern Recognition, arXiv:1506.01195v2.

[17] Rashedi Nia, K., 2017. Automatic Building Damage Assessment Using Deep Learning and Ground-Level Image Data, Thesis Submitted in Partial Fulfillment of the Requirements for the Degree of Master of Science in the School of Computing Science Faculty of Applied Science.

[18] Vetrivel, A., Gerke, M., Kerle, N., Nex, F., Vosselman, G., 2017. Disaster damage detection through synergistic use of deep learning and 3D point cloud features derived from very high resolution oblique aerial images, and multiple-kernel-learning, ISPRS J. Photogram. Remote Sensing, http://dx.doi.org/10.1016/j.isprsjprs.2017.03.001

[19] Chen, J., Jin, Q., Chao, J., 2012. Design of Deep Belief Networks for Short-Term Prediction of Drought Index Using Data in the Huaihe River Basin, Hindawi Publishing Corporation, Mathematical Problems in Engineering, Volume 2012, Article ID 235929, 16 pages, doi:10.1155/2012/235929

[20] Liu, Y., Wu, L., 2016. Geological Disaster Recognition on Optical Remote Sensing Images Using Deep Learning, Procedia Computer Science, 91, pp. 566 – 575.

[21] Nor Khuzaimah Binti Amit, S., Shiraishi, S., Inoshita, T., Aoki, Y., 2016. Analysis of Satellite Images for Disaster Detection. Geoscience and Remote Sensing Symposium (IGARSS), 2016 IEEE International, pp. 5189- 5192.

[22] Frizzi, S., Kaabi, R., Bouchouicha, M., Ginoux, J., Moreau, E., Fnaiech, F., 2016. Convolutional Neural Network for Video Fire and Smoke Detection, Industrial Electronics Society , IECON 2016 - 42nd Annual Conference of the IEEE, pp. 877- 882.

[23] Zhang, Q., Xu, J., Xu, L., Guo, H., 2016. Deep Convolutional Neural Networks for Forest Fire Detection, International Forum on Management, Education and Information Technology Application (IFMEITA 2016), Published by Atlantis Press.

[24] Zhang, Q., Y. Wang, Q. Liu, X. Liu, and W. Wang. 2016. "CNN Based Suburban Building Detection Using Monocular High Resolution Google Earth Images." IEEE International Geoscience and Remote Sensing Symposium (IGARSS) 661 – 664. doi:10.1109/IGARSS.2016.7729166.

[25] Yuan, J. 2016. "Automatic Building Extraction in Aerial Scenes Using Convolutional Networks." arXiv:1602.06564.

[26] Vakalopoulou, M., K. Karantzalos, N. Komodakis, and N. Paragios. 2015. "Building Detection in Very High Resolution Multispectral Data with Deep Learning Features." IEEE International Geoscience and Remote Sensing Symposium (IGARSS) 1873 – 1876. doi:10.1109/IGARSS.2015.7326158.

[27] Alidoost, F. and Arefi, H., 2016. Knowledge based 3D Building Model Recognition using Convolutional Neural Networks from Lidar And Aerial Imageries, Int. Arch. Photogramm. Remote Sens. Spatial Inf. Sci., XLI-B3, 833-840, doi:10.5194/isprs-archives-XLI-B3-833-2016.

Framework for Iranian 3D SDI in CityGML

Behnam Alizadehashrafi

Faculty of Multimedia, Tabriz Islamic Art University, b.alizadehashrafi@tabriziau.ac.ir

KEY WORDS: External code lists, CityServer3D, Iranian 3D SDI, CityGML, interoperability

ABSTRACT:

Three-dimensional Spatial Data Infrastructure (3D SDI) is normally used to describe metadata relevant to the collection of technologies, technical methods and processes, policies and institutional arrangements that facilitate the access to 3D spatial data and extraction of information from geospatial DB. This paper describes a framework for 3D geospatial data infrastructure based on OGC Standards in Iran specially Tabriz as one of the oldest cities with more than 3000 years history. The external code lists based on local culture, vegetation and heritage landmarks were proposed for indexing 3D city structures and furniture of Tabriz city. These code lists can be used between different governmental agencies as a communication tool and utilized for indexing in the 3D spatial database. There are some predefined code lists from other developed and developing countries such as Germany and Malaysia, which can be utilized for Iranian context along with additional codes. These external code lists can be defined for all the street furniture, sculptures, and façade textures in some sort of applications such as city planning, built environment, disaster management and etc. The external code lists can also be used for the components of the buildings or of the façade in different layers as an entity such as windows, doors and backgrounds to enhance the usage of 3D SDI for a variety of privileges from end-users to professionals in the near future for different organizations and management levels. The framework for web-based application for connecting to CityServer3D was introduced in this research paper. CityGML as a standard data exchange format have been utilized for developing Iranian 3D SDI and implicit geometry representation has been used to avoid lagging while rendering the 3D models during navigation in the 3D virtual environment.

1 Introduction

The framework attempts to utilize the available Open Geospatial Consortium (OGC) Web services such as Web3D Service. Features that have been implemented by (Basanow, Neis, Neubauer, Schilling, & Zipf, 2008) seem very appropriate with some modification to suite local requirements in Iran. Semantic modeling and Surveying technology like total stations, terrestrial or airborne laser scanners or photo matching techniques via AgiSoft Photoscan software can be utilized for 3D low poly virtual geometry reconstruction to a certain extent along with textures. This means that neither hidden parts nor the meaning of the surfaces or their belonging to specific object types can be extracted from these techniques. The same situation applies for the multitude of 3D models that are created within CAD and computer graphics systems like SketchUp or Autodesk's 3D Studio Max. These models generally consist of geometry and appearance information, but do not represent thematic information and the meaning of the objects. Thus, they also cannot be used for BIM applications. (Nagel, Stadler, & Kolbe, 2009) discusses several aspects of CityGML including the characteristics of the language. CityGML is a standardized information model which puts focus not only on the objects' geometry but also on their semantics, topology, and appearance. Key features of CityGML are:

- Objects may comprise coexisting geometric representations for different levels of detail (LOD concept).
- Topological relations between objects can be recognized via links between geometries (XLink concept).
- Complexity of the variable in the geometry, semantic and coherent structures (Stadler & Kolbe, 2007).
- Aggregation hierarchies on the part of both geometry and semantics support complex object structures (hierarchical structuring).

Building Information Models (BIMs) can be used as a detailed semantic modeling the same as CityGML and external code lists. It might be employed for enabling interoperability between varieties of applications in the near future. BIM-based Integrated Project Delivery might be a common process for managing a project via distributed systems. Urban management tasks such as disaster management, delivery of goods and services, and cityscape visualization are managed by using GIS and modeling tools. Some of these tasks such as response time for fire management, require detailed geometric and semantic information about buildings in the form of geospatial information, while tasks such as visualization of the 3D virtual city require less (geometric and semantic) information. Nowadays service-oriented architectures are becoming more popular in terms of enabling integration and collaboration over distributed environments. An enhancement for a BIM Web Service pattern proposed by (Isikdag, Underwood, Kuruoglu, & Rahman, 2011) called RESTful BIM that will help interoperability. Unfortunately, until now there is no complete interoperability and transfer of semantic data and spatial relationships from building models to the geospatial environment except FME software to some extent.

Nowadays due to availability of broadband and high-speed internet, emergence of service-based architectures is feasible for remote applications to inter-operate using standard web interfaces. Services can be based on thin-servers along with thicker client side web-based application or thick-servers interoperating with thin client side application as a service. Furthermore because of unlimited number of clients, distributed systems, parallel processing and multithreading can be employed for higher efficiency and better response time. The service-orientated system enables loose coupling of applications over the web. Several applications can communicate and interact with each other without having the detailed knowledge of each other's working environment. Each of these applications or data layers that take part in such a web-based interaction in a serving form as a data or component or application service is known as a web service. Service Oriented Architectures (SOA) is software architecture built upon web services. Although the trend in the software industry is towards enabling application interoperability over web services or SOA, the Architecture, Engineering, and Construction (AEC) industry is still not fully benefiting from the service oriented approaches, as the focus of the industry is still very data integration oriented.

2 CITYGML

2.1 Servers and Clients of CityServer3D

The server stores data in the database, accessible via variety of interfaces. In addition to querying the stored data in its own database, it is also possible to query additional data sources. The CityServer3D uses a meta-model to handle this concept. After processing the query, the result can be transferred in various ways to other server's functional unit or clients via different interfaces in 2D or 3D formats. The interoperability of the server must be guaranteed for data exchange securely and confidently. E-commerce can be used on the system based on the server components for authentication and transactions monitoring and recording. The system consists of different layers such as interface layer (IL), converter layer (CL), functional layer (FL), data schema layer (DSL) and database management system layer (DBMSL). The DBMSL is based on relational concept and Oracle Spatial and DSL composed of GeoDB1, GeoBase2, which can be employed not only for geometry but also for storing thematic and spatial classification of the data sets. The controller unit (CU) controls the interaction between layers (See Fig. 1). Two tools are integrated for the clients of CityServer3D to manage the contents and access the 3D city model. Firstly, a web based visualization system and secondly, management of the database for importing and exporting data is necessary for the clients system (Haist & Coors, 2005).

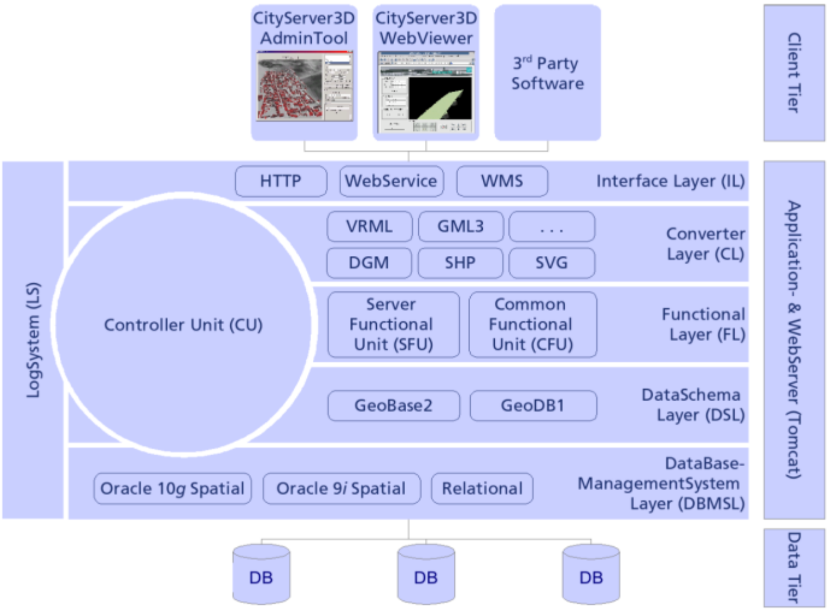

Figure 1: (Haist & Coors, 2005) Architecture of the CityServer3D

2.2 Iranian 3D spatial data infrastructure

To achieve the integration of those spatial data, applications and services, a 3D geospatial data infrastructure has to be built in order to connect the existing information "islands". The core component of this data infrastructure is a domain specific ontology that specifies the knowledge stored in the overall city information model. CityGML is a candidate for such ontology (Groger, Kolbe, & Czerwinski, 2009). It was accepted as an OGC standard for the representation, storage and exchange of virtual 3D city and landscape models. CityGML is based on a rich, general purpose information model in addition to geometry and appearance information. For specific domain areas, CityGML also provides an extension mechanism to enrich the data with identifiable features under preservation of semantic interoperability. This extension mechanism is essential to make use of CityGML in various other applications such as flood simulation and energy management. From BIM, the industrial foundation classes (IFC) developed by the International Alliance for Interoperability (IAI 2007) is a well-defined data model for data interchange of building information models. The definition of a mapping of both CityGML and IFC is a future challenge that would result into a city information model at all levels from city-wide models to high detailed building information model. The second challenge towards a 3D geospatial data infrastructure is the definition of standard interfaces to access distributed data sources. These interfaces will enable individual access to the relevant information sources for a specific task. The OGC working group 3D Information Management (3DIM) is developing such interfaces to support a framework of data interoperability for the lifecycle of building and infrastructure investment: planning, design, construction, operation, and decommissioning. Web service specifications for visualizing 3D city and landscape models are needed (Schilling & Kolbe, 2010). The Iranian 3D SDI aims to provide 3D information to many users within the existing Iranian Geospatial Data Infrastructure (IRGDI) framework. This IRGDI, basically contains various 2D spatial data and layers for cadastral information in Tabriz. The current research project IT department of municipality in Tabriz could be part of "bigger picture" of the proposed 3D SDI to serve the community with appropriate interface especially applications like navigation, urban planning, police simulation and crime monitoring system, building management, homeland security, and 3d cadastral information which is missing at the present moment.

For instance, in Tabriz 3D project the semantic information were defined along with external code lists and Iranian 3D SDI within CityServer3D. Information such as, name, roof type, number of the floors under the ground level, number of the floors above the ground level and statues along with external code list for them. CityServer3D has a very nice graphic user interface for adding data and attributes similar to data definition language and data manipulation language in database for end-users. The system automatically updates CityGML file based on defined external code lists. LOD4 also tested for faculty of Multimedia in Tabriz Islamic Art University and also many statues within the city (See Fig. 2).

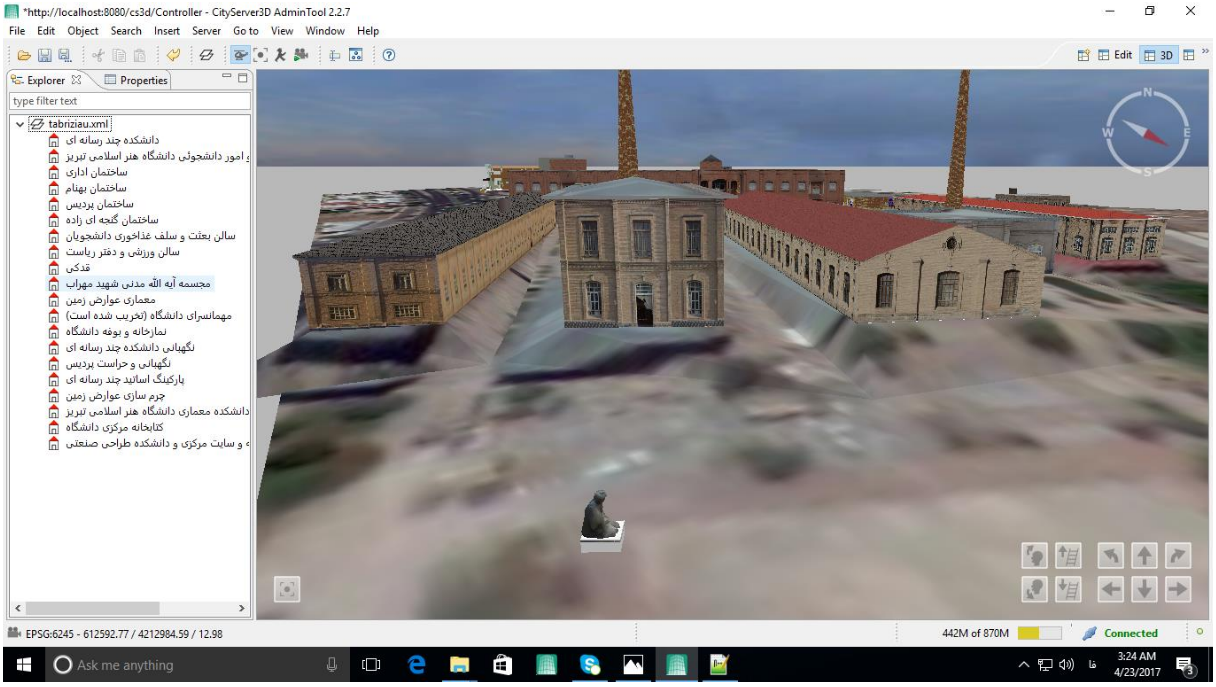

Fig 2. Semantic 3D modeling of Tabriz Islamic Art University in CityServer3D and CityGML based on 3D SDI.

3 A SUSTAINABLE 3DSDI

3.1 Standardized Web Services

Developing 3D data infrastructures along with general SDIs in particular is an important issue to achieve sustainability. Mostly in temporary limited research projects the collected data gets lost when the project is finished because of the absence of the persons or researchers who know where the data is, how to make use of the data, which formats are available, how to update and maintain and etc. To avoid these kinds of problems the spatial data for Iranian 3DSDI should be stored in a standardized way and provided by different geographical web services along with documentations and instructions for usage. With the use of the standards of the Open Geospatial Consortium (OGC) it is possible to gain interoperability, which means that the data can not only be used by the web application but also it can be accessed with any GIS system supporting OGC standards. This method guarantees flexibility in further usage of the data beyond project duration. For instance, the web atlas is fed by four different OGC-Web-Services (OWS) listed as following (Auer, Höfle, Lanig, Schilling, & Zipf, 2011).

- WMS for the 2D map presentation
- WFS for vector data
- WPS for analysis processing
- W3DS for the 3D scenes

This can be implemented for Iranian 3D SDI as well. Before 2010 W3DS was in the state of an OGC discussion paper to become a new standard (Schilling & Kolbe, 2010) and now it is. Iranian 3D SDI started from Tabriz 3D project based on these initiatives in Faculty of Multimedia at Tabriz Islamic Art University.

3.2 Integration of Data Infrastructure Design

Integration of an existing XML document database and service used and maintained by the historians into the 3D SDI design was a challenging work on the service infrastructure level. This XML database stores the text-scientific results, transcriptions, catalogue of meta-data for the inscriptions, context data about inscription sites and caves and other information. The XML documents about the inscriptions sites, caves and the metadata documents have been supplemented with a spatial component in form of geographic coordinates. This opens up the potential of spatial analysis and visualization of the stored information. As the XML documents do not make use of geographic standard formats it cannot be distributed by OGC Services directly. To enable a standardized access to the data as well as to support the given structure of the XML database, an automated conversion step has been integrated which pulls new documents, whenever they are available, from the XML database and writes them as Simple Features into a spatially enabled PostgreSQL12 database with PostGIS extension (See Fig. 3). From this source, the information can be distributed easily by the different OGC services to the web client or any other GIS client. Archiving of new XML data is feasible via XML editors such as notepad++ along with database connection and ensures automated propagation update of the PostGIS database that new features will be automatically shown on the map client and are available for GIS analysis through standardized geo-data interfaces. In this case the OGC-WMS and OGC-WFS interface is provided by the Open Source software GeoServer. The OGC-WPS has been realized with pyWPS using GRASS-GIS processes behind it while the W3DS is an implementation of the University of Heidelberg (Basanow, et al., 2008). The provided data can be received via user-friend graphic user interface (GUI) which can convert the data to XML schema before feeding in the form of XML database.

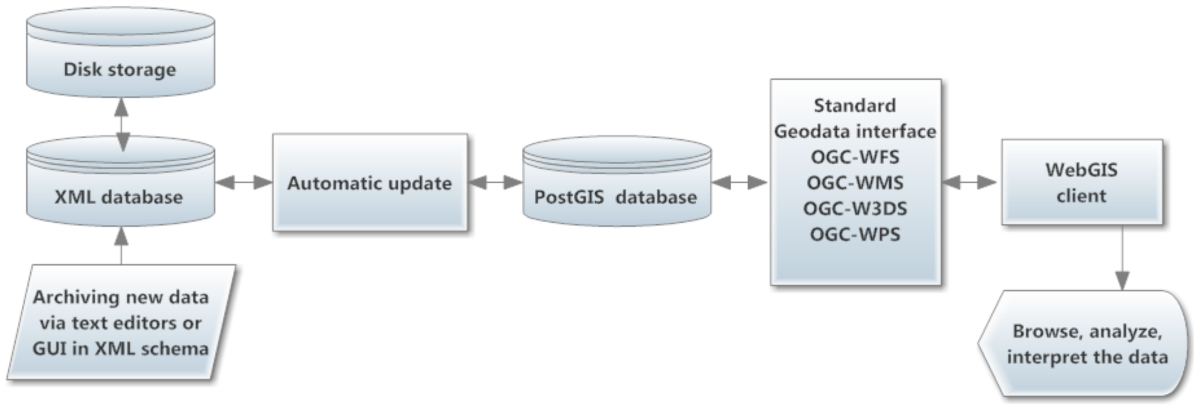

Fig 3. (Auer, et al., 2011) Integration of an XML-Document Service into the spatial data infrastructure

4 Code lists and External Code lists

In order to represent the object attributes of the city, having an enumerative range of values is necessary and the concept of dictionaries as provided by GML should be used. The values are defined in a file called CityGML_ExternalCodeLists.xml, which comes with the CityGML schema document, but is not a normative part of this schema, since it might be modified, augmented, replaced by users or other communities. The actual values in the file CityGML_ExternalCodeLists.xml are a suggestion of the SIG 3D (Special Interest Group 3D). In the process of designing semantic and thematic information for 3D city objects, these predefined attributes are necessary to assign to these objects which can be standardized for each area and country such as Iran. Attributes are employed to classify the objects and recognize them via queries or clicking and selecting the objects within 3D virtual environment of CityServer3D. It is similar to indexing system and a unique value relates to each attribute within a single file. These values are defined according to the name of attribute. The files are placed in a directory, which is called code lists. The code lists for the predefined objects in Germany can be extracted from the CityGML schema and the data can be changed, modified, enlarged and replaced according to requirement in Iran. These code lists is initially equipped by SIG 3D. These code lists are defined by Open Geospatial Consortium (OGC) in CityGML.

The external code list file defines attribute values and assigns a unique identifier to each value. In a CityGML instance document, an attribute value is denoted by an identifier of a value, not by the value itself. These identifiers are known terms for the operators and users. Thus, printing or typing errors are avoided and it is ensured that the same concept is denoted the same way, by the same identifier and not by two different terms with identical meaning. This is why the use of code lists facilitates semantic and syntactic interoperability, since they define common terms within an information community. Furthermore, the dictionary concept enables more than one term to be assigned to the same dictionary entry, thus the same concept may be explained in different languages. To differentiate between the languages, code spaces are used. An example for an enumerative attribute is RoofType, which is defined by the external code list file as "1000" (See the appendix).

'DefinitionCollection' element is used in the dictionary concept for representing the values of an attribute, where each value is given by a Definition entry. In CityGML a definition entry is identified by the name element, which is qualified by the SIG 3D code space. The unqualified name element represents the value of the attribute and an optional description defines the value. CityGML does not use GML identifiers (gml:id) to link to attribute values, since IDs are restricted syntactically, and must be globally unique, which is not feasible for code lists (Groger, et al., 2009).

For instance, external code lists of the building model can be summarized in the following types, whose valid values are explicitly enumerated in an external code list.

- BuildingClassType
- BuildingFunctionType
- BuildingUsageType
- RoofTypeType
- BuildingInstallationClassType
- BuildingInstallationFunctionType
- BuildingInstallationUsageType
- IntBuildingInstallationClassType
- IntBuildingInstallationFunctionType
- IntBuildingInstallationUsageType
- BuildingFurnitureClassType
- BuildingFurnitureFunctionType
- BuildingFurnitureUsageType
- RoomClassType
- RoomFunctionType
- RoomUsageType

5 Interoperability and 3D conversion process

Different formats can be exported from SketchUp Trimble such as WRL, DAE, 3DS, XML, KMZ and CityGML. 3D model in Collada file format can be utilized via MultiPatch feature class within ArcScene and ArcGlobe. It is also possible to create the MultiPatch feature class automatically via "Arc tool box -> 3D analyst tools -> conversion -> from file -> import 3D files". Unfortunately importing the WRL file format into SketchUp is not possible until now but 3DS. This is why the process of converting the WRL file format to SKP file format can be done through 3DMAX software. In this case the WRL file format can be imported to 3DMAX software and 3DS file format can be exported. The 3DS file format can be utilized to import the 3D model into SketchUp. By means of using FME or CityGML plugins for SketchUp it is possible to convert any 3D model in SketchUp to CityGML. It is better to make a group for each 3D model in SketchUp before exporting the CityGML file. It can be applied to avoid breaking down the 3D building to its components as many buildings tag within CityGML. The semantic information and code-lists can be added in via CityServer3D interface which can be added automatically to the connected MySQL database. It is possible to create Web3D-Service Interface via JavaScirpt to visualize CityGML files and use Google spreadsheets for defining, manipulating and updating data. In this case selecting, hovering the mouse on the 3D models, aggregating and many spatial analyses would be possible.

6 Implicit geometry in CityGML

CityGML supports implicit geometries, prototypic objects, scene graph concepts such as vegetation model, city furniture and generic objects. Implicit geometry is a kind of prototypical geometry which can be generated once and reused unlimited number of times based on 9 well known parameters (3 for rotation, 3 for translation and 3 scale factors). The implicit geometry can be an external file in different formats such as VRML, DXF or 3Ds Studio MAX on a local or remote machine and loaded to CityGML scene via URL. Alternatively, it can be defined by a GML3 geometry object (Gröger et al., 2008). This concept can be utilized to represent uniform shapes such as coconut or palm trees, street furniture and so etc. It can solve the lagging and rendering problems while visualization and navigation and also as component can be used to reduce the data size tremendously for web based applications.

7 Proposed external code lists for Tabriz area

External code list specifies the attribute value of city objects and gives unique identification. In CityGML, external code lists define most of the city objects separately, which are recommended by (Special Interest Group 3D) SIG3D. The code list is mainly used for the semantic and syntactic interoperability to define the objects in information field. All the required code lists are not available in CityGML external code lists though it covers most of the city objects. Some code lists are proposed according to the suitability for Iran especially in building façade types based on personal interests on constructions according beauty and price. Some examples of external code lists proposed for Iran for different city objects such as rubbish bins, statues and etc.

8 Conclusions

In this paper, the definition of SDI and 3DSDI are clarified and some reasons are given for using these metadata as standard methods between governmental sections for better interoperability. CityGML and Iranian 3D Spatial Data Infrastructure (IR3DSDI) along with semantic and thematic definition of the objects within a 3D virtual city were discussed in detailed via BIM or geospatial data. Sustainable 3DSDI was addressed and some methods to prevent data losses in the process of interoperability were highlighted. The process of conversion between different 3D models and also implicit geometry representation within CityGML were declared. The use of code list was addressed for indexing semantic information. Some code lists were proposed for street furniture and vegetation based on Irann culture, environment and weather in Tabriz as a developed test infrastructure. The idea of 3DSDI can be further developed and extended for whole urban areas in Iran along with 3D virtual visualization, analysis and 3D cadastral data for municipality.

9 Appendix

```
<gml:DefinitionCollection gml:id="id356">
  <gml:description>Codelist derived from German authoritative standards  ALKIS/ATKIS (www.adv-online.de) by S. Schlueter and U.
Gruber</gml:description>
  <gml:name>RoofTypeType</gml:name>
    <gml:definitionMember>
      <gml:Definition gml:id="id357">
        <gml:description></gml:description>
        <gml:name codeSpace="urn:d_nrw_sig3d">1000</gml:name>
        <gml:name>flat roof</gml:name>
```

```
    </gml:Definition>
  </gml:definitionMember>
  <gml:definitionMember>
    <gml:Definition gml:id="id358">
      <gml:description></gml:description>
      <gml:name codeSpace="urn:d_nrw_sig3d">1010</gml:name>
      <gml:name>monopitch roof</gml:name>
    </gml:Definition>
  </gml:definitionMember>
 ….
</gml:DefinitionCollection>
```


References

Alizadehashrafi, B. (2012) Towards enhancing geometry textures of three-dimensional city elements. PhD thesis, Universiti Teknologi Malaysia, Faculty of Geoinformation and Real Estate.

Auer, M., Höfle, B., Lanig, S., Schilling, A., & Zipf, A. (2011). 3D-Sutras: A web based atlas of laser scanned Buddhist stone inscriptions in China. Paper presented at the International Conference on Geographic Information Science, Utrecht, The Netherlands.

Basanow, J., Neis, P., Neubauer, S., Schilling, A., & Zipf, A. (2008). Towards 3D Spatial Data Infrastructures (3D-SDI) based on open standards - experi-ences, results and future issues. In P. Z. S. P. F. F. E. VanOosterom (Ed.), Advances in 3d Geoinformation Systems (pp. 65-86).

Gröger, G., Kolbe, T., Czerwinski, A. and Nagel, N. (2008). OpenGIS® City Geography Markup Language (CityGML) Encoding Standard. [Online]. [Accessed].

Groger, G., Kolbe, T. H., & Czerwinski, A. (2009). Candidate openGIS cityGML implementation specification.

Haist, J., & Coors, v. (2005). The w3ds-interface of cityserver3d. European Spa-tial Data Research (EuroSDR). Next Generation 3D City Models, 63-67.

Isikdag, U., Underwood, J., Kuruoglu, M., & Rahman, A. A. (2011). Geospatial Views for RESTful BIM. In U. I. J. Underwood. (Ed.), IRMA-International.org (Vol. 2, pp. 10).

Munankarmi, M. (2011). 3D Semantic City Modelling of Putrajaya Area, Malay-sia Master of Science, Stuttgart University of Applied Sciences, Stuttgart.

Nagel, C., Stadler, A., & Kolbe, T. (2009). Conceptual requirements for the auto-matic reconstruction of building information models from uninterpreted 3D models. International Archives of Photogrammetry, Remote Sensing and Spatial Information Sciences, 38.

Rahman, A. A., Alizadehashrafi, B., Hanifah, F. A., Majeed, Z., A., Aziz, A., & Coors, V. (2011). PUTRAJAYA 3D – THE MALAYSIAN 3D CITY MODELLING INITIATIVE SESAC 2011 International Surveyors Con-gress, 10.

Schilling, A., & Kolbe, T. H. (2010). Draft for Candidate OpenGIS Web 3D Service Interface Standard.

Stadler, A., & Kolbe, T. H. (2007). Spatio-semantic coherence in the integration of 3D city models. Proceedings of 5th International ISPRS Symposium on Spatial Data Quality ISSDQ 2007 in Enschede.

Evaluating the Susceptibility of Ungauged Watersheds to the Risk of Floods Based On Geomorphometry Using QGIS

Dennis Theuri Gitundu

Dedan Kimathi University of Technology, Kenya, dennis.gitundu@dkut.ac.ke

KEY WORDS: DEM, Flash Floods Risk, Geomorphometry, QGIS, Watersheds

ABSTRACT

There is an increase in flooding occurrences and frequency due to climate change and population pressure, leading to greater risk of damage to infrastructure and environment, lost livelihoods and casualties. Knowledge of flood hazards as well as vulnerabilities and the way they change over time, is a fundamental prerequisite in designing action plans for reducing flood disaster risk. In many developing parts of the world with observed flood incidences, the lack of gauging stations inhibits the implementation of a full flood forecast system since the hydrological response cannot be modelled. It is, however, possible to assess the risk of flooding using the morphology of the watersheds since the morphology intrinsically contains information that is useful in indicating their exposure to floods. The availability of global coverage Digital Elevation Models (DEMs) makes it possible to delineate stream networks and watersheds for any modelled part of the world. The streams and watersheds are then used in computing morphometric parameters. This paper describes a workflow that may be implemented in determining the susceptibility of watersheds to flash flood risks based on geomorphometric parameters using QGIS, an open source GIS software. The paper briefly examines different methods of stream definition that consider the variability in drainage density over extensive and heterogeneous regions. The stream network is then modelled following the approaches of previously related studies. In addition, the delineated streams are redefined to conform to the Strahler definition of stream segments. Outlet points are objectively generated on the redefined stream segments and used to delineate corresponding watersheds. Finally, geomorphometric parameters are derived from the computed stream network and watersheds, normalized and combined to derive a risk factor for each watershed. The correlation between the derived parameters and stream discharge may be used to ascertain the susceptibility of watersheds to flood risks.

1 Introduction

Watersheds are important spatial reference units within which water-related processes can be modelled and monitored as well as units for environmental monitoring and management (Vogt et al., 2007). One such process is channel discharge which is useful in assessing flood occurrences. Flooding is the most common environmental hazard worldwide (NDA, 2015) and has the greatest damage potential of all natural disasters (United Nations, 2004). The risk of flooding is now greater due in part to climate change and population pressure. Risk assessment at the watershed level may be carried out to determine the nature and extent of flooding. This is done with an aim of reducing the harmful consequences associated with flooding such as loss of lives and property, disrupted economic activities and environmental damage.

There exists hydrological models which are applied for the understanding of the flood character as well as for flood forecasts and assessment of flood risks. Commonly used hydrological models include the Hydrologic Engineering Center's Hydrologic Modelling System (HEC-HMS) (Hydrologic Engineering Center, 2015), The TOPography based hydrological MODEL (TOPMODEL) (Beven *et al*., 1995), The Identification of unit Hydrographs and Component flows from Rainfall, Evaporation and Streamflow data (IHACRES) (Croke *et al*., 2005) and The Soil and Water Assessment Tool (SWAT) model (Arnold & Fohrer, 2005). Many of these models rely on information such as precipitation, soil characteristics, vegetation cover, elevation datasets and stream flow information to model the hydrological response of a watershed (Tarboton, 2003). Within data sparse regions and ungauged watersheds, it is, however, challenging to model their hydrological response with a sufficient level of confidence. A tentative flood risk assessment for such data sparse regions may be provided through the assessment of the morphological characteristics of watersheds. The morphology of a watershed may reveal information such as the magnitude of peak and mean runoff that is useful in indicating its flood exposure through the analysis of factors that contribute to flow and discharge. Such characteristics include slope, drainage density and basin area among other quantifiable morphological characteristics or the geomorphometric parameters of watersheds.

The geomorphometric parameters depend on characteristics of the hydrological network. This implies that with an accurate stream network we can derive reliable parameters and subsequently a better assessment of flood risks within a watershed. One aspect of the accuracy of hydrological networks is the drainage density which varies between hillslopes and valleys (Tarboton et al., 1992) as well as from one location to another based on soil, vegetation, and climate among other factors (Vogt et al., 2007). There exist different methods and algorithms which are spatially adaptable to the varying drainage density (Montgomery & Dietrich, 1992; Tarboton et al., 1992; Tarboton & Ames 2001; Vogt et al., 2007; Passalacqua et al., 2012). It is therefore imperative to delineate hydrologic networks taking into account the spatial variability of drainage density between different locations. This is particularly true for large and heterogeneous watersheds.

2 Study area

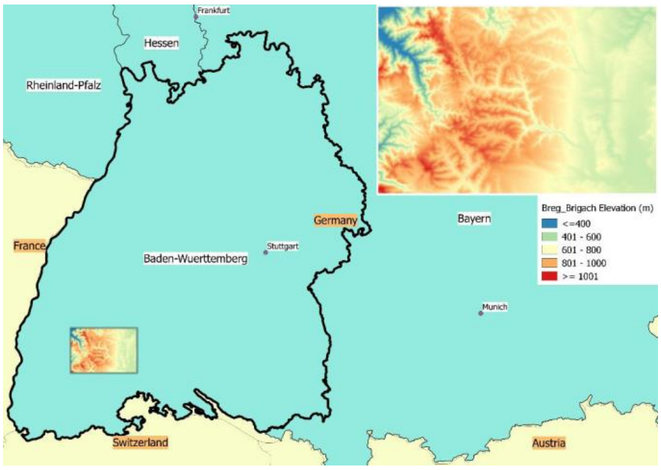

Figure 8: The location of the Breg and Brigach catchments in Baden-Wuerttemberg Germany. The DEM (upper right corner) shows the elevation of the catchment. The catchment generally slopes from the West to the East.

The area of interest for this study was the Breg and Brigach sub-catchments within the state of Baden-Württemberg, Germany (Fig. 1). The selected location covers a total area of 1080.2 km2. The Breg and Brigach rivers form the headstreams for the Danube, which is the longest River within the European Union.

3 Methodology

Following the approaches of Schröder and Omran (2013) we delineate stream networks as well as watersheds and thereafter derived and combined geomorphometric parameters in order to derive flood risk maps. Streams and watersheds were initially delineated from a DEM by modelling stream flow direction and flow accumulation. A suitable threshold value was applied to the flow accumulation grid to derive the stream networks. The streams were redefined to conform to the definition of a Strahler (Strahler & Chow, 1964) stream. Outlet points were determined for each correctly defined stream segment and used to define the watershed for each stream. The geomorphometric parameters were then computed from the delineated streams and watersheds, normalized and combined to produce flood hazard maps. Within the described workflow, there are some key issues which must be considered in order to derive accurate stream networks as well as watersheds and subsequently accurate geomorphometric parameters. The issues described in this paper are:

1. How do we objectively define the initiation threshold value for delineating streams?
2. Are the streams defined correctly to conform to the definition of a stream according to the rules applied in their ordering, for example Strahler rules?
3. How do we objectively generate pour points?

3.1 Defining the initiation threshold value for stream delineation

The premise of this study was to provide a tentative risk assessment within data scarce areas thus the constant drop analysis by Tarboton and Ames (2001) was preferred since it only requires a DEM as input data. Their work considers that there is a distinction in terrain between hillslopes where flow disperses and channels where flow accumulates. Channel cells were identified as upward curved grid cells by computing the plan curvature of the DEM. The identified upward curved cells were applied as a weight field to the flow accumulation grid to identify the most probable stream cells. Using the constant drop analysis, the mean drops of the first order streams and higher order streams were compared against each other in a t-test and the threshold value resulting in smaller statistical differences was selected as the most suitable. The selected value was applied to a weighted flow accumulation grid to determine the most probable stream cells.

3.2 Redefining stream cells to conform to Strahler rules

The selected stream channel cells were ordered according to Strahler rules. By definition, sequential stream segments of the same order form a Strahler stream. At every confluence, however, a new stream segment was formed resulting in a higher stream count. This would affect some of the geomorphometric parameters which rely on the stream count such as bifurcation ratio and stream frequency. This is illustrated in figure 2 where a new stream segment begins at every point of confluence. This was corrected using the workflow shown in figure 3. The computed stream network was initially split according to the different orders. In an iterative process according to the number of created layers, each stream layer was dissolved to form continuous segments. The result of this, however, was multipart features. The multipart features were split into single parts so that each stream was identifiable as a single object. During the dissolving process, streams of the same order that converge were dissolved into one layer that could not be separated by the multipart to single part algorithm. A stream layer of order n was, therefore, split by a higher order stream layer of order n+1. This was done in order to split streams of the same order that converge to form a higher order stream.

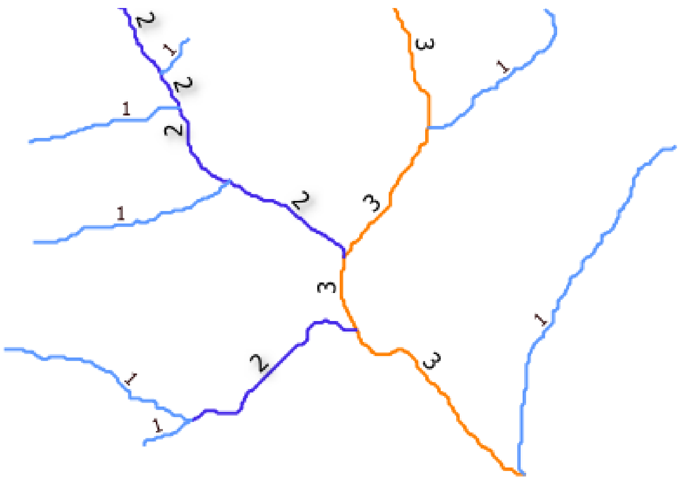

Figure 9: Delineated stream segments. At every confluence, a new segment is created. The numbers indicate the order of the stream according to Strahler rules.

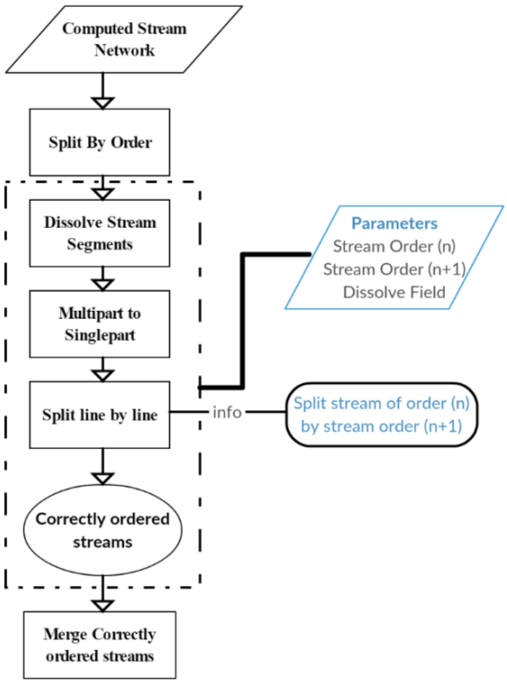

Figure 10: Workflow to redefine the stream network according to Strahler rules

3.3 Generating pour points and delineating watersheds

To delineate the watersheds, a pour point was identified for each correctly defined stream segment. These points mark the outlet of the stream segment. The outlet was identified as the point on each stream segment with the highest contributing area value using the workflow shown in figure 4.

Figure 11: Workflow for generating pour points.

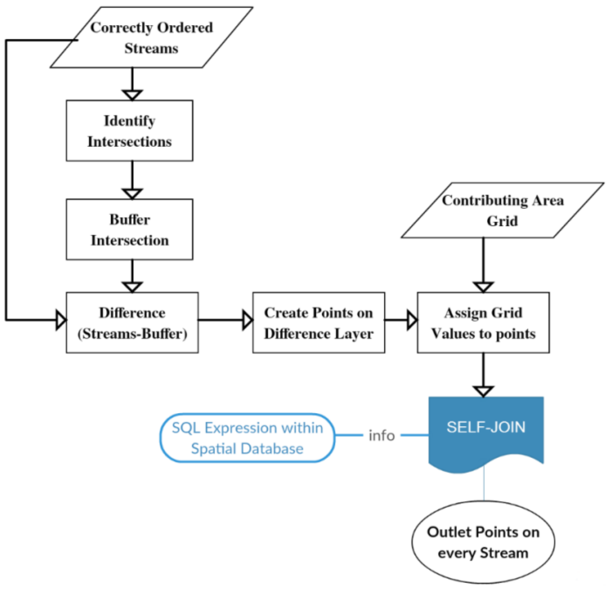

The locations of confluence were identified using an intersection tool. A buffer was created around this point and used to erase parts of the stream segments which corresponded with the confluence pixel. This was necessary because the confluence represents multiple sub-watersheds. Points were then generated on the new stream segments. Using a spatial join operation, values from the flow accumulation grid cells were assigned to corresponding points. These points were imported into a database from which the point with the highest accumulation value was identified using a self-join. The identified pour points were then used to delineate the watershed for each stream segment.

3.4 Computing geomorphometric parameters

The geomorphometric parameters of interest are provided in table 1. In-built functions within QGIS were used to determine the geometries of the streams and watersheds. The length of the streams, for example, was subsequently used in computing the drainage density within each watershed. Geoprocessing functions such as join and intersection were used to obtain stream counts of each order within a watershed. Stream count was then used to determine parameters such as bifurcation ratio and stream frequency. Relief parameters were determined for each watershed using zonal statistics where the watersheds represented the zones of interest and elevation values were derived from the DEM. The other morphometric parameters were calculated using the field calculator according to the formulae provided in table 1.

Table 1: Linear, Areal and Relief Geomorphometric parameters under consideration in this study.

(Adapted from Hajam et. al, 2013)

Linear Parameters	**Symbol**	**Formula**
Stream Order	Sμ	Hierarchical rank
Bifurcation Ratio	Rb	R_b = Nμ / Nμ +1 Where, Rb = Bifurcation ratio, Nμ = No. of stream segments of a given order and Nμ +1= No. of stream segments of next higher order.
Areal Parameters	**Symbol**	**Formula**
Basin Area	A	The area from which water drains into a common stream and boundary determined by opposite ridges.
Drainage Density	Dd	Dd = Lμ/A Where, D_d = Drainage density (Km/Km2) Lμ = Total stream length of all orders and A = Area of the basin (Km2). ++73
Drainage Frequency	Fs	Fs = Nμ/A Where, Fs = Drainage frequency. Nμ = Total no. of streams of all orders and A = Area of the basin (Km^2).
Infiltration Number	If	If = $D_d \times F_s$ Where, D_d = Drainage density (Km/Km2) and F_s = Drainage frequency.
Circularity Ratio	R_c	$R_c = 4\pi A/ P2$ Where, A = Basin area (Km^2) and P= Perimeter of the basin (Km)
Relief Parameters	**Symbol**	**Formula**
Basin Relief	H	H = Z – z where Z = Maximum elevation of the basin (m) and z = Minimum elevation of the basin (m)
Relief Ratio	R_r	$R_r = H / L_b$ where H = basin relief (m) and L_b = Basin length (m)
Basin Slope	Sb	$Sb = H / L_b$ where H and L_b are given above

3.5 Flood risk assessment

The computed geomorphometric parameters were normalized to a common evaluation scale of between 1 and 10 with higher values indicating higher flood risks. Quantities such as basin area and drainage density have a directly proportional relationship to the risk of floods, therefore low values of these quantities represented low flood risk and vice versa. Quantities such as the bifurcation ratio and basin area have an inverse proportional relationship to the risk of floods. Therefore, for these parameters the normalization of the values was done such that the lower the value, the higher the flood risk. The normalized values for each watershed were summed together and classified into four classes using equal interval classification. This was done to provide a visually interpretable map.

4 Results and discussion

4.1 **Threshold value and extracted stream network**

From the constant drop analysis a value of 161.87m2 was obtained as the critical contributing area for stream initiation. This represented the value from the weighted accumulation grid with an absolute t-test value less than 2, which is the 95% confidence interval. Using this value the highest order stream according to Strahler rules was the Order 5 stream. The average stream densities (Figure 5) was computed using a moving average window. A Topographic Position Index (TPI) based landform classification (Gallant & Wilson, 2000) was used to distinguish between the flat areas (East) and the hillslopes (West) shown in figure 5.

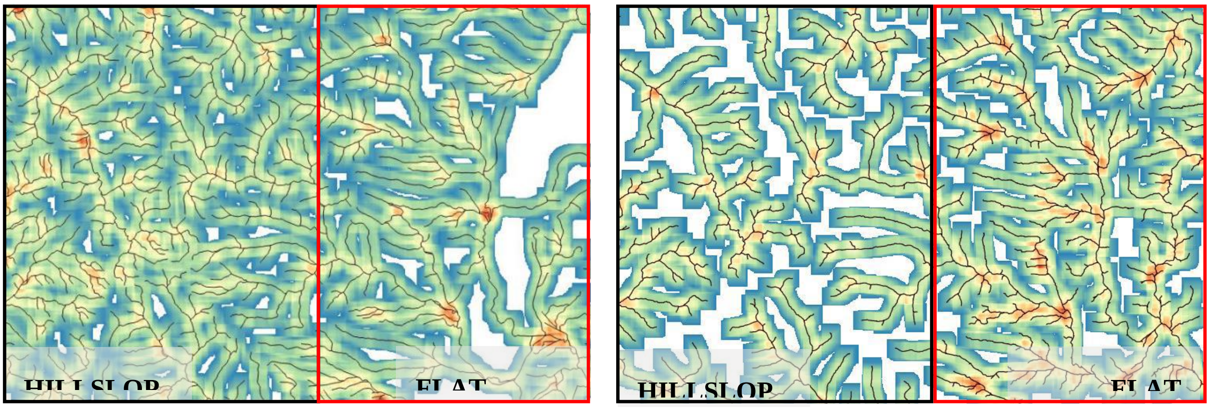

Within the hillslopes, a lower drainage density was obtained compared to the reference stream network. This

Figure 12: Average stream densities for the computed streams (left) and the reference stream networks (right).

implies that a lower threshold value was used which resulted in a lower drainage density. Within the flat areas, however, a higher drainage density was obtained. While this is typical of flat areas in hydrological modelling since flow is forced from high lying areas to low lying areas, the implication is that the resolution of the DEM was not sufficient to capture the variations in terrain in the flat areas.

4.2 Redefined stream segments

Figure 6 compares the extracted (left) and the redefined (right) stream networks. The streams have been labeled with their corresponding Strahler order number. More segments were identified in the computed stream network. This is because a new segment begins at every confluence. According to the Strahler rules, sequential stream segments of the same order form a Strahler stream. The requirement is to have the correct number of streams according to Strahler rules in order to derive important quantities such as the bifurcation ratio. Sequential stream segments of the same order were therefore dissolved to continuous stream segments.

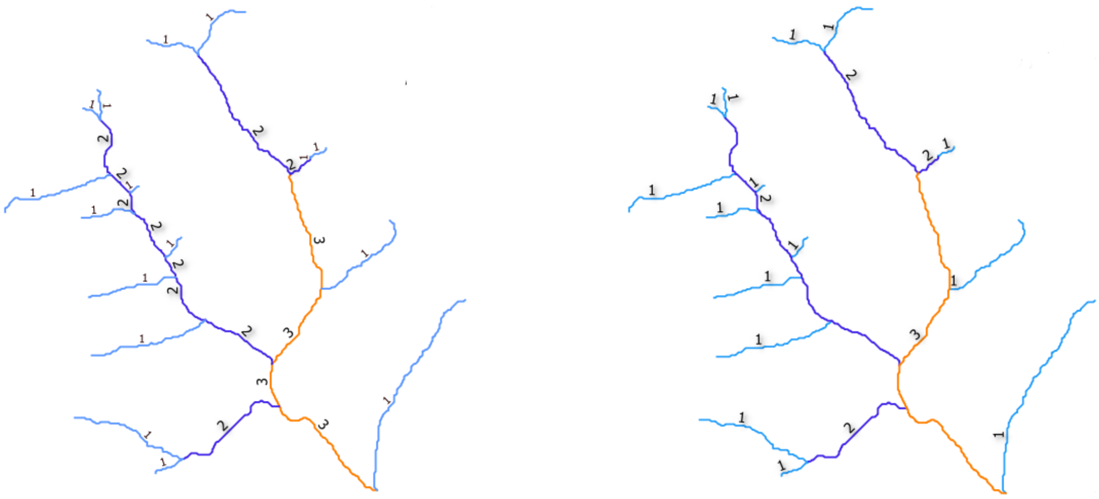

Figure 13: Computed stream segments (left) and the redefined stream segments (right).

4.3 Pour points and watersheds

The workflow objectively generated pour points on each correctly defined stream segment (Figure 7 (left)). The points represent the outlet of each stream and were further used to define the sub-watershed for each stream segment. Figure 7 (right) shows an example of an order 5 watershed containing all the lower order stream segments contributing drainage to the order 5 stream. The outlet point for the order 5 watershed is seen at the lower right end of the watershed (in red).

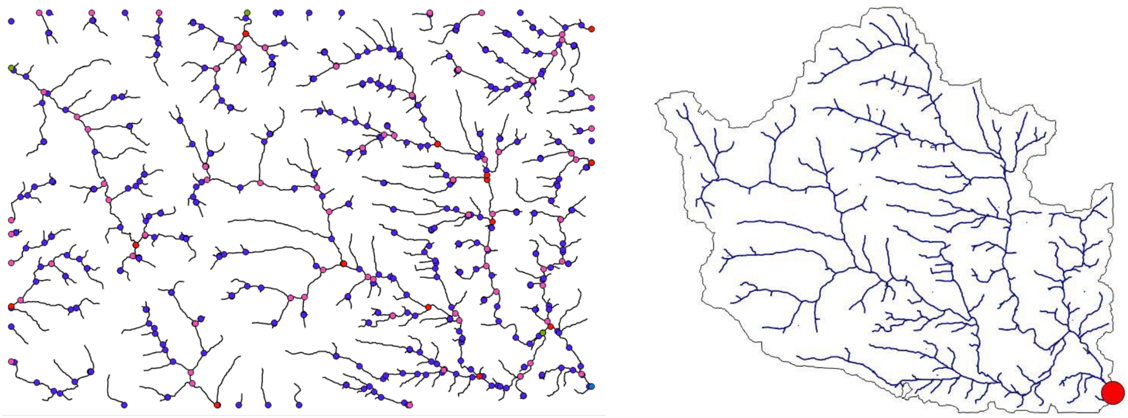

Figure 14: Pour points generated on every stream segment (left) and the delineated order 5 watershed (right).

4.4 Flood risk map

The final flood risk map was obtained by summing up the individual geomorphometric parameters in a multi-criteria approach. Equal influence was assumed for each parameter. An example of the resulting flood risk map is shown in figure (8) for the order 3 watershed. The flood risk map has been classified into four classes using the equal interval classification for visual interpretation. Smaller watersheds as well as watersheds with higher drainage densities, high elongation ratios, and lower bifurcation ratios had a higher risk of flooding. This is because a high drainage density and frequency, small watershed area, high circularity and elongation ratios, and high relief ratio indicate high discharge, peak time and volume hence a higher flood risk.

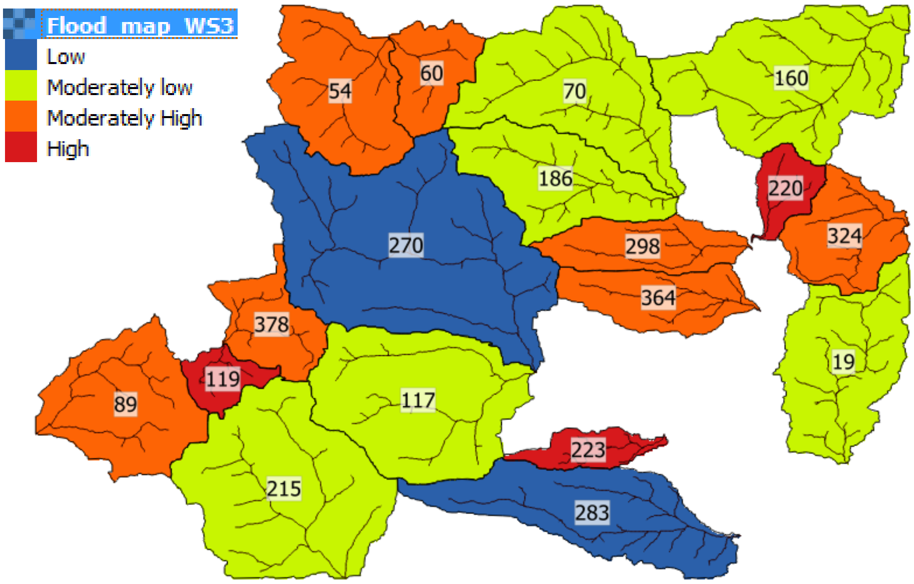

Figure 8: Flood risk map for the order 3 watersheds in Breg and Brigach catchments.

5 Conclusion

The workflows described in this paper were implemented within QGIS. Flood risk assessment based on geomorphometry requires only a DEM as input data. This approach may therefore be used to provide a tentative flood risk assessment within data scarce areas by evaluating physical terrain descriptors which affect discharge and timing of surface flow. With the availability of global coverage DEM datasets, it is possible to use these approaches for any part of the world. The most critical task in this workflow is the delineation of stream networks. The accuracy of the delineated streams will provide a solid basis for computing the geomorphometric parameters.

The selected threshold resulted in a lower drainage density at the hillslopes. Large and heterogeneous areas may be stratified into regions of spatial homogeneity based on factors that affect drainage density as well as runoff in order to account for the variability of drainage density. There exists other spatially adaptive algorithms and methods for defining stream segments. A comparison of these methods may be undertaken to determine the optimal conditions within which these methods may be used. Equal influence of each computed geomorphometric parameter was assumed because the actual quantitative influence of each parameter on the risk of floods is not sufficiently known. The parameters may, further, be correlated with the hydrological response to define the quantitative relation with the risk of flooding.

REFERENCES

Arnold, J. G., and Fohrer, N., (2005). SWAT2000: Current capabilities and research opportunities in applied watershed modeling. *Hydrological Processes*, 19, 563-572.

Beven, K. J., Lamb, R., Quinn, P., Romanowicz, R., and Freer, J. (1995). TOPMODEL, in Singh, V. P. (Ed.), Computer Models of Watershed Hydrology. *Water Resource Publications*, Colorado. 627-668.

Croke, B., and Jakeman, A. (2004). A Catchment Moisture Deficit module for the IHACRES rainfall-runoff model. *Environmental Modelling and Software*, 19, 1-5.

Croke, B., Andrew, F., Spate, J., and Cuddy, S. (2005). IHACRES User Guide. Technical Report 2005/19. Second Edition. iCAM, School of Resources, Environment and Society. User Guide. Canberra, Australia: The Australian National University.

Hajam, R. A., Hamid, A. and Bhat, S. (2013). Application of Morphometric Analysis for Geo- Hydrological Studies Using Geo-Spatial Technology –A Case Study of Vishav Drainage basin. Hydrol Current Res, 4(3):157. doi:10.4172/2157-7587.1000157

HFA. (ND) Hyogo framework for Action: Report on Word Conference for Disaster reduction. Retrieved October 7, 2015 from http://www.unisdr.org/we/coordinate/hfa

Hydrologic Engineering Center. (2015). Hydrologic Modelling System HEC-HMS Applications Guide. CA: US Army Corps of Engineers, Institute for Water Resources.

Montgomery, D. R., and Dietrich, W. E. (1992). Channel initiation and the problem of landscape scale. Science, 255, 826-830. Retrieved from http://apcg.uoregon.edu/amarcus/geog607w09/ Readings/Montgomery-Dietrich1992_Sci_Channel-Initiation.pdf

NDA. (ND) Natural Disaster Association. Natural Hazards: Flooding. Retrieved October 7, 2015 from http://www.n-d-a.org/flooding.php

Passalacqua, P., Belmont, P. and Foufoula-Georgiou, E. (2012), Automatic channel network and geomorphic feature extraction in flat and engineered landscapes, Water Resources Research, 48, W03528. doi:10.1029/2011WR010958.

Schröder, D. and Omran, A. (2013). Terrain Analysis for Flash Flood Risk Mapping. Proceedings Applied Geoinformatics for Society and Environment (AGSE), (pp. 1-8) Ahmedabad, India.

Strahler, A. N., and Chow, V. T. (1964). Quantitative geomorphology of drainage basins and channel network. In. Handbook of Applied Hydrology, McGraw-Hill Book Company, New York, USA.

Tarboton, D. G. (2003). Rainfall-Runoff Processes. A workbook to accompany the Rainfall-Runoff Processes Web module. Utah State University. Retrieved from http://www.engineering.usu.edu/dtarb/rrp.html

Tarboton, D. G. and Ames, D. P. (2001). Advances in the mapping of flow networks from digital elevation data. In World Water and Environmental Resources Congress, Orlando, Florida. Retrieved 2015 from:

http://www.unc.edu/courses/2010spring/geog/591/001/readings/tarboton_asce2001.pdf

Tarboton, D. G., Bras, R. L. and Rodriguez-Iturbe, I. (1992). A physical basis for drainage density, Geomorphology, 5 (1/2), 59-76. doi: 10.1016/0169-555X(92)90058-V

United Nations. (2004) Guidelines for reducing flood losses. Retrieved October 16, 2015 from https://sustainabledevelopment.un.org/content/documents/flood_guidelines.pdf

Vogt J. V., Soille P., de Jager A., Rimavičiūtė E., Mehl W., Foisneau,… Bamps C. (2007). Developing a pan-European Database of Drainage Networks and Catchment Boundaries from a 100 Meter DEM. In M. Wachowicz and L. Bodum (Eds.), Proceedings of the 10th AGILE Int. Conference on Geographic Information Science. Aalborg University, Denmark. Retrieved 2015 from http://ccm.jrc.ec.europa.eu/documents/

Influence of Elevation above Sea Level and Forest Type on Estimation of Forest Canopy Height Using ICESat/GLAS – Case study: Hyrcanian forests of Iran

Manizheh Rajab Pourrahmati[*a,b], Ali A. Darvishsefat[a], Nicolas Baghdadi[b]

a Faculty of Natural Resources, University of Tehran, Karaj, Iran, b IRSTEA, UMR TETIS, 34093 Montpellier, France – *corresponding author email: manizheh.pourrahmati@teledetection.fr, mrajabpour@ut.ac.ir

KEYWORDS: ICESat/GLAS, Hyrcanian forests of Iran, Forest canopy height, Forest type, Elevation above sea level

ABSTRACT:

Measuring forest biophysical parameters is important for forest management and ecosystem health monitoring. Heterogeneity of Hyrcanian forests in terms of vertical and horizontal makes the measurements and estimations difficult and doubtful. This research aims to assess accuracy of estimation of maximum canopy height (H_{max}) and mean Lorey height (H_{Lorey}) of Hyrcanian mountainous forests using lidar space borne data of ICESat/GLAS, and also influence of elevation above sea level and forest type on the estimations. GLAS extracted metrics were regressed against field measurement data using three statistical methods of multiple linear regression (MLR), random forests (RF) and artificial neural network (ANN). A 10-meter digital elevation model (DEM_{10}) was employed to decrease the recognized effect of terrain slope on lidar waveforms. In order to assess the influence of forest type and elevation, statistic parameters were calculated in three forest type classes of pure Fagus orientalis*, mixed* Fagus orientalis *and* Carpinus orientalis-Quercus macranthera*, and three elevation classes of <300 m, 1300-1500 m and > 1500 m. Concerning Hmax, best result was obtained using an MLR based on waveform parametric metrics and terrain index extracted from DEM10 with an RMSE of 5 m. The accuracy of this model increased to 3.9 m in pure* Fagus orientalis*, and 3.8 m in elevation class of 1300-1500 m which is also mostly covered by pure* Fagus orientalis*. Regards to H_{Lorey}, an ANN model based on waveform nonparametric metrics acquired from principal component analysis (PCA) showed the highest accuracy of 3.4 m which increased to 2.4 m and 2.6 m in pure* Fagus orientalis *and 1300-1500 m elevation, respectively. The results confirm the effect of forest type and mixture, and also elevation of sea level besides terrain slope on GLAS estimates. It is expected to achieve more accurate estimations by adding such qualitative information to GLAS regression models.*

1. Introduction

Forests are of extreme importance to humans in many ways. They are watersheds, and have economic, environmental and climate control benefits. Forests help to keep the carbon cycle and other natural processes working and help reduce climate change. The increasing importance of sustainable forest management and ecosystem health monitoring encourages researchers to find precise, yet low-cost methods in measuring biophysical parameters of forest as the primary step.

Information about vertical structure of forest specifically height is important for ecosystem health assessment, site fertility, volume, biomass and carbon cycle measurement and monitoring (Namiranian, 2007; Cairns *et al.*, 1995). However in situ measures provides the most precise information of forest height, for very large heterogeneous forests, measuring quantitative and qualitative properties of forest on the ground would be prohibitively expensive, time consuming and laborious. This highlights the importance of remotely sensed techniques in estimation of forest biophysical parameters.

Lidar is an active remote sensing system which is able to detect height of objects by measuring time delay between laser transmission and reception. Space borne lidar of ICESat/GLAS (Ice, Clouds, and Land Elevation Satellite/Geoscience Laser Altimeter System), launched into the space in 2003, has been used to retrieve forest canopy height and biomass in several researches (e.g. Lefsky *et al.*, 2005; Lefsky *et al.*, 2007; Rosette *et al.*, 2008a; Sun *et al.*, 2008; Chen, 2010; Duncanson et al., 2010; Saatchi et al., 2011; Mitchard *et al.*, 2012; Baghdadi *et al.*, 2014;). The most concerning point about GLAS data is waveform extent broadening over sloped area, and difficulties of canopy top and ground peak identification due to mixed vegetation and ground returns (Lefsky *et al.*, 2007; Chen, 2010). According to the complex condition of Hyrcanian mountainous forests in the north of Iran, vertically and horizontally, even and uneven aged stands, presence of diverse broadleaf species, severe topography, etc., this research aims to assess accuracy of estimation of maximum canopy height (H_{max}) and mean Lorey height (H_{Lorey}) using ICESat/GLAS in such area, and also influence of elevation above sea level and forest type on the estimations.

2. Study area and data description

This research was performed in temperate deciduous broadleaved forests of Nowshahr as part of Hyrcanian forests in the north of Iran (Fig. 1). It contains different forest type covering a wide range of elevation above sea level from 100 to 2200 meters with slopes ranging from flat to greater than 80%.

Two GLAS products (GLA01 and GLA14) provided by NASA national snow and ice data center (NSIDC) were used to extract required information. The data were acquired during L3I (October 2007) and L3k (October 2008) GLAS missions.

Field data were collected during September 2013 and May 2014. In total, 60 circle plots with diameter of 70 m (average size of GLAS footprints) were measured at the location of GLAS shots. Diameter at breast height of all trees greater than 7.5 cm (DBH > 7.5 cm), height of 10 dominant trees, species and environmental parameters (slope, aspect and elevation) were recorded within each plot. Two biophysical parameters including maximum canopy height (H_{max}) and mean Lorey height (H_{Lorey}) were calculated based on collected data.

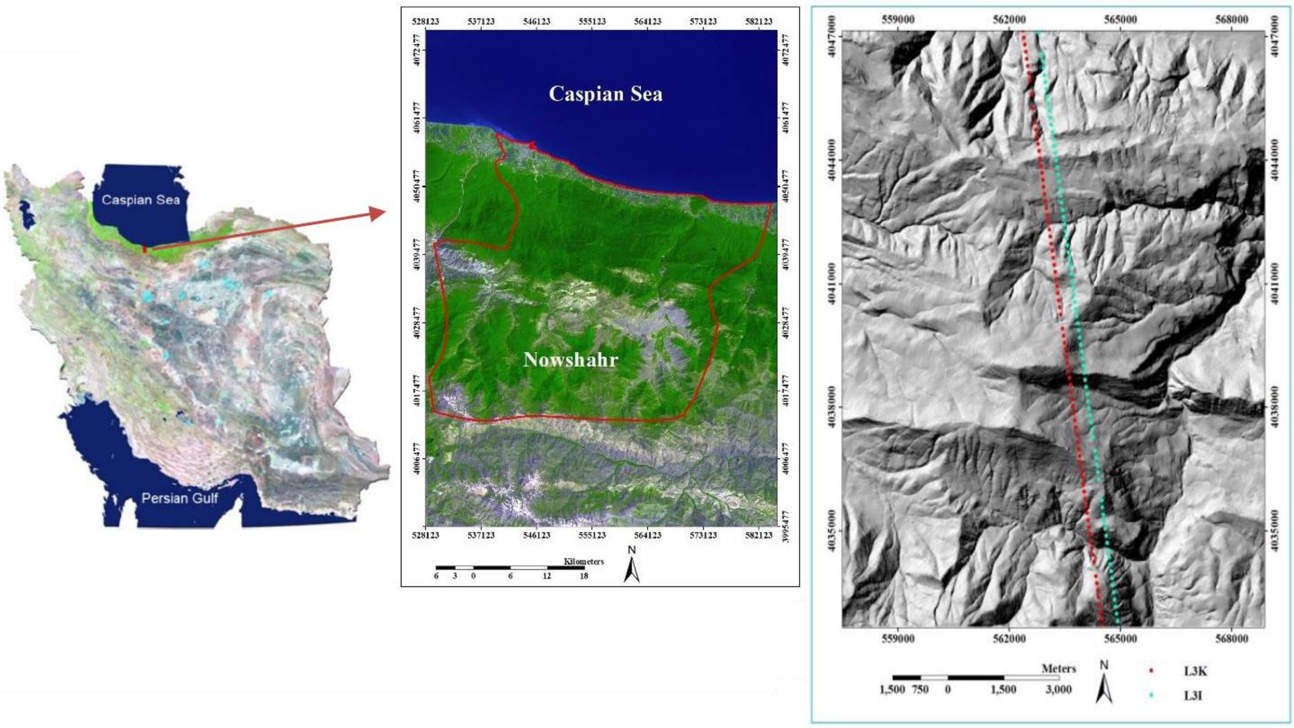

Figure 1: Location oft he study area in the north of Iran (two left maps) and Lidar footprints over hillshade of the study area (right map)

3. Methodology

Within each GLAS footprint, laser reflected energy by all intercepting objects results a waveform representing vertical profile of laser-illuminated surface. Two sets of metrics were extracted from waveforms including parametric metrics that were defined as vertical distance between different positions of waveform and ground peak (W_{ext}, H_{trail}, H_{lead},

H_{25},H_{50},…), and nonparametric metrics that are principal components (PCs) produced from principal component analysis (PCA) (Rajab Pourrahmati *et al.* (2016)).

GLAS extracted metrics were regressed against field measurement data using three statistical methods of multiple linear regressions (MLR), random forests (RF) and artificial neural network (ANN) to estimate maximum canopy height (Hmax) and mean Lorey height (HLorey). In order to reduce known terrain slope effect on GLAS waveforms (Lefsky *et al.*, 2007; Chen, 2010; Rajab Pourrahmati *et al.* (2016)), terrain index (TI10), representative of topography information, derived from a 10-meter digital elevation model (DEM10) was added to the models. Five-fold cross validation was used to validate the models. In order to assess the influence of forest type and elevation, the data were classified into three forest type classes of pure *Fagus orientalis* (F.o), mixed *Fagus orientalis* (F.o-other) and pure and mixed class of *Carpinus orientalis-Quercus macranthera* and other species (C.o-Q.m), and three elevation classes of <300 m, 1300-1500 m and > 1500 m. This classification is based on distribution of field data (60 plots) and is not representative of all conditions in the study site. Statistic parameters were calculated before and after classification.

4. Results

According to statistical parameters of root mean square error (RMSE), Akaike information criteria (AIC) and adjusted R-squared (R^2_a), best result concerning H_{max} was obtained using an MLR model (Equation 1) with an RMSE and R^2_a of 5.0 m and 0.85, respectively. The accuracy of this model is 3.9 m, 5.7 m and 5.8 m in F.o, F.o-other and C.o-Q.m classes, respectively (Fig. 2a). Moreover, calculation of accuracy in elevation classes of <300 m, 1300-1500 m and > 1500 m resulted the RMSE of 8.4 m, 3.8 m and 5.1 m, respectively (Fig. 2b).

$$H_{max} = -0.0042W_{ext}^{2.5} + 0.386W_{ext}^{1.5} + 3.549\ln(H_{50}) -0.052TI_{10}^{1.5} + 21.22 \qquad (1)$$

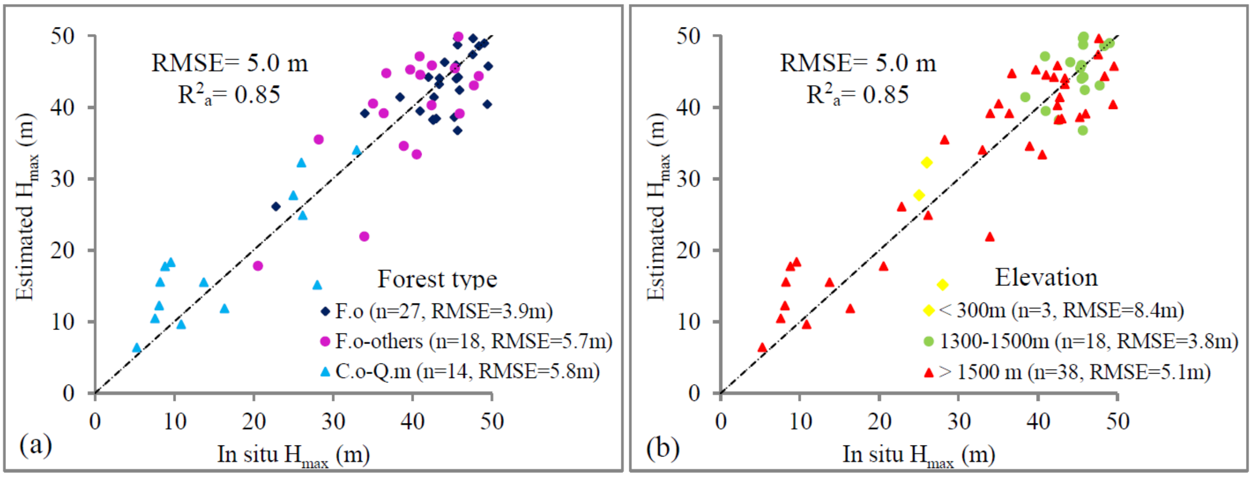

Fig. 2. Estimated H_{max} using an MLR model (Eq. 1) versus in situ H_{max} classified by a) forest type, and b) elevation above sea level.

Regards to H_{Lorey}, the best result was obtained using a three-layer neural network model employing only three first PCs of PCA and W_{ext}. It produced an RMSE and R2a of 3.4 m and 0.87, respectively. Accuracy of the model increased in F.o class (RMSE=2.4 m), and it is equal to 3.5 m and 4.2 m in F.o-others and C.o-Q.m classes, respectively (Fig. 3a). As it is observed in figure 3b, this model produced an RMSE of 7.6 m, 2.6 m and 3.2 m in elevation classes of <300 m, 1300-1500 m and > 1500 m, respectively.

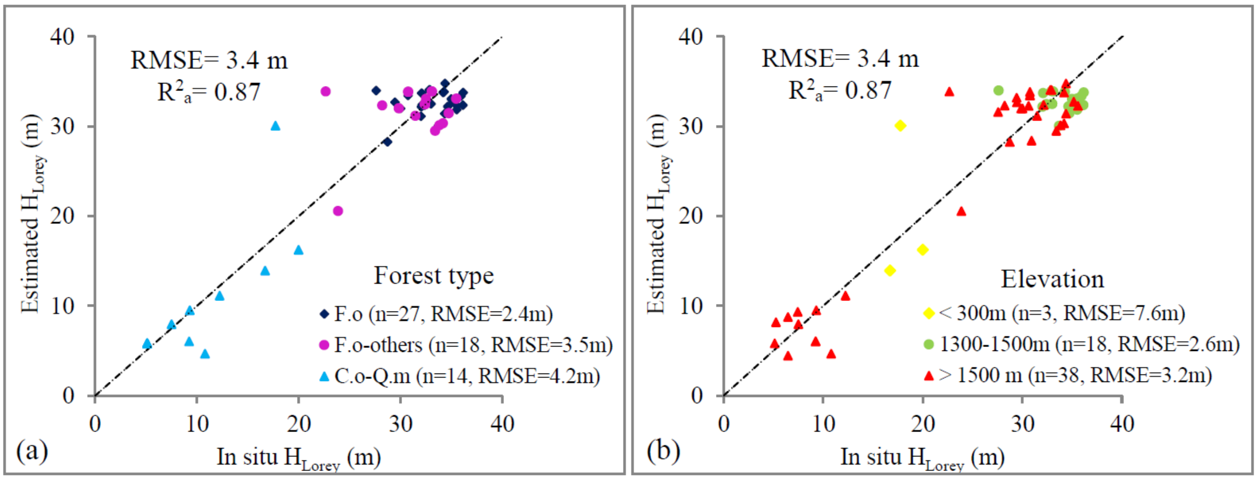

Fig. 3. Estimated H_{Lorey} using an ANN model versus in situ H_{Lorey} classified by a) forest type, and b) elevation above sea level.

According to the results, accuracy of estimations for both H_{max} and H_{Lorey} increases in pure stands (dark blue points representing pure *Fagus orientalis* class in figure 2.a and figure 3.a). It is worth to mention that pure *Fagus orientalis* class includes one-story even-aged stands. The homogeneity in vertical and horizontal structure of forest reduces mixed returned signals and leads to less noisy waveforms. In other words, over heterogeneous stands the ground peak might correspond to the objects under first story that do not represent terrain surface within a footprint (Chen, 2010) which is likely in two other forest type classes. It should be mentioned that the most errors regard to H_{max} (Fig. 2) refer to plots covered by short sparse stands over a sloped terrain. In such condition top of the highest object within a footprint is not necessarily at the top of the tallest tree, and could be a shorter tree on a higher elevation or even terrain instead of any vegetation (Chen, 2010). Lack of efficiency of GLAS data to estimate forest structural parameters, accurately, was also stated by Nelson (2010).

According to the result of height estimation in three elevation classes, the accuracy of estimations does not show a definite trend (Figure 2.b and figure 3.b). Both H_{max} and H_{Lorey} models have better performance in 1300-1500 m which includes mostly plots covered by pure Fagus orientalis. The lowest accuracy belongs to < 300 m class which could be as a result of lack of sufficient samples in this class, and also presence of bushes and shrubs understory which makes error in identification of ground peak.

5. Conclusion

This research investigated the influence of elevation above sea level and forest type on estimation of forest canopy height using ICESat/GLAS data. The results show a decrease in accuracy of estimations from pure *Fagus orientalis* towards mixed *Fagus orientalis* and pure and mixed class of *Carpinus orientalis-Quercus macranthera* and other species (RMSE F.o < F.o-other < C.o-Q.m). Concerning sea level elevation, the best result was obtained in 1300-1500 m which includes mostly plots covered by pure *Fagus orientalis*. This confirms the interaction effect of these two factors on the canopy height estimation using GLAS. It is worth noting that according to the complexity of study area in terms of topography and forest structures, horizontally and vertically, definite interpretation on influence of each individual factor is challenging. Nevertheless, it is expected to achieve more accurate estimations by adding such qualitative information to the GLAS regression models.

REFERENCES

Baghdadi, N., G. Maire, I. Fayad, J.S. Bailly, Y. Nouvellon, C. Lemos & R. Hakamada, 2014. Testing different methods of forest height and aboveground biomass estimations from ICESat/GLAS data in Eucalyptus plantations in Brazil. *IEEE Journal of Selected Topics in Applied Earth Observations and Remote Sensing*, 7(1): 290-299.

Cairns, M., J., Barker, R. Shea & P. Haggerty, 1995. Carbon dynamics of Mexican tropical evergreen forests: influence of forestry mitigation options and refinement of carbon-flux estimates. *Interciencia*, 20(6): 401-408.

Chen, Q., 2010. Retrieving vegetation height of forests and woodlands over mountainous areas in the Pacific Coast region using satellite laser altimetry. *Remote Sensing of Environment*, 114: 1610-1627.

Lefsky, M.A., M. Keller, Y. Pang, P.B. de Camargo & M.O. Hunter, 2007. Revised method for forest canopy height estimation from Geoscience Laser Altimeter System waveform, *Journal of Applied Remote Sensing*, 1: 1-18.

Lefsky, M.A., D.J. Harding, M. Keller, W.B. Cohen, C.C. Carabajal, F.D. Espirito-Santo, M.O. Hunter, R. de Oliveira & P.B. de Camargo, 2005. Estimates of forest canopy height and aboveground biomass using lCESat, *Geophysical Research Letters*, 32(22): 1-4.

Mitchard, E.T.A., S.S. Saatchi, L.J.T. White, K.A. Abernethy, K.J. Jeffery, S.L. Lewis, M. Collins, M.A. Lefsky, M.E. Leal, I.H. Woodhouse & P. Meir, 2012. Mapping tropical forest biomass with radar and spaceborne lidar in Lop´e National Park, Gabon: overcoming problems of high biomass and persistent cloud. *Biogeosciences*, 9: 179-191.

Namiranian, M., 2007. Measurement of Tree and Forest Biometry, 1st Edition, University of Tehran, ISBN: 964-03-5439-2, 574pp (In Persian).

Nelson, R., 2010. Model effects on GLAS-based regional estimates of forest biomass and carbon. *International Journal of Remote Sensing*, 31(5): 1359-1372.

Rajab Pourrahmati, M., Baghdadi, N., Darvishsefat, A.A., Namiranian, M., Fayad, I., Bailly, JS., & Gond, V. (2016). Capability of GLAS/ICESat Data to Estimate Forest Canopy Height and Volume in Mountainous Forests of Iran. *IEEE Journal of Selected Topics in Applied Earth Observations and Remote Sensing*, 58(11), 5246-5261.

Rosette, J.A.B., P.R.J. North & J.C. Suarez, 2008a. Vegetation height estimates for a mixed temperate forest using satellite laser altimetry, International Journal of Remote Sensing, 29(5): 1475-1493.

Saatchi, S.S., H.L., S. Brown, M. Lefsky, E.T. Mitchard, W. Salas, B.R. Zutta, W. Buermann, S.L. Lewis, S. Hagen, S. Petrova, L. White, M. Silman & A. Morel, 2011. Benchmark map of forest carbon stocks in tropical regions across three continents, Proceedings of the National Academy of Sciences USA, 108(2): 9899-9904.

Sun, G.K.J. Ranson, D.S. Kimes, J.B. Blair & K. Kovacs, 2008. Forest vertical structure from GLAS: An evaluation using LVIS and SRTM data, *Remote Sensing of Environment*, 112: 107-117.

Identification of Char Lands & Suitability Analysis of Cropping in Dry (winter) Season on Teesta-Jamuna River Basin in Bangladesh

Mohammad Kamruzzman*, A H M Tajul Islam, Zahid Hasan Siddiquee, Md. Ashraful Islam

Institute of Water Modelling, ICT-GIS Division, Dhaka, Bangladesh – mkz@iwmbd.org; tis@iwmbd.org; zhs@iwmbd.org; afl@iwmbd.org

KEYWORDS: Char Land, Suitability, Sandbar cropping, sand index;

ABSTRACT:

Bangladesh is a riverine delta in South Asia crisscrossed by hundreds of rivers, located in the confluence of Ganges and Jamuna. Situated in the downstream these rivers carry billions of tons' siltation from their origin to destination, the Bay of Bengal. During monsoon (November and extends up to the end of March) both banks of these rivers become inundated therefore the livelihood of the local people are disrupted. After the flood water is dispelled it leaves thousands of hectors of barren fertile land known as Chars (extended river banks and river islands formed from sedimentation – are extremely vulnerable to natural disasters). The livelihood of Char Lands is mainly fishing or husbandry, as there is not adequate opportunity for farming as being most of the land buried under sands. This research paper attempts to identify the Permanent and Temporary Char Lands in Teesta-Jamuna, Padma River catchments using Remote Sensing and GIS Technology as well as suitability of sandbar cropping on these lands. The study jurisdiction is from Teesta Barrage to the confluence of Padma Jamuna River confluence with a total length of approximately 451 km. Four bands Sentinel 10 m spatial resolution Satellite image, Landsat 8 OLI_TIRS are used to identify the Char Lands supported by Remote Sensing Software. A NDWI (Normalized difference Water index) and Char land index would be used to automate the unsupervised classification. To differentiate the seasonal variation, temporal image of February to December was collected for last couple of years attributed by their stability. These unexplored Char Lands can be considered as great resources as the lands are very fertile therefore can be used for cultivating sandbar cropping. This sandbar cropping technology is expected to diminish the food scarcity of North-Western people in a sustainable way thus will ameliorate the disaster resilience to seasonal flood.

1 Introduction

1.1 Background

Maximum Bangladesh is one of the largest deltas in the world, is facing the adverse effects of climate change with riverbank erosion and flood water inundation during monsoon. This has resulted in loss of agriculture crops, livestock and homesteads. The amount of cultivable land is reducing every year in an ever-changing landscape. Sandbar cropping has made a positive impact in converting these unfertile barren sandbars into food producing lands (Sondossi, 2001). This has aided in providing climate-resilient livelihoods to the vulnerable farmers by strengthening their food security. After each rainy season, large sand islands (Char Lands) appear in the main rivers of Bangladesh. Cropping on the sandbars involves digging small pits in the sand and lining the pits with compost to grow pumpkin, squash, and other high value crops and vegetables. Large-scale irrigation is not necessary as the land (considering it is in the river basin) is close to the river channel. The pumpkins produced on the sandbars can be stored in people's houses for over a year, greatly assisting poor households by providing an income source, food security, and a way to manage lean seasons. Sandbar cropping has given displaced peoples a way to transform barren landscapes and 'mini deserts' into productive.

* Corresponding author.

This study targets to discover the Char-lands of Jamuna, Teesta and Padma Rivers as well as the suitability of sandbar cropping. The suitability includes finding the sandy chars which remain stable during the dry season (October to March). Since there is no record on Char-lands in this area, this study is focused to measure it using satellite images. Therefore, the present study has combined with RS, GIS technology using free source Sentinel images and Landsat images in year 2015-16.

2 Study Area

In Bangladesh, the river mainly affects the five northern districts of Rangpur Division: Gaibandha, Kurigram, Lalmonirhat, Nilphamari and Rangpur (BBS, 2011). The study area will cover both banks and the Char Lands of Teesta Padma River; Starting from Teesta Barrage (Lat- 26.1786, Long- 89.0523) to the confluence of Jamuna-Teesta (Lat- 25.4892, Long- 89.6974). The total length of all the segment of Teesta River is approximately 101.80 km. The study area will cover both banks and the Char Lands of Jamuna, Teesta and Padma Rivers. Starting from Teesta Barrage to the confluence of Jamuna Padma confluence and Padma River from Rajshahi Town to Jamuna Padma confluence. The total length of all the rivers are approximately 451 km.

The River alignments are buffered into area coverage with a uniform distance from the river alignment. This distance(s) were measured by the maximum width of Rivers covering all the chars. The higher buffer distances were considered for wider rivers. The River alignments are buffered into area coverage with a uniform distance from the river alignment. The maximum width of River measured this distance covering all the chars. The buffer distance of these River is considered as 2.5 km in both banks.

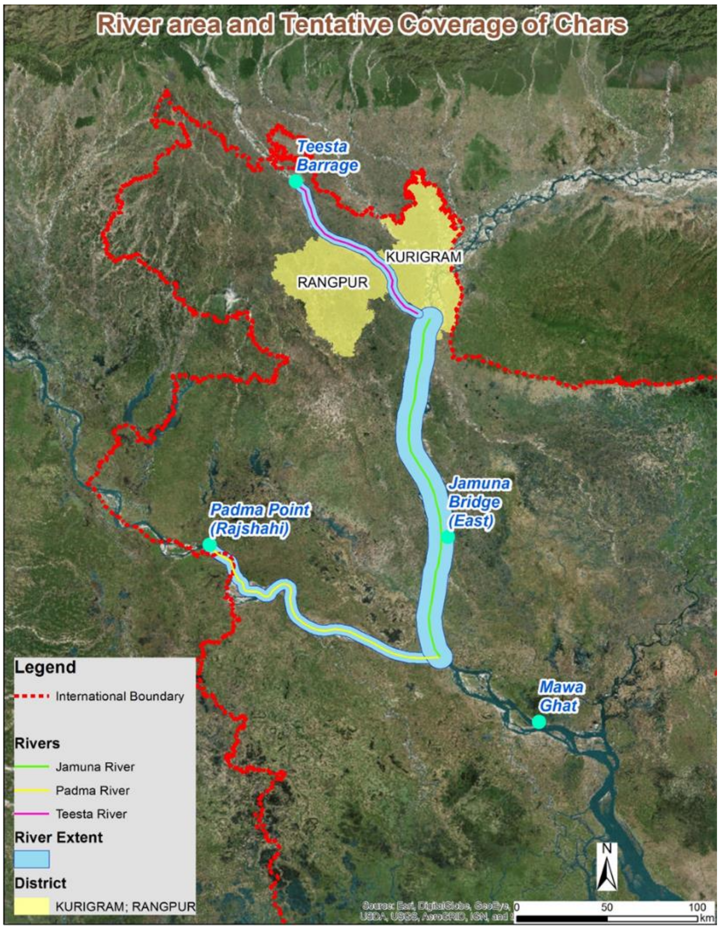

Figure 1: Study Area

3 Materials & Methods

3.1 Data

The Char-land identification was carried out using Remote Sensing Technology. The image of Sentinel image was used to extract the area of Char-lands; the spatial resolution is 10m-20m. The basic data of the study area are Landsat satellite images of February, October and December, year 2015. United States of Geological Survey (USGS) provides (Path 138 and Row 43) images in the earth explorer website: http://earthexplorer.usgs.gov. All satellite images have taken at dry seasons. Atmospheric corrections were done for accuracy of the information that was extracted from different Landsat images. Geometric corrections were performed to fix each image into the UTM-45N projection. Because of flat land, the orthogonal transformation was not performed. All images were resampled with the nearest neighbor method to a common resolution of 10m. Erdas Imagine software has been used for processing satellite images and analysis of the riverbank data.

3.2 River Identification

The Normalized Difference Water Index (NDWI) is a satellite index derived from Near-Infrared (NIR). The Normalized Difference Water Index (NDWI) is a new method that has been developed to delineate open water features and enhance their presence in remotely-sensed digital imagery. The NDWI makes use of reflected near-infrared radiation and visible green light to enhance the presence of such features while eliminating the presence of soil and terrestrial vegetation features. It is suggested that the NDWI may also provide researchers with turbidity estimations of water bodies using remotely-sensed digital data.

The NDWI was derived using principles similar to those that were used to derive the NDVI. The NDWI is calculated as follows:

NDWI= (GREEN - NIR)/ (GREEN + NIR)

NIR: Near infrared (860nm, Band 5, Landsat 8).

Where GREEN is a band that encompasses reflected green light and NIR represents reflected near-infrared radiation. The NDWI product is dimensionless and varies between 0 to 1, depending on the leaf water content but also on the vegetation type and cover.

3.3 Char land identification

An Unsupervised or Supervised Classification identifies wide range of features, but only topsoil features were identified. A char land index can be used for getting a quick and accurate output. The formula for a char index was computed as following-

Char land index = (RMAX+BMAX+GMAX) / (RMIN+BMIN+GMIN)

Char land index will be classified as four class. The dimension and range varies between 30 to 100. According to suitable study and classification it is classifies as vegetation, shrub, moisture and pure sandy area. After the classification, the thematic raster will be converted to the vector data for further analysis using ArcGIS Software.

4 Analysis & Discussion

The results of this study include two parts; the first result shows the identification of char land mainly sandbar in different time in a year, the other one is the brief explanation of important of sand bar, impact on sustainable agriculture and sustainable development.

4.1 River Identification

4.1.1 Water Index Calculation

NDWI can be presented in the form of maps and graphs, providing information both on the spatial distribution of the vegetation water stress and its temporal evolution over longer time periods. This allows for the qualitative and quantitative comparison of the intensity and duration of the NDWI anomalies with recorded impacts such as yield reductions, low flows, lowering of groundwater levels.

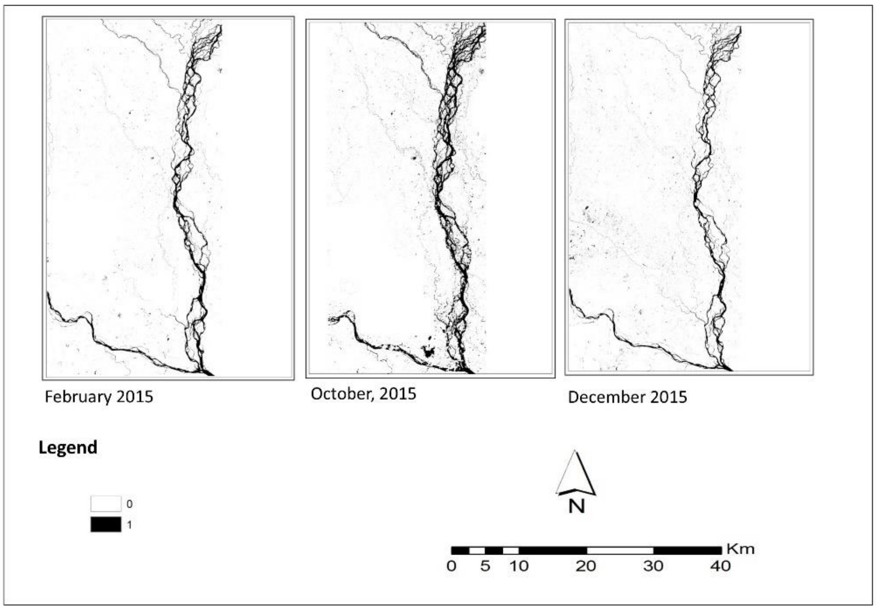

Figure 2. River index of February, October, December, 2015

The NDWI product is dimensionless and varies between 0 to 1, depending on the leaf water content but also on the vegetation type and cover. High values of NDWI correspond to high vegetation water content and to high vegetation fraction cover. Low NDWI values correspond to low vegetation water content and low vegetation fraction cover. In period of water stress, NDWI will decrease.

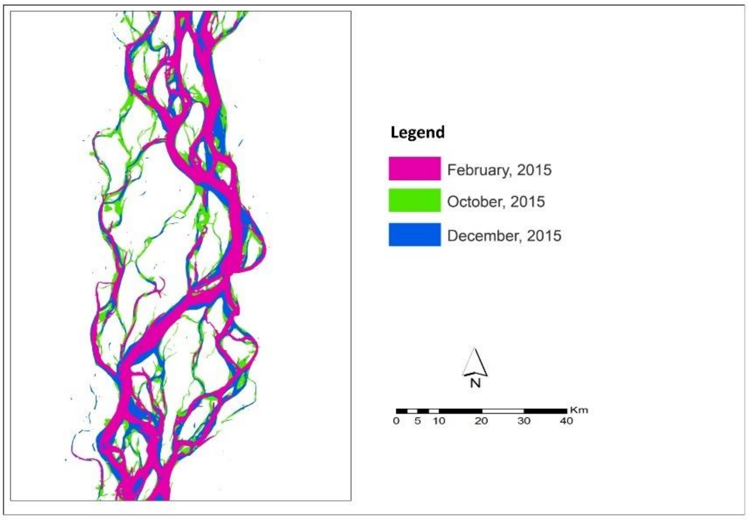

Figure 3. River identification of February, October, December, 2015

The figure 2 represents the water index map that is river of the study area. From the water index is identified that water or not. The NDWI product is dimensionless and varies 0 to 1. The value 0 represent other types and the value 1 represent the water area of February, October and December of 2015. The figure 3 represent the river in different three time in 2015.

4.2 Char land identification

Char land is identified from char land index which is modified of normalized bare soil index. Char land identification generally refers to identification of sand bar in the study area. The char land is classified in different types as sand, wet sand, vegetation with sand and pure vegetation. The figure 4 represents the classification of the area. Three different time has been selected for this study. In year 2015 month of February, October, December three different classification is representing in figure. The four-different color represent the four classifications.

Table 1. Char land classification value

Class name	Value range
Vegetation	31-36 31-36
Sand	36-40 36-40
Moisture sand	40-45 40-45
Pure sand	45-85 45-85

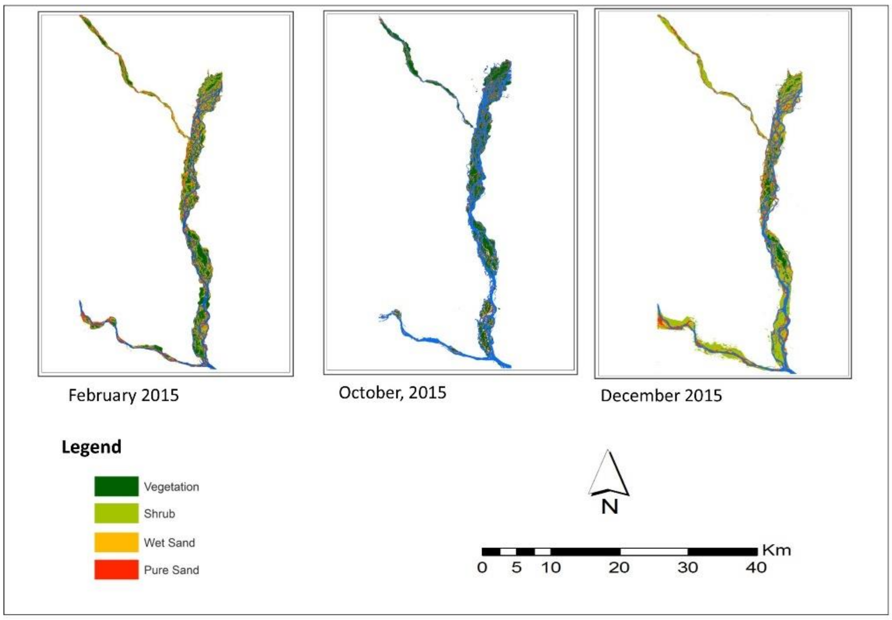

Figure 4. Char land classification of February, October, and December, 2015

According to the classification the sand and vegetation is dominant type. Sand area is different in different time of year. The figure 4 and table 2 represent the char land classification and four different color shows distinct different of three times images. In October, the river contains huge water, as a result the area of char land shows minimal area. But in later period, in winter the water quantity is low that's why char land focuses more than other times.

In all reaches, sand area was less in October than in February, supporting the conclusion. From October to December, sand area decreased in all reaches.

Table 2. Char land identification of February, October, and December, 2015

Class Name	**February, 2015 (Sq Km)**	**October, 2015 (Sq Km)**	**December, 2015 (Sq Km)**	**Region**
Soil & Vegetation	910.98	1104.45	350.35	Vegetation Region
Soil & Shrub	660.80	366.52	1498.29	
Wet Sand	688.14	156.73	651.93	Sandy

Pure Sand	478.13	97.83	424.97	Region
Total Area (Sq. Km)	2738.05	1725.53	2925.54	
Total Area (Hectare)	273805	172553	2922554	

The long-term investigation should provide the sediment and erosion trend in recent year of the study area thought historical map. The Figure 5 shows a sandbar sediment area in recent year. The area of sandbars reduces from October to December. The other phenomenon of sandbar change show as table 4, the lagoon area also reduces gradually from February. These phenomena tell us that the sandbar was increase rapidly in different month in a year. The sandbar index is an important factor for knowing sediment and erosion trend condition. We can use the winter and the summer image for sandbar study.

Figure 5 shows the area of vegetation shrub, moisture and pure sandy area. In October three area of sand is lowest because it is the post rainy season and December has the moistest sand area because it is the driest season. As sandy area remains for four to seven months in a year this is important for year-round cultivation.

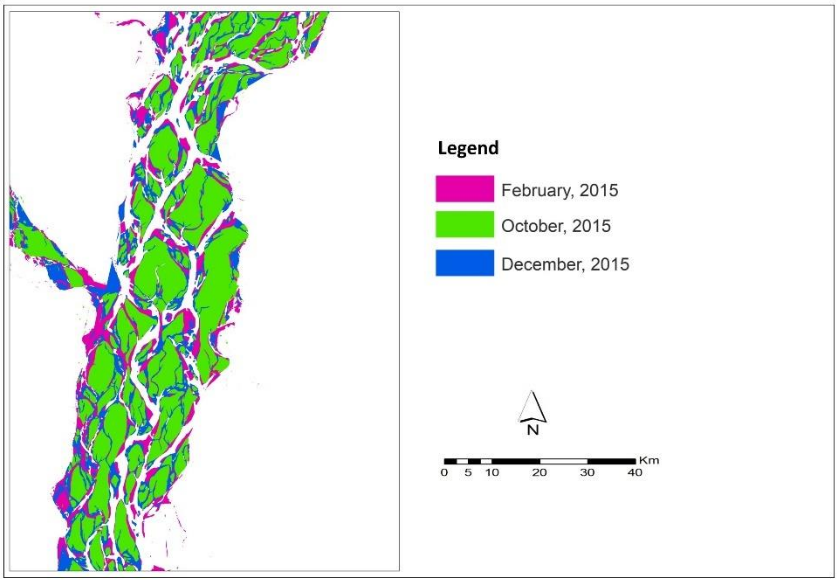

Figure 5. Char land identification of February, October, and December, 2015

The most important finding from these research is the sandbar area is different in different time period. In driest season the area is highest and in wet season it is in lowest, according to figure. The highest number of area 2925 sq. km are in 2015 as char land. Within this area around 424 sq. km are sandbar. The sandbar is important for sandbar cropping this is an elementary factor for sustainable development through sandbar cropping. This study has great potentiality for future development in integrated research in water sector.

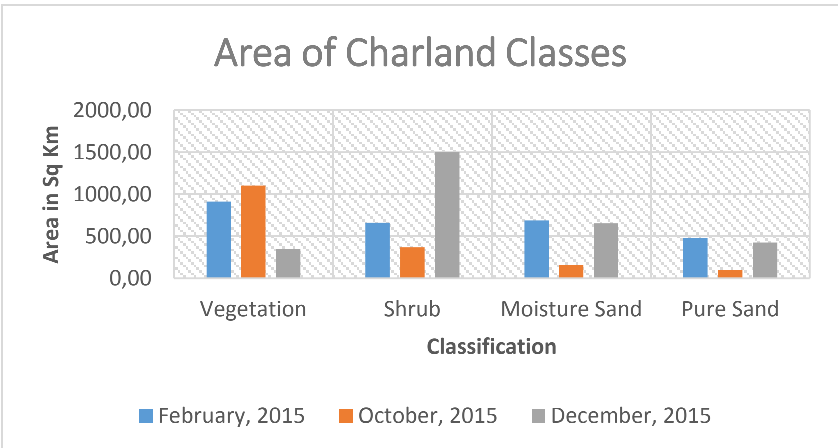

Figure 6. Area of char land classification 2015

4.3 Sandbar Cropping

At the end of rainy season in mid-November, as the water level in the rivers recede, sandbars start to emerge. These sandbars are brought under cultivation using the sandbar cropping technique. The sandbar cropping technique is a pit cultivation approach, adapted to the sandbars to grow pumpkin, squash and watermelon. Pits are dug in the sandbars and are lined with manure and compost. Jute sacks are used in locations where ground water is very poor. Seeds are placed in the pits and are carefully monitored for the next few months with periodic irrigation and nursing as required.

4.3.1 Sandbar Cropping – the sustainable development

In Bangladesh, monsoons flood and erode river embankments, wash away houses and agricultural land, and displace over 200,000 people that take shelter in public places or migrate to urban areas. In the northwest region of Bangladesh, the yearly flooding creates nearly insurmountable poverty conditions and disenfranchises those living on the riverbanks. When the monsoon subsides and the rivers recede, thousands of hectares of transitional land (sand-covered silty riverbeds) emerge and exist for six to seven months. Bangladesh, home for one of the largest deltas in the world, is facing the adverse effects of climate change with riverbank erosion and flood water inundation during the annual monsoon. This has resulted in loss of agriculture crops, livestock and homesteads. The amount of cultivable land is reducing every year in an ever-changing landscape. Sandbar cropping has made a positive impact in converting these unfertile barren sandbars into food producing lands. This has aided in providing climate-resilient livelihoods to the vulnerable farmers by strengthening their food security (Practical Action Bangladesh, 2012).

Every year millions of people in Bangladesh are effected by flooding and riverbank erosion. With most parts of the country being less than ten meters above sea level, cyclones, storm surges and seasonal floods are common yearly events. Over-population is forcing extremely poor people to inhabit unstable riverbanks and flood-prone areas. Every year more than 100,000 end up becoming environmental refugees and are forced to relocate as their houses and livestock are washed away and their farms are flooded or eroded by rivers (Unnayan Onneshan, 2012).

Climate change has worsened the situation. The rise in temperature and unpredictable rainfall patterns have resulted in increased river flow, frequent and severe floods, higher river bank erosion, prolonged drought and increased salinity intrusion. As rivers recede, large sand islands called sandbars emerge. Sandbars containing sand and silt, being non-conducive for vegetative growth, end up as barren lands. Practical Action, an International NGO, has developed ‘sandbar cropping’ techniques in partnership with local communities to cultivate these silts deposited sandbars to grow vegetables like pumpkin, squash and lettuce (Practical Action Bangladesh, 2011). In four of the northern districts of Bangladesh, sandbar cropping has helped many landless families to diversify their incomes and overcome seasonal food shortages, thereby helping them to adapt to the changing environment.

If you have questions about the technical content, submission procedure, layout, or editorial requirements, please contact the relevant individual of the meeting organizing committee.

5 Conclusion

The amount of cultivable land is reducing every year in an ever-changing landscape. Sandbar cropping has made a positive impact in converting these unfertile barren sandbars into food producing lands. From the research, In October three area of sand is lowest because it is the post rainy season and December has the moistest sand area because it is the driest season. As sandy area remains for four to seven months in a year this is important for year-round cultivation. These sandbars are brought under cultivation using the sandbar cropping technique. The results of this study shows the identification of char land mainly sandbar in different time in a year, has a great impact on sustainable agriculture and sustainable development.

References

BBS 2011, Bangladesh Bureau of Statistics 2011.

ILO 2009 “Green Job Assessment in Agriculture and Forestry sector of Bangladesh”, International Labour Organisation, Bangladesh, April 2009.

Unnayan Onneshan, 2012 “Innovative Agricultural Adaptation a Case Study on Sandbar Cropping in Sirajgonj, Bangladesh”, RESOLVE.

Practical Action Bangladesh 2012 “Accessing and Retaining Access to the Sandbars by Extreme Poor, Practical Action Bangladesh, EPR-shiree, March 2012.

Sondossi, H. A., and Schmidt, J. C. (2001). “GIS as a tool for studying the geomorphology of fine-grained deposits in the Colorado River in Grand Canyon National Park,” final report in partial fulfillment of contract 1425-98-FC-40-22640, 45 p.

Practical Action Bangladesh, 2012 “Learning from Phase-1”, PFP-shiree Project, Practical Action Bangladesh, 22 April, 2012

Data Collection, Flood Forecasting & Warning Message Dissemination Through Smartphone In Changing Climate

Md. Mahbubur Rahman [a*], Md. Zahid Hasan Siddiquee [a], Md. Ashraful Islam [a], A S M Muntaheen [a]

[a] Institute of Water Modelling, House 496, Road: 32, New DOHS, Mohakhali, Dhaka-1206,(Bangladesh) – mhb@iwmbd.org, zhs@iwmbd.org, afl@iwmbd.org, mut@iwmbd.org

KEY WORDS: Flood Forecasting, Warning center, Telephonic, Android, IWRM

ABSTRACT:

Global warming and climate change are the emerging threats for Bangladesh. Riverine and flash flood are imminent in almost every year. The Flood Forecasting & Warning Centre (FFWC) is the custodian for generating and disseminating forecast and warning manages for beneficiaries. FFWC used to collect water level data from the gauge readers through manual/telephonic system which is time consuming, less reliable and erroneous to some extent. In practice, it is done through phone call with a hand-written register book. Since the gauge readers provide data from the field only once in a day, the forecast and warning cannot be delivered more than once in a day. To reduce these problems Islamic Relief, Bangladesh and the FFWC initiated a pilot project to automate the system utilizing ICT technology including smartphones. Each gauge reader has a mobile phone and the collected the data are sent through SMS. An SMS Solution App for android is made where data can be converted from SMS format to plain text format. Then the text format data is transferred to computer from android phone. After that the text format SMS data is imported into SMS Solution software. All input massages are filtered, processed and stored in database. The process data is used to create a pre-formatted CSV file for a flood forecast model input. Flood forecast model uses this data for forecast. Generated forecast data is imported to the SMS solution software. Then flood forecasting massages are generated and disseminated both in English and local language (Bangla). This system has enabled FFWC to collect the data with more reliability, low cost, in more quickly. which ultimate contributes to generate better flood forecast and warning massages. This smart phone-based solution brought the Integrated Water Resources Management one step ahead in building resilient communities with special reference to climate change induced disaster like riverine and flash flood.

1. Introduction

1.1 Background

Flood Forecasting in Bangladesh is the responsibility of the Flood Forecasting and Warning Center (FFWC) of Bangladesh Water Development Board (BWDB). This center was established in 1972 and is fully operative in the flood season, from 1st April to 31st October, as directed by the Standing Orders for Disaster (SOD) of the Government of Bangladesh. The objectives of flood forecasting and warning are to enable and persuade people along with organization to be prepared for the flood with a review to taking necessary steps in order to increase safety as well as reducing damage. Its goal is to alert the 'combat' agencies to enhance their preparedness and to motivate vulnerable communities to undertake protective measures. The basis of flood forecasting is measurements of rainfall and water level which are used to interpret the present flood situation and generate flood forecasts.

The hydrological data collected through the monitoring are used as input to a numerical model which forms a core component of the forecasting system. The results of the model computations are used as the basis for the preparation of a

[*] Corresponding author.

range of flood warning products, including warning bulletins and inundation maps. FFWC disseminates these through a variety of media, including email, fax and the Internet via its own dedicated web site.

Bangladesh is located in the North-eastern part of South Asia Stretching between latitude 20°34´ N and 26°38´ and longitudes 88°01´ and 92°41´ E. The country is the lowest riparian of the three great rivers of the world, the Ganges, Brahmaputra and Meghna. With a limited land area of about 147,540 sq-km, the country provides drainage route of a huge catchment area, which over 92.5% of its land mass (ADPC and PAOS 2004). Its Flood Management is complex in nature due to geographic location. High variability of spatial and temporal distribution of water resources causes many problems for the country. Excessive water is available during the monsoon whereas water scarcity prevails during the dry period. Monsoon flood management is a challenge for Bangladesh for various reasons like food security and reduction of flood damages to support the economic development. There is some indication that flood hazard risks are changing due to natural and human–induced factors. Process related to human interventions include rapid urbanizations and unplanned development of flood plains, soil erosions due to over tilling and certain flood management activities. There are also upper riparian interventions such as flood embankments, damming of rivers and deforestation that are affecting river flows. In addition, global climate change could be affecting hydrology and water resources of Bangladesh's river network, a vast part of the country's surface is lower than 6 meters above sea level, which may ultimately result in more seriously flooding in future (DHI, 2005). Among the various aspects of flood management, flood forecasting is very efficient tools for flood management. Only physical measure like construction embankment or dams cannot be used for total flood management purposes. On the other hand, flood forecasting is rather simple tool which can be easily applied with little efforts. Considering the whole aspect of complexity of floods in Bangladesh, the Government of Bangladesh has taken the initiative for effective flood management. FFWC is the national institution responsible for flood forecasting activities. It provides forecasts and warnings to many national level organizations. The objective of the study is to automate the process of system mainly water level data collection and disseminated of model generated flood forecasting and warning message dissemination through smartphone.

2. Current status of Flood Early Warning

In 1972 the Flood Forecasting and Warning Centre (FFWC) was established to contribute to reducing the loss of life and the economic damage caused by riverine floods. Over the past decades various studies and pilot programs have been carried out to understand the effectiveness of the current Flood Early Warning System and to suggest as well as test improvements. These projects were explained in the Combined Evaluation Report submitted in April 2014. Forecasts for the major and secondary rivers in the central region of the country are of acceptable quality, but messages are often not effectively conveyed. There is a formal institutional disaster management structure (Disaster management committees at National, District upazila and Union levels) set up under the Department of Disaster Management (DDM). This consists of Disaster Management Committees (DMCs) at each level being supported by Disaster Management Information Centers (DMICs) up to Upazila level.

The strong penetration of mobile services in Bangladesh, 75% of the population (BTRC, 2014), offers opportunities to enhance this communication and dissemination component. Mobile service techniques have been tested successfully in Bangladesh for early warning i.e. SMS by ADPC (ADPC and PAOS), Interactive Voice Response (IVR) by DDM, Cell Broadcasting by Comprehensive disaster management Programme (CDMP) and DDM, Bulk SMS by DDM.

3. Present Hydro Meteorological data collection and Flood forecasting system

The flood forecasting system comprise of their core components, which includes data acquisition network, flood modelling systems and the dissemination of forecasts and warning. The basis of Flood Forecasting and warning is the monitoring of rainfall and water level measurements and the data at filed stations are used to both interpret the present food situation and also to predict future flooding. The data acquisition process can be these:

- A near real time monitoring system under BWDB covering Bangladesh with which rainfall and water level measurements are collected.
- A data exchange agreement with India through which FFWC obtains rainfall and water level in India.
- Meteorological data from Bangladesh Meteorological department (BMD)

The data acquired by FFWC are processed and stored in a database, from where they are accessed by numerical models which form the basis of flood forecasting and warning systems. The flood watch system integrates the data with the modelling system. MIKE 11, a one-dimensional river modelling system developed by DHI Water & Environment, Denmark has been used in FFWC to compute water level and discharge in the river systems. FFWC produces water level forecasts at 38-gauge stations on different rivers up to 72 hours. (FFWC, 2011).

4. Early Flood warning & Forecasting system

The main objective of the system is the acquisition of water level and rainfall data from observation stations through SMS (through GSM network) and pre-process is for Flood Forecast Model input. It will provide quality data in less time and eliminate the redundant jobs for parsing and processing. Data pre-processing for flood model will be achieved through a few clicks. To achieve the goal and objective we have identified the following major activities which are to be carried out listed below;

4.1 Design SMS based Data Acquisition and Processing System

Conceptual design is depicted in different steps (see fig 1 and 2)
Step -1 Create and Send SMS from gauge reader's cell phone;
Step -2 Receive SMS by cell phone connected to application server;
Step -3 FFWC Android apps will create SMS File for system import module.
Step -4 Import SMS File to store observed water level in database server;
Step -5 Pre-process and export data for forecast generation (Flood Forecast model);
Step -6 Disseminate forecast info through SMS to gauge readers;

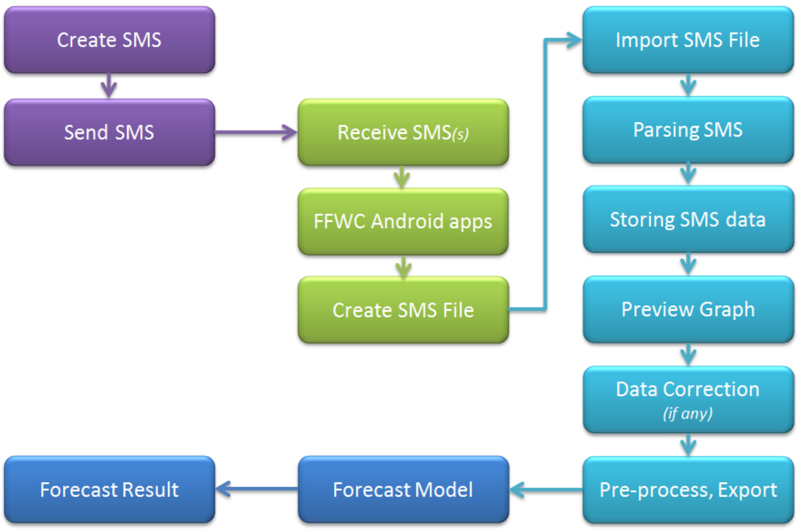

Figure 1. Early warning system detail activity

4.2 Development of the System

Two major application software development steps have been carried out. One is, FFWC Android Apps has been developed using Java. The other is, we have developed System (SMS Software) incorporating all features and functionalities.

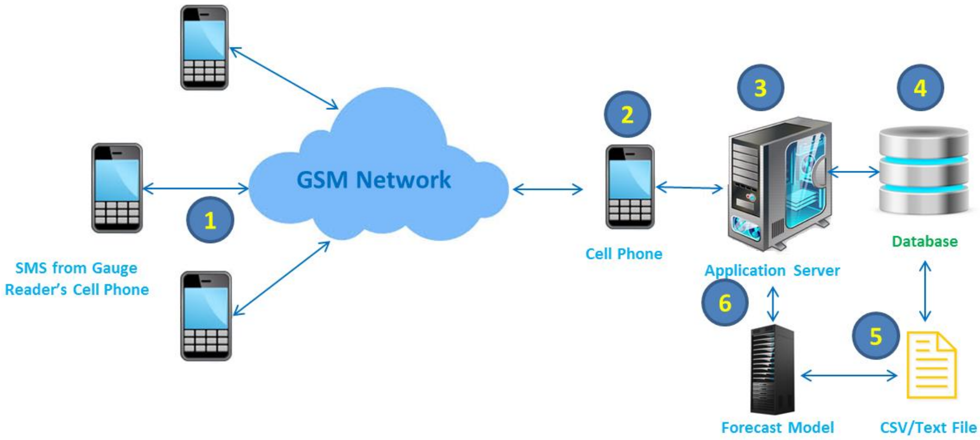

Figure 2. Conceptual form of Early warning system

5. Discussion

In SMS system, each gauge reader has a mobile phone. They collect the data and send it through SMS to the FFWC internal phone. An SMS Solution App for android is created where data can be turned from SMS format to plain text format. Data is collected from mobile phone's SMS by user from Android phone with the help of "SMS Solution for FFWC" app and a SMS text file will generate in internal storage of that android phone. Then data will be transfer to the data folder in application. This process considered as a Select SMS File to Import in SMS Solution for FFWC apps. After importing SMS successfully. The data will be processed and stored in data centered.

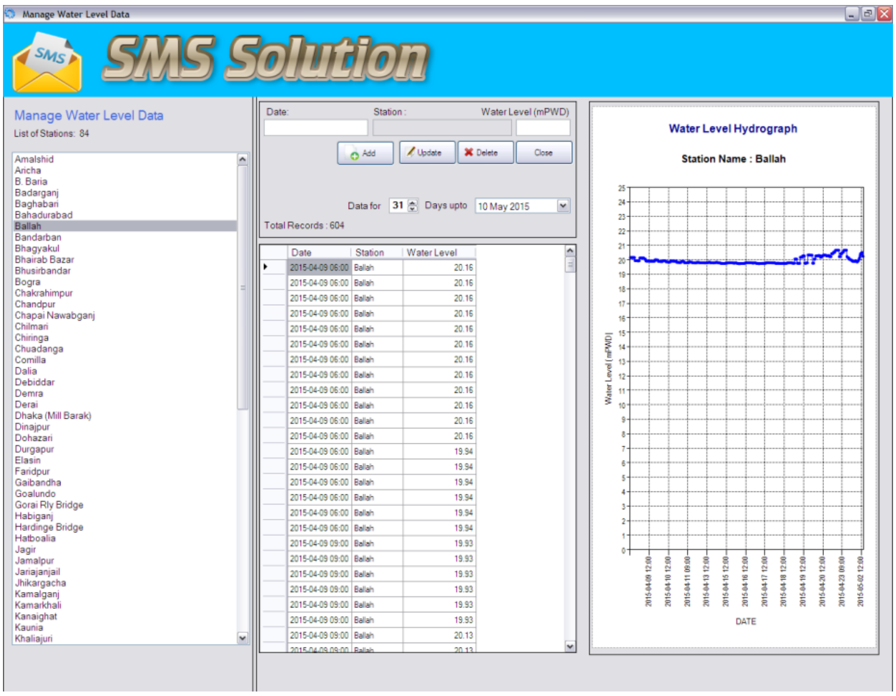

Figure 3. Early warning system water level data

The SMS import being finished, all the SMS need to be processed and stored in database. To process and store SMS data it needed to be a system. A 'Filtered SMS Data' window will appear. After data processing, has been done, user can process the station wise water level data. In water level data user are able to see the station wise Water level data and Water level hydrograph. Similarly, they can manage can manage the station wise rainfall data and rail fall hydrograph. They can also generate hydrograph for specific period of time such as 5/6/7 days etc. up to 31 days.

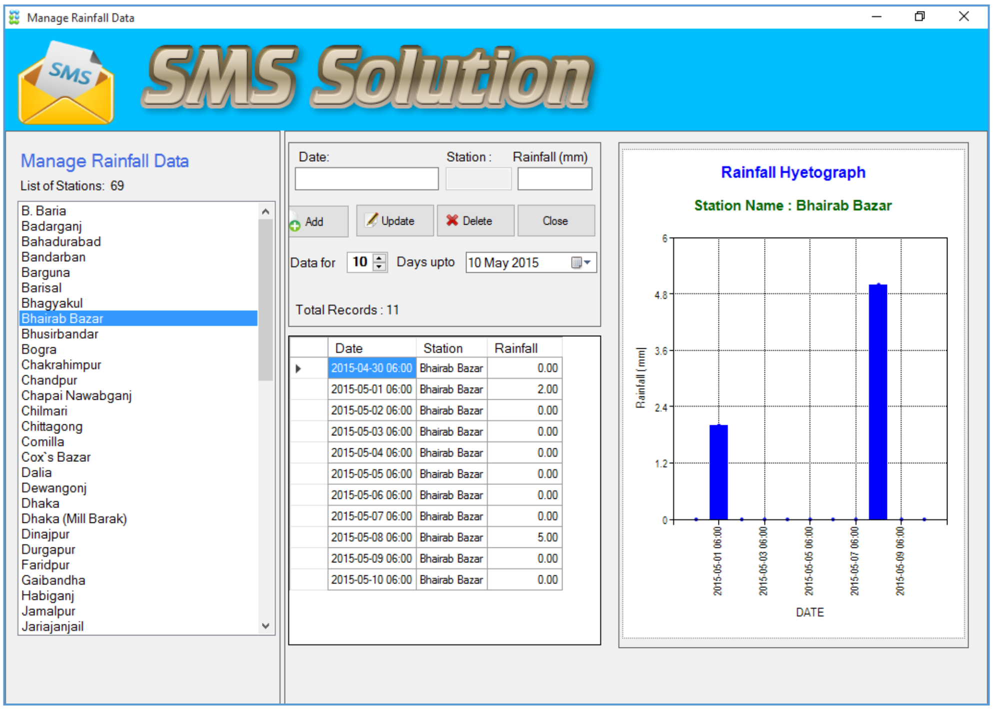

Figure 4. Early warning system rainfall data

To create forecast SMS first user, need to import forecast data (which is generated based on model data). In this stage forecast massage will be created. The massage will also be created in local language (Bangla) for local level people who has little knowledge in English. Figure 5 show an interface of application interface and disseminated message.

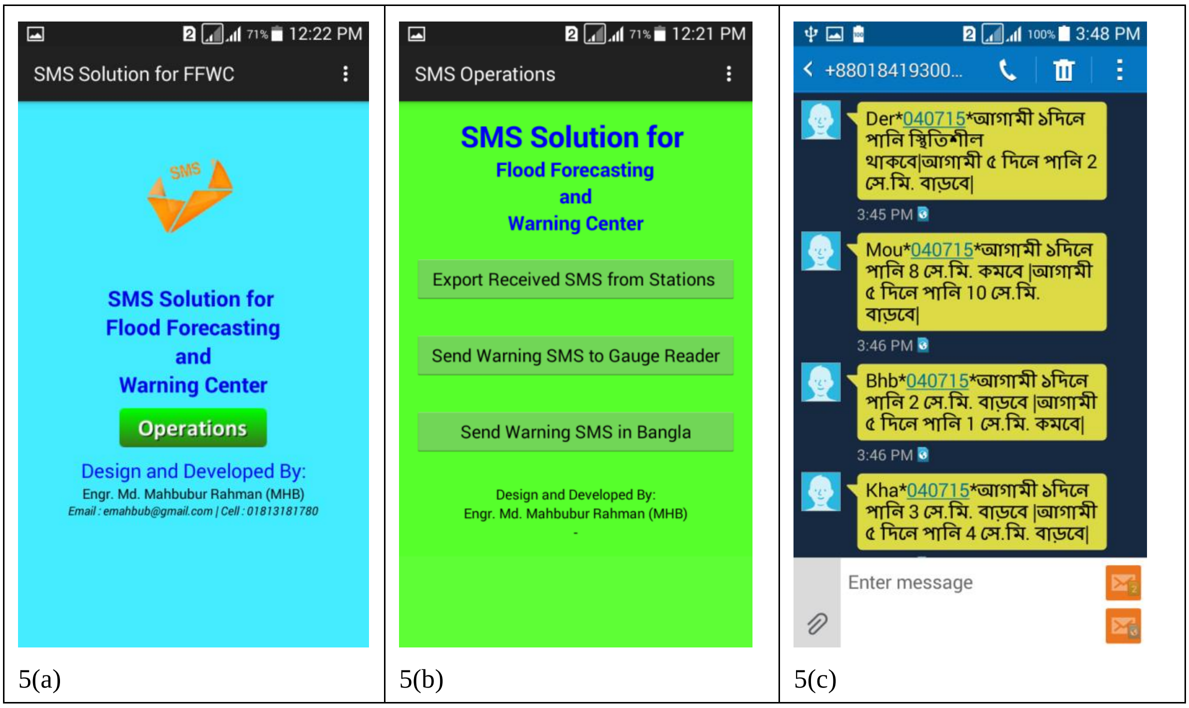

Figure 5. Early warning system application interface (5a) (5b); Generated massage in local language (5c)

After creating the massages, they are sent the file by Android phone using FFWC android app. This way it can also send warning SMS to gauge Reader. It might take a few minutes to perform the operation.

6. Outcomes – benefits and response

It is clear from the evaluation that the end users were able to really use this warning information to take protective actions to reduce losses to their livelihoods. User utilize the social network in the community to take more effective actions in response to the warnings. This include getting help from the gauge readers, UP chairman, agricultural officers, NGO staff and DC operators and family in order to more effectively carry out their response actions. Support is provided through manual labor and by offering advice on the best actions to take. They were able to bear the costs from household savings. However, on the other hand, the poor transportation facilitates (including a lack of boats and poor road quality), lack of manpower, lack of safe storage places, and limited access to financial support, constrained the end user's ability to effectively respond to the warnings. Furthermore, it was clear that there was only limited livelihood advisory information is available at the local level including information on agricultural, livestock (cattle rearing), fish culture and health, which could be useful in combination with a warning message.

However, the following Improvement have been made:

- Improved Data quality, less error and less cost.
- Improved accuracy of flood forecasting.
- Reduced time to processing of data
- Faster forecast result
- Daily flood forecast to local communities through mobile SMS

7. Conclusion

At present flood forecast are being using deterministic and probabilistic forecast approaches. The study shows that the forecast quality gradually deteriorated where forecast intervals moved further away from the time of forecast. Short range forecast is used to evacuation and emergency planning whereas medium and long range forecast is used for agricultural planning which is essential to build food security. As probabilistic model, can play an important role to increase the present short-term lead-time to medium to long range lead-time, so more focus should be given on its improvement. Improvement of data collection system as well as regional cooperation is also necessary for increasing lead-time.

References

ADPC and PAOS. 2004. *National Consultation Workshop on Climate Forecast Applications in Bangladesh*: Experimental Forecasts. Bangkok: Asian Disaster Preparedness Centre, Thailand and Georgia: Program on Atmospheric and Oceanic Sciences, Georgia Institute of Technology, USA.

BTRC, 2014. Bangladesh Telecommunication Regulatory Commission Annual Report 2014-2015. http://www.btrc.gov.bd/sites/default/files/paper_files/Annual%20Report%20Book.pdf

DHI, 2005. *Consolidation and Strengthening Flood Forecasting and Warning Services.* Dhaka: Ministry of Water Resources, Final Report Volume 1: Main Report.

FFWC, 2010. *Annual Flood Report-2010*. Dhaka: Bangladesh Water Development Board.

FFWC, 2011. *Annual Flood Report-2011*. Dhaka: Bangladesh Water Development Board.

The Landslide Hazard Map of Bogota: A Risk Management Initiative

Niny Johana Zamora

Risk management and climate change Institute (Instituto distrital de gestión del riesgo y cambio climático), - nzamora.idiger@gmail.com

KEYWORDS: Landslides, Bogota, GRASS GIS, Risk management, Hazards, Model Builder

ABSTRACT:

A land management plan (Plan de Ordenamiento Territorial, POT) is an instrument for planning the landuse of a a territory considering physical, social and economic aspects. In the frame of the POT's upgrading, the risk management plays an important role in conservation of human lives, prioritization of territory's landuse as well as the formulation to reduce the fiscal vulnerability of the territorial institutions when a disaster occurs e.g. landslides. Landslides represent a rampant danger in Bogota's hillside area because of accelerated urban growth, steep topography, low quality materials and abundant rain among other factors. It is calculated that more than 3 500 000 people live in such risky zones.

This paper presents the methodology followed to obtain a landslide hazard map -which will be in force in 2017- produced by an interdisciplinary team formed by geologists, geotechnical and GIS specialists.

Conveniently, Open Source and commercial software was used: since the study area covered a considerable part of Bogota's urban region 16 000 ha, the vast volume of information demanded a quite efficient and robust software. Thus, GRASS GIS software was used to carry out many geoprocessing tasks, while automation of some geoprocesses was implemented with commercial software. The methodology used consists of the combination of two partial results, the first one regarding to susceptibility and triggering variables affecting the hillside stability while the second had to do with stability of natural slopes.

To obtain those variables, geoprocessing was performed and in some cases very specific geomorphology algorithms, such as Terrain Classification from SAGA GIS, were used. At the end, map algebra was applied to combine them. Furthermore, stability of natural earth slopes was analysed with the support of hydrological modelling in GIS. From this new hazard map, civil works for disaster mitigation will be performed or resettlement of affected people will be recommended.

1 Introduction

The current Plan de Ordenamiento Territorial (POT) of Bogota and its corresponding landslide hazard map were released in 2000. The dynamic of the landscape due to natural and human events lead to an imperative necessity of updating the landslide hazard map of Bogota. For configuring the new map a high resolution DEM was used as one of the most important inputs. In addition, orthophotos and Google Earth were reviewed. Conversely, specific open source was used to carry out some geoprocessing tasks yielding more precise results. The current hardware capacity eased the work allowing producing a map in a short period of time.

Moreover, hydrological modelling granted a more accurate slope's family delimitation and a Visual Basic (VB) application developed to find the main inputs for the Slopes Natural Methodology (MTN) made the process expedite and provided reliable results. Utilisation of the same methodology used 18 years ago, allowed accomplishing a comparison between the old map and the new map. With the results the factors that more significantly influenced the method can be distinguished.

The resulting map is derived from a model that takes into account different factors and combines statistical with probabilistic methods. Like in every model a simplification of reality is made selecting the most relevant aspects that affect an event in this case stability of slopes. An appropriate way for validating the model is comparing the known hazard levels of morphodynamic processes located in the study's area with those ones yielded by the map. If they produce an acceptable level of adjustment, the model will give satisfactory results and will be adopted.

In the context section some aspects that affect the stability of hillside in Bogota are described. Virtues of Open Source and commercial software are addressed. In the methodology section an overview of both methodologies implied in the model is given. The risk management component highlights the dynamic inherent to the hills stability and therefore the requirement to constant monitoring. Contrasting map section set out the criteria used to combine the partial map results. Finally, implications of this study are briefly explained.

2 Software and geoprocessing

2.1 Format vector

Vector format was used for addressing the geographical processes, since it was necessary continuously to verify the partial results obtained when summing up the different features. Likewise, it was necessary to check more than an attribute or characteristic of specific areas in order to prove that the method provides proper results. This procedure is not possible in raster type data.

Furthermore, most of the information was given in vector format; therefore not conversion of data was required.

2.2 Automation and software

In the project, commercial software and open source software were available. For executing combinations of layers, GRASS was used exploiting its efficient performance. Some others processes implemented in GRASS are described subsequently.

2.2.1 Topology fixing

Since vector format was mainly used, there were topology issues. To overcome them, the topology nature of GRASS GIS was exploited. Automatic corrections of topology errors are possible to be done with the Clean Vector Map module of GRASS. In this way GRASS becomes a useful tool; manual repair would have been done in absence of it. Correction of topological errors should be made carefully. For example, when land use layer is corrected, aerial images can be checked to guarantee a matching to the correct land use polygon.

2.2.2 Smoothing

Combination of many layers results in small angles and unpleasant forms in some cases, thus, smoothing process was essential. Performance with commercial software was not optimal since the polygons shape was rounded without conservation of topology, which bring about a dataset of unconnected polygons. For smoothing the final results the Chaiken algorithm from GRASS –which can be found under the Topology Maintenance menu- was implemented yielding quite acceptable results.

2.2.3 Watersheds basins

Accomplishment of watersheds delimitation was executed with GRASS, which provided efficient results. Other software may be sensitive when the size of exterior watershed basin is small e.g. 1000 Ha. Those watersheds might present an unpleasant delimitation which would not obey the terrain forms providing inaccurate results.

2.2.4 Automation

When automation of processes was necessary e.g. figures production, routines programmed using the ArcPy module from ArcGIS as well as Model Builder models were implemented. These tools are friendly and ease to use.

Model Builder iterating virtues were utilised. Later on, in the MTN methodology there is a practical situation where a simple model was developed for separating a dataset in subdatasets depending of a name of each one. (Figure 5).

3 Context of landslides in Bogota

Bogota is located in the geographic centre of Colombia, in a east Andes mountains plateau, to 2630 m above sea level, with a 177 598 ha area. It is formed by 20 regions, its population according to estimates exceeds 8 080 734.

From the physical perspective, Bogota is formed by two important terrain zones. The first one is a flat zone located in the central and north western part where the population majority live. There the terraces and alluvial valleys of Bogota River and its affluent and wetlands are predominant. The second zone is mountainous and frames the city in the south and eastern side. In this zone the East Hills (Cerros Orientales) are important. (Adapted from Comunidad Andina, 2009)

Accordingly, and due to its hydro-meteorological, geological, geotechnical characteristics, the mountainous zones as well as the flat ones are constantly under natural processes of transformation where the terrain forms change because of frequent precipitations, erosive action of water curses and susceptibility of rocks and soils when these are disintegrated and dragged. In addition, inadequate human interventions contribute to the occurrence of different type of landslide phenomena and flooding. (Adapted from Comunidad Andina, 2009)

The mentioned phenomena are considered hazardous. The ridges belonging to the Bogota's Hills have a natural susceptibility to landslides due to its geology and geomorphology. In addition, human intervention has an impact: the operation of quarries as well as the use of territory for construction of houses without the fulfilment of minimal requirements. (Adapted from Comunidad Andina, 2009)

It is important to mention, that Bogota is - according to the Colombian Code of Seismic- Resistant Constructions- located in an intermediate earthquake zone. Furthermore, the city has soils with potential zones of seismic waves' amplification, others with liquefaction, others are expansive and some of the constructions are too vulnerable to earthquakes effects. In the city, landslides are produced along the ridges as well as in its foothills' strips: East Hills, South Hills, Suba (region located in Northwest of Bogota). (Adapted from Comunidad Andina, 2009)

Bogota's climate has an impact in life of Bogota`s inhabitants and causes important economical losses. The city is situated in the Intertropical Convergence Zone (ITCZ) which has influence in the rainwater regime. Additionally, the variability reflected in intensity, frequency or magnitude is due to Global Climate Change and cold and hot phenomena of Pacific Ocean "El Niño" and "La Niña". The ITCZ leads to two periods of intensive rainfalls: the first one in months of March, April and May; the second one during the months: September, October and November. During these periods there is a significant coincidence in the increase of landslides reports. (Adapted from Comunidad Andina, 2009)

4 Procedure and methods

Threat zoning landslide investigations aim to the importance of tackling a combination of methodologies which are supplemented. A complete inventory of processes of instability of study region should be present as well as a completed geomorphologic characterization. Statistic, deterministic or probabilistic methods should be considered in the landslides analysis in accordance to the Colombian law.

The method used should allow a comparison to the current landslide hazard map, additionally there was existing information that could be upgraded and also, human factor must have been considered. This could be accomplished by mean of using SES method. (Sistema cuantitativo de evaluación de estabilidad acronym in Spanish. In English Stability Evaluation Semicuantitative System). This heuristic method has the disadvantage of being subjective. Hence, an additional method is used MTN (Método de taludes naturals acronym in Spanish. In English Natural Slope Method). The process followed to obtain the landslide hazard map of Bogota 2016 is illustrated in figure 1.

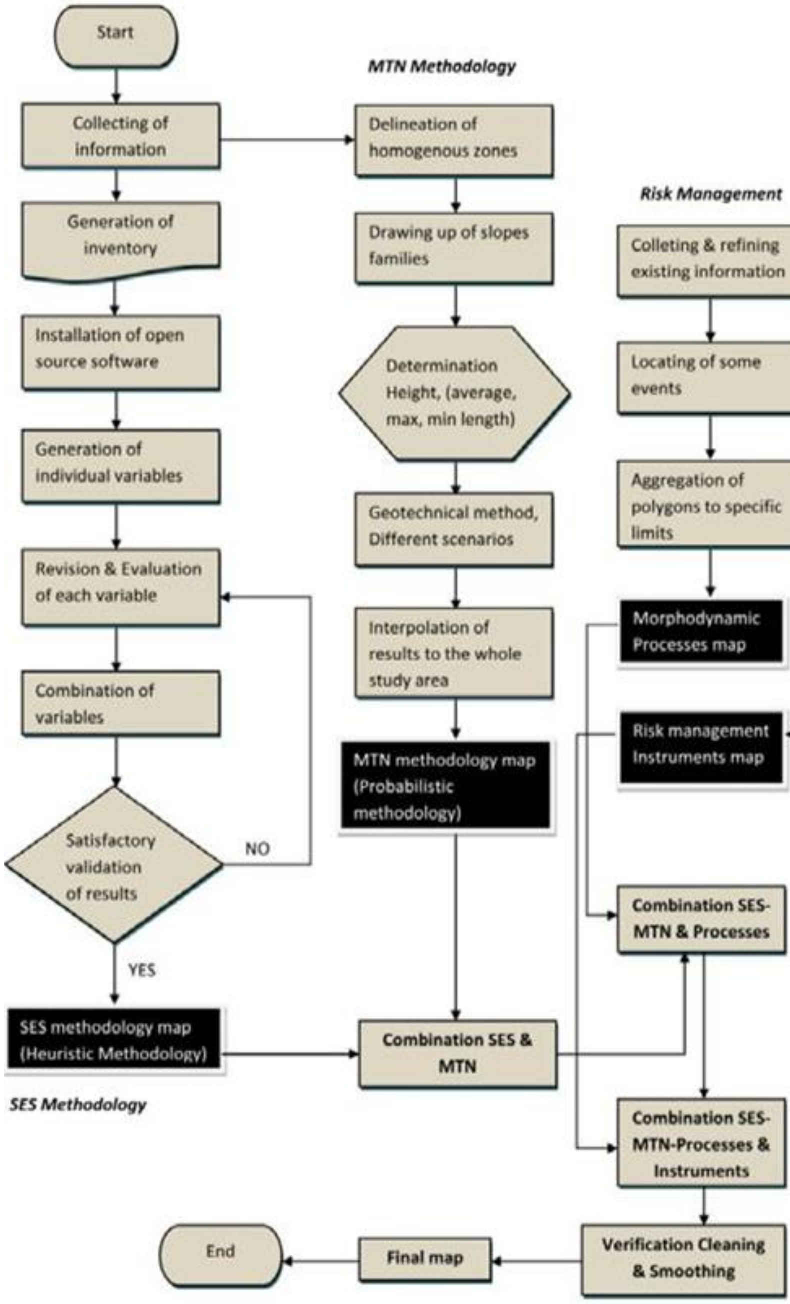

Figure 1: Landslides Hazard Map Procedure

4.1 SES Methodology

The SES methodology is a heuristic method based on categorizing and weighting of factors causing instability according to the expected influence of these in the occurrence of landslides. Such methods are known as indirect, and its results could be extrapolated to regions without landslides with a similar combination of factors, taking into account adequate expertise.

4.1.1 Description of methodology

The methodology uses eight variables grouped in 2 categories, the first one is related to the intrinsic conditions of terrain: material, terrain condition, drainage and landuse, the second group associated to triggering factors: climate, earthquake, erosion and human factor. The figure 2 shows these variables and the main inputs for each one.

In the methodology followed in 2000 eight parameters are assessed (Figure 2). These parameters give particular stability conditions, defining homogeneous zones that can be calibrated with the landslide processes.

A layer that depicts each variable is configured, in which variability intervals are assigned according to its influence to landslides stability. To study and retrieve a map from each variable a group of specialised professionals worked in gathering and preparing information. To visualise and geoprocess the information, the free and Open Source QGIS was used.

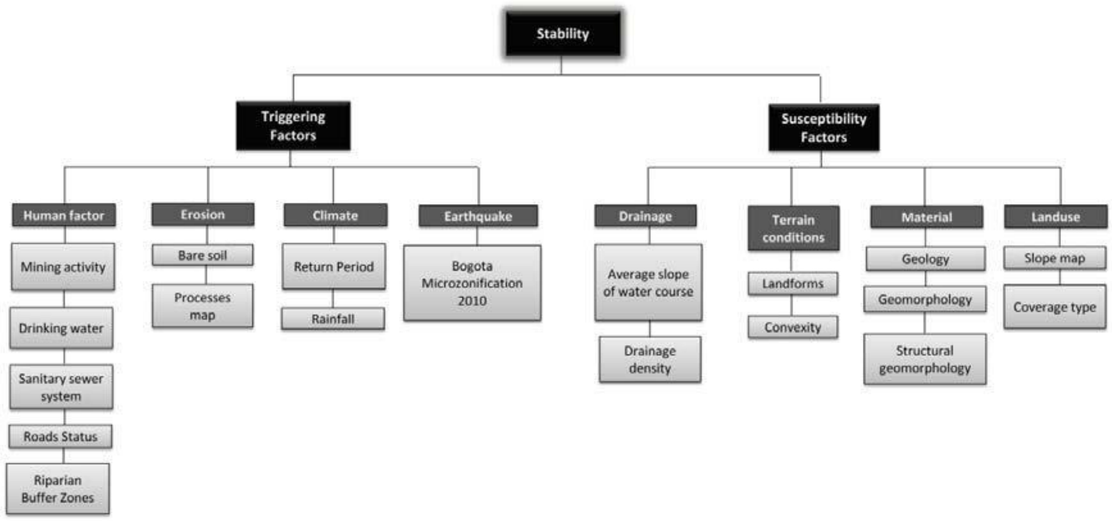

Figure 2: Variables of SES Method

The combination of the different factors in each parameter and the sum of the rating from each one, result in a stability rating (SR) from where a level of relative hazard can be defined. Stability can be expressed as the sum of ratings

SR=Human Factor +Erosion +Climate+Earthquake +Drainage +Terrain condition +Material + Landuse

For assessing each variable combination of vector information was tacked or in the case of landuse coverage vector was converted to raster to be then combined with the slope map. Terrain condition parameter will be explain with a higher level of detail.

4.1.2 Terrain conditions variable

Stability conditions are associated to morphometric characteristics and morphodynamic processes. In the analysis, slope as well as convexity were necessary to evaluate. To get this variable the algorithm Terrain Surface Classification from

SAGA GIS was used. The difference in terrain condition variable is evident -when comparing with this one from the previous study- since the landforms obtained with the algorithm depicts the terrain landforms with a much higher level of detail. The algorithm takes into account the DEM (a 5 m resolution DEM), slope, convexity and texture. (See Figure 3).

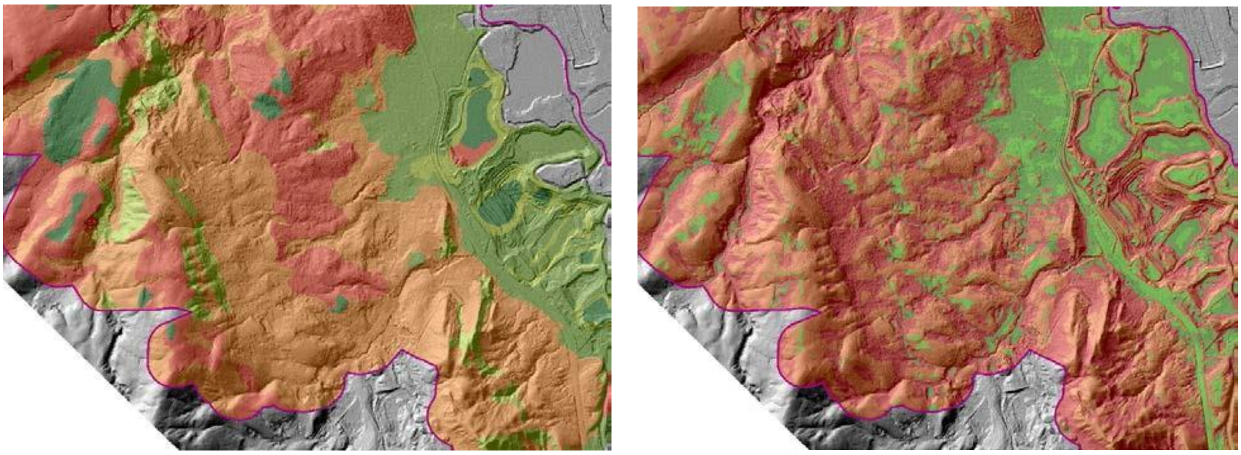

Terrain condition previous study

Terrain condition current study with SAGA GIS

Figure 3 Comparison Terrain condition variable

4.1.3 Final result of SES methodology

The result of combining triggering with susceptibility factors (see figures 9 and 10) give a final stability result, where the rating were made based on probabilities taking into account a normal distribution (Figure 4). Important to note is the higher a value is, the better is its behaviour. The media and standard deviation were 166.671119 and 20.634558 respectively. The results for categorizing the SES method are shown in table 1.

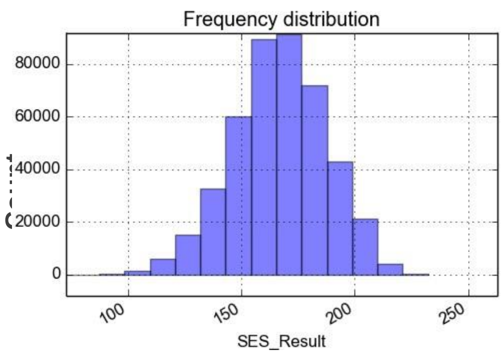

Category	Symbol	1998	POT 2016	Ranges
Very High	VH	126	125,4	SR < 125,4
High	H	151	146,0	125,4 < SR < 146,0
Medium	M	157	**166,7**	146,0 < SR < 187,3
Low	L	177	187,3	187,3 < SR < 207,9
Very Low	VL	202	207,9	SR > 207,9

Figure 4 Frequency distribution of SES methodology result & Table 1 Ranges of SES methodology, 1998 result and 2016 update result

4.2 MTN (Método de Taludes Naturales) Methodology

For the MTN accord to the previous study the basic principle consisted in a measurements family of the H values and its correspond length (both measured in m) applied in segments of a mountain composed by homogeneous materials regarding to origin and composition. These are related by mean of the functional basic equation:

$$H = A\,L^{b} \qquad (1)$$

Where H and L are height and length respectively. A and b are constants in a potential regression equation. The parameter b can expresses convexity of the region.

Homogeneous zones are the starting point for determining the slope families. In each homogeneous zone it is required to estimate a dataset of heights and lengths of slopes to establish a potential type regression which defines each family. The delimitation is a crucial task in the methodology. An acceptable family definition, presents excellent performance in the potential regression correlation with a value of R>0.95

Delimitation of slopes families was achieved using hydrological modelling: small watershed units which in turn would be intersected with the synthetic rivers or accumulation rivers representing as a result very homogeneous zones. Here is important to mention that despite that the fact homogeneous areas were found after evaluating the regression for each family should be discarded because of R<0.95, which emphasized again how sensitive is the method and how important is an adequate delimitation process.

Once the similar zones are defined the measurements should fulfil the following requirements (See figure 6):

- The measurements start in inferior contour line.
- The interval between the inferior contour and the next one located immediately in superior level should evaluated. Only the perpendicular distances between both intervals are calculated.
- Afterwards, the arithmetic average should be measured, which correspond to the distance or average distance.
- Three distances should be registered: average, maximal and minimal lengths.
- For the next measurement the starting point is again the inferior contour line, but this time two contour intervals should be covered.
- The procedure should be repeated until all the intervals between the inferior contour and the superior height are covered.
- The family of natural slope is formed by a main slope (the longest one) and the other slopes. (See figure 6, main slope 2814_2).

The assignment described above for taking the measurements would be cumbersome if it was made manually since the families have different sizes and covered different number of contour lines. Therefore, an application in Visual Basic was programmed. Initially the coordinates for yielding the distances were separated by family, using a model in Model Builder which iterates and groups according to the name's family. (In figure 6 name family is 2814). That model is shown in figure 5.

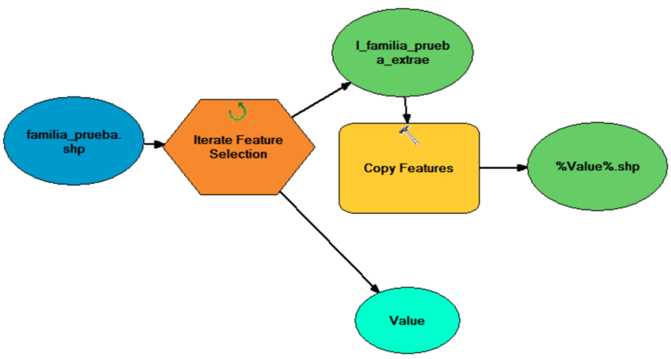

Figure 5 Separation of coordinates by families

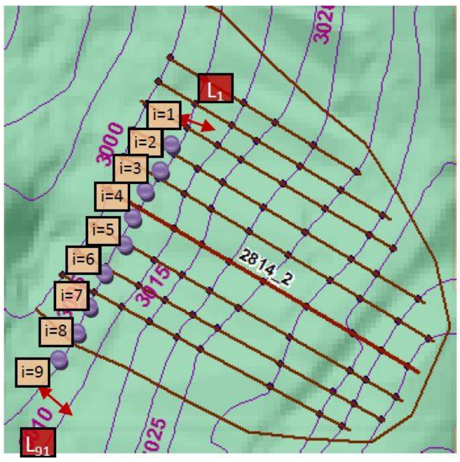

Figure 6 Slope family and its distances

These groups of coordinates would the input in the VB application. The principle for determining the distances is illustrated in figure 6. Average distance is calculated with the following equation:

$$L_5 = \frac{\sum_{i=1}^{n} L_{ir}}{n}$$

where

L_5=Average length in a 5m height

L_{ir} = Distance from the inferior contour intersections (represented in purple in the figure 6) to the next contour intersections (first measurement)

n= Number of slopes that formed a family, in this case n=9

Table 2 shows the result for the slope family illustrated in figure 6. Here the utility of the VB application is evident since this family has 9 slopes which intersect with the contours 79 times.

To find the distances the Euclidean distance formula is used:

$$d= \sqrt{(x_p - x_i)^2 + (y_p - y_i)^2}$$

Where x_p e y_p are the inferior contour coordinates, x_i e y_i are the analysed contour coordinates, d= distance.

For the final result the application yields a summary table with average, maximum and minimum length for the whole number of delineated families. For each family a similar table like this showed in table 2 was calculated. These results are the input for the posterior complex geotechnical analysis and study.

H-2814	Average-2814	Maximum-2814	Minimum-2814	Length-2814
5	7,33356147	8,98440664	5,44836937	L1
10	14,1675147	16,0439931	12,5635029	L2
15	19,8772509	23,0041568	18,253848	L3
20	27,4256795	31,3201408	24,2235138	L4
25	35,0314211	40,6715744	29,0876877	L5
30	45,0626193	48,5720247	41,9799049	L6
35	53,3672421	54,7080691	51,4844678	L7
40	59,351225	61,5365003	58,0367608	L8
45	65,0611987	66,3068185	64,5787205	L9

Table 2 Measurements summary for family 2814

These values are given as input to a geotechnical program. Some processes are executed where a set of different scenarios like seismic effect, rain plus seismic, and different periods of time (long, medium and short) are analysed. This procedure aims to get Safety Factors (SF) that evaluates the slope stability for each family. In the general scenario a total SF is found. These factors are assigned to the centroid, and both ends of the main slope (See figure 6) for interpolation effects.

4.2.1 Evaluation of MTN

SF	Values
Minimum	0.15733952
Mean -1σ	0.38578301
Mean	0.97912966
Mean+1σ	1.5724763
Maximum	3.56908764

MTN Hazard	1998 Values	2016 Values
VH	total_SF ≤ 0.60	total_SF≤ 0.50
H	0.6< total_SF ≤ 1.1	0.5< total_SF ≤ 1.1
M	1.1 <total_SF ≤ 1.9	1.1 < total_SF ≤ 1.7
L	1.9 < total_SF ≤ 3.4	1.7 <total_SF ≤ 2.3
VL	total_SF > 3.4	FS_total > 2.3

Table 3a Intervals for MTN hazard level selection &Table 3b Levels of hazard MTN methodology

From the safety factors, statistical parameters are obtained. In this way, the intervals for determining the different hazard levels (From very low to very high) are obtained. (See Table 3a).

With a standard deviation of 0.59334664 intervals are defined, where a mean value SF =1.1 (value used in the previous study this one from 1998) gives a better adjustment than this one from 2016, therefore 1.1 was used as mean. The values to define hazard intervals are shown in table 3b.

4.3 Risk management

Apart from these to partial results, SES and MTN risk management component was considered in landslide map preparation. Instruments and processes were included.

4.3.1 Instruments

The risk management instruments include different types of technical concepts which evaluate hazard for improving and updating the given information in the normative plan (POT). Thus, for assessing hazards the starting point is the hazard given in the landslide map. Additionally, existing information from previous studies and diagnoses accomplished in the area should be collected.

Relevant information can cover geological units, geomorphology, active or potential processes morphodynamic processes, and drainage characterization.

Furthermore, information regarding to land use, and triggering factor like precipitation, human factor (cut and fillings, runoff and superficial water management) and seismicity is included.

Field work should be done to verify physical conditions of the sector under study. There, landslides susceptible zones are delimitated and finally the hazard is defined.

4.3.2 Scales compatibility

Since the risk management instruments are generated to provide a mayor level of detail, it is found that the scale of the existing instruments were not compatible with the scale of the landslides hazard plan (1:5000). The detailed concepts can be yielded in a 1:500 or 1:1000 scales, thus, the input entities could not be depicted individually. To reduce the scale of these polygons a concave hull can be drawn around them. This can be done with the aggregation polygons tool of ArcGIS or with the Convex Hull tool from QGIS as illustrated in figure 7.

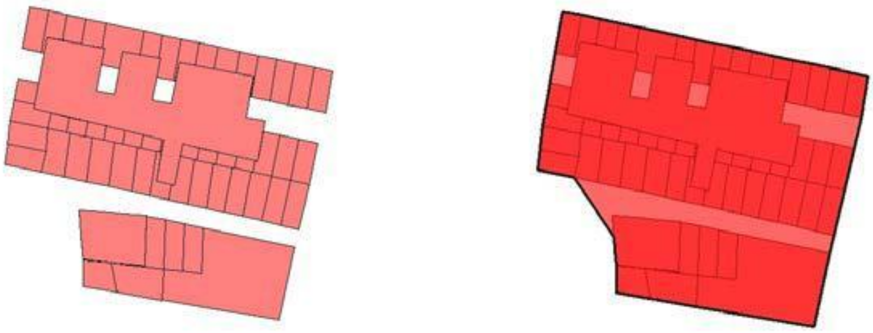

(a) (b)

Figure 7 Aggregation of risk management instrument polygons. (a) Individual lots. (b) Individual lots after being grouped

4.3.3 Processes

For preparing a processes inventory the initial point is to evaluate the morphodynamic processes; those which are active are considered to have high hazard. A landslides inventory collects information regarding to geographic distribution, intensity, magnitude, current status and failure mechanism of these ones. This information is used in zoning hazard processes, mainly in parameters definition and variables to use and in rating and calibration of zoning maps.

Depending on the identified activity from each process, a qualitative probability was assigned, the table 4 shows the process type and its corresponding probability.

Process	Probability
Active process	Very high
Incipient process	High
Colapsed process	Medium
Stabilised process	Low

Table 1: Hazard according the probability of processes

4.4 Contrasting of maps

Having obtained the inputs: hazard maps for the SES and MTN methods with 5 categories of hazard (Tables 1 and 3), map of instruments of risk management with 3 categories (High, Medium, Low) and processes map with 5 categories, the following procedure was executed:

- **a)** Elaborating of different overlapping models with different levels of conservatism taking into account the intervals to define the hazard levels in tables 1 and 3 (1998 and 2016 values). Four combinations were resulting, from them the more appropriate combination was chosen. The SES and MTN maps selected for obtaining the final map are shown in figure 11a and 11b respectively. (See below Models, section 4.1.1)

- **b)** Assignation of probabilities of failure.

4.4.1 Models

To validate the adjustment of the different combinations a special tool was used: that calculated the percentage of coincidence between the hazard yielded by the combination SES+MTN and hazard of processes which was known. A higher percentage of coincidence was the criterion to decide the winner combination.

At the beginning the matrix 1 (See table 5) –that overlaps SES and MTN-was tested where Very high hazard (VH), High (H), Medium (M), Low (L) and Very low (VL). However when the results were validated with the processes map the adjustment was not satisfactory. Likewise a second adjusted matrix was applied. (See table 5, matrix 2).

Once the resulting overlapping maps from performing the matrix 2 were depicted, it was found that for slopes <10° and >45°, this overlapping did not provide an acceptable performance. The MTN methodology is applicable in zones different from this range. This limitation of the methodology is currently being studied. Consequently, for this slope range the matrix 3 was applied (table 6), in which the SES methodology has preponderance. The resulting map after applied this matrix is illustrated in figure 11c

Afterwards, the processes layer was overlapped with the selected combination MTN-SES using the matrix 4. (Table 6)

The result from matrix 4 was then overlapped with the instruments of management risk. Since the processes having high threat must have entire predominance over the whole information, the result MTN-SES-Processes-Instruments was then overlapped with high hazard processes returning the final landslide hazard map of Bogota (Figure 11d)

		SES				
	CAT	**VH**	**H**	**M**	**L**	**VL**
MTN	**VH**	VH	VH	H	H	M
	H	VH	H	H	M	M
	M	H	H	M	M	L
	L	H	M	M	L	L
	VL	M	M	L	L	VL

(Matrix 1)

		SES				
	CAT	**VH**	**H**	**M**	**L**	**VL**
MTN	**VH**	VH	H1	H2	M1	M2
	H	H1	H2	M1	M2	M3
	M	H2	M1	M2	M3	L1
	L	M1	M2	M3	L1	L2
	VL	M2	M3	L1	L2	VL

(Matrix 2)

Table 2: Matrix 1 Conservative Matrix SES-MTN Matrix 2 Adjusted Matrix SES-MTN

MTN \ SES					
CAT.	VH	H	M	L	VL
VH	VH	H	M	L	VL
H	VH	H	M	L	VL
M	VH	H	M	L	VL
L	VH	H	M	L	VL
VL	VH	H	M	L	VL

(Matrix 3)

MTN+ SES \ PROCESSES				
CAT.	VH	H	M	L
VH	VH	VH	VH	VH
H	VH	H	H	H
M	VH	H	M	M
L	VH	H	M	L
VL	VH	H	M	L

(Matrix 4)

Table 6 Matrix 3 10°>slopes >45 & Matrix 4 SES-MTN & processes map algebra

5 Impact and results

Landslide hazard levels resulting from the new map are depicted in figure 8. The graphic illustrates the dominance of the level of hazard type medium with 64%, which indicates that for a considerable part of the studied area more specific studies must be developed when a construction project is scheduled.

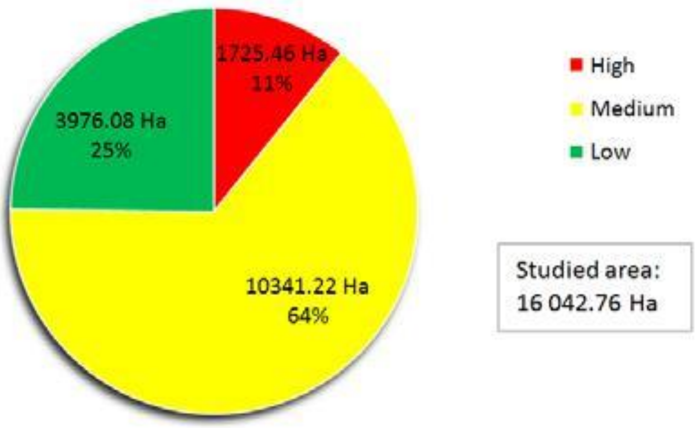

Figure 8: Landslides hazard map pie

This map has an impact in development of Bogota. It is said that risk management is development management. From this map, new suitable areas for housing projects can be defined. When a project is located in low landslide hazard, specific zone's studies are not needed.

Success of risk management depends on continuous monitoring of likely zones to suffer a landslide. Special attention should be paid to areas characterized in the map as high and medium threats. Since stability conditions are based on diverse triggering and susceptibility factors, the hazard levels are dynamic, therefore new specific studies should be performed. Hence, this map cannot be interpreted as a definitive map of landslides hazard.When comparing with the previous map hazard levels obtained in 1998, changes in hazard levels can be attributed to the following reasons:

Updating in inputs like seismic acceleration periods (input used in earthquake variable) or inclusion of new climatic stations (input used in Climate variable) could bring about a hazard level can suffer improvement (for example high to medium) or worsening (low to medium).

In addition, reforestation and clean of colluvial deposits could have contributed to improve conditions. Inclusion of risk management instruments could have generated more precise results regarding to hazard zoning.

Mitigation measures have an influence in hillside changing geomorphology when housing projects are constructed which improve existent conditions. In addition, human factor plays an important role in stability of slopes, changing the previous conditions.

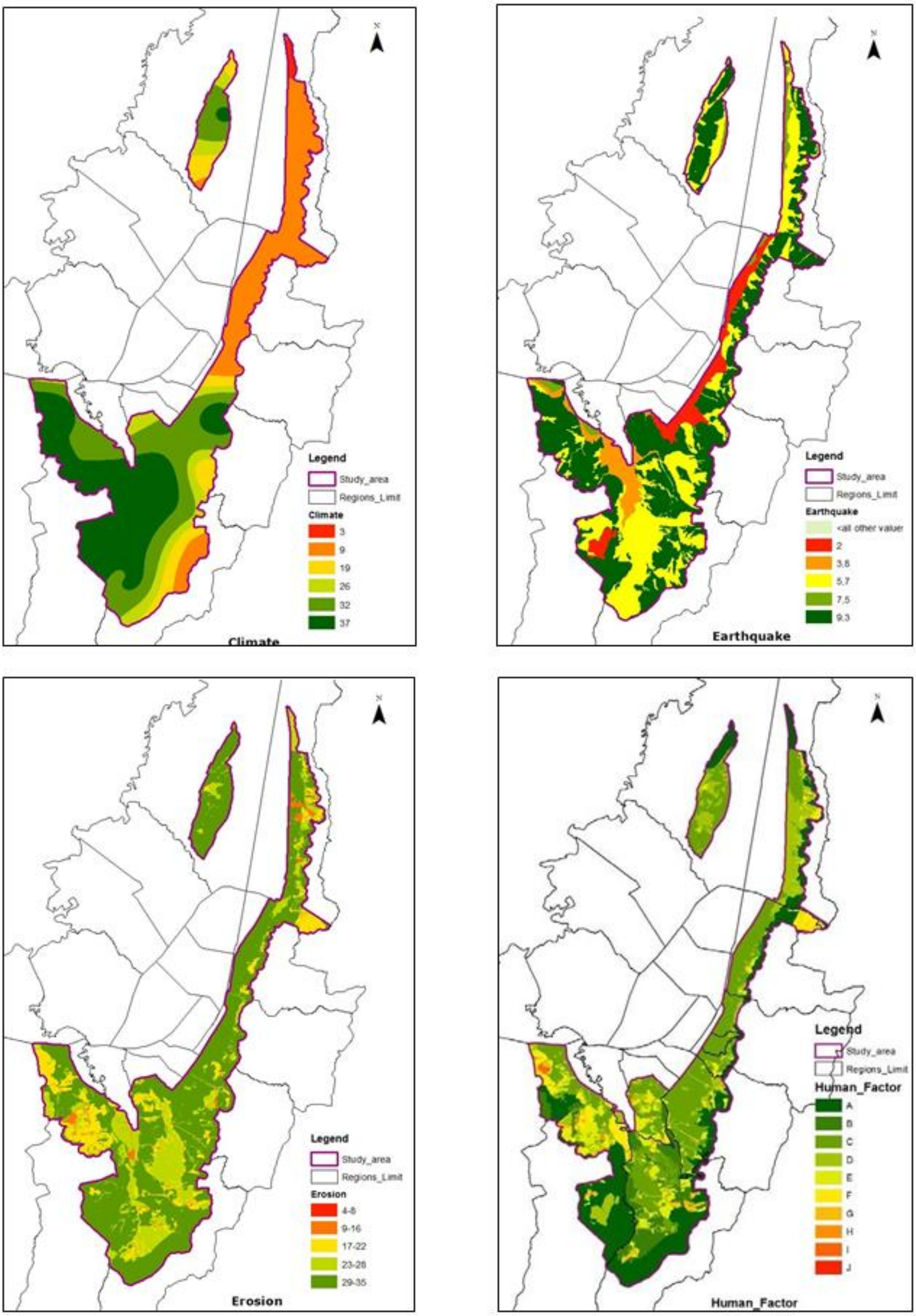

Figure 9: Triggering variables

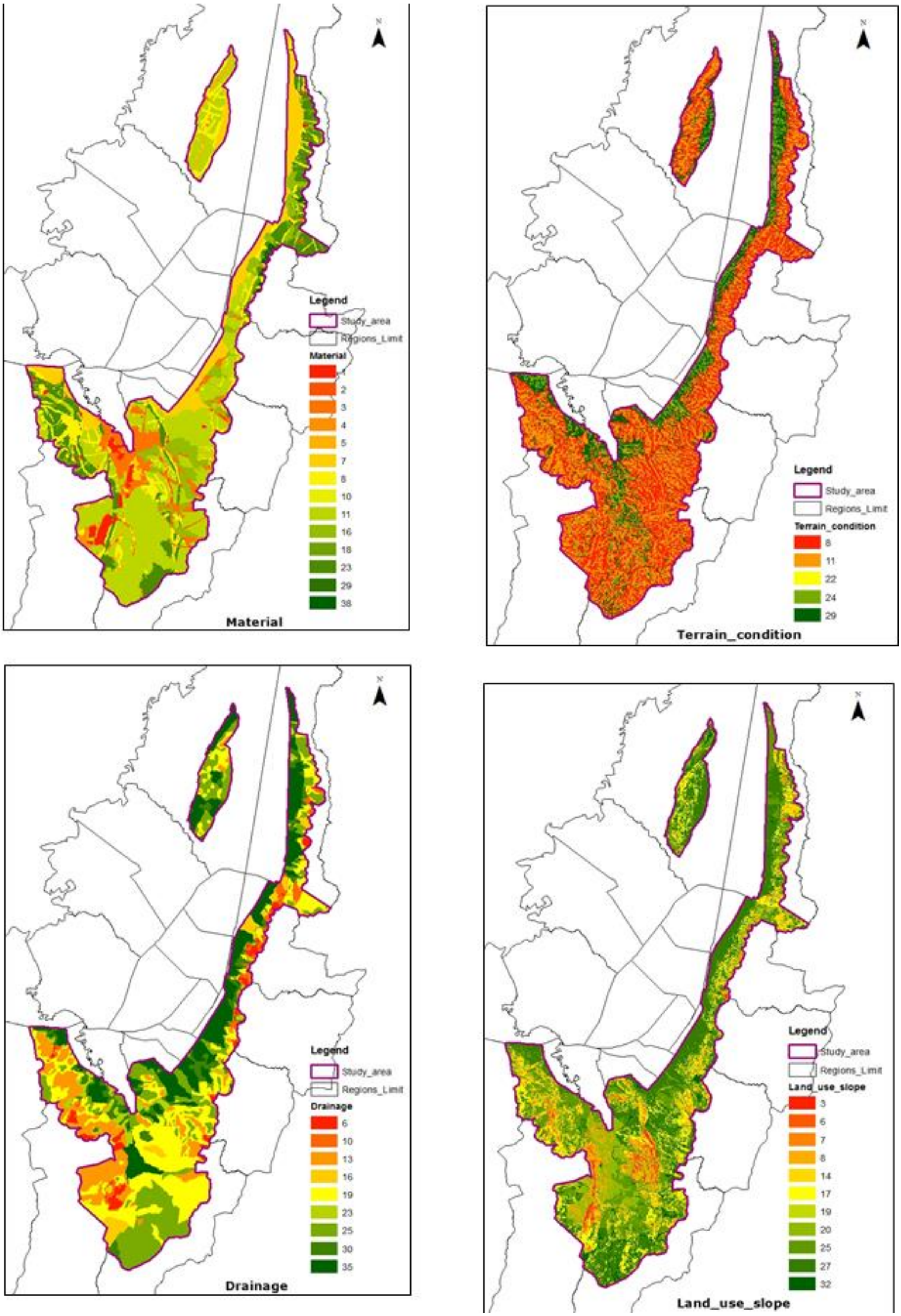

Figure 10: Susceptibility variables

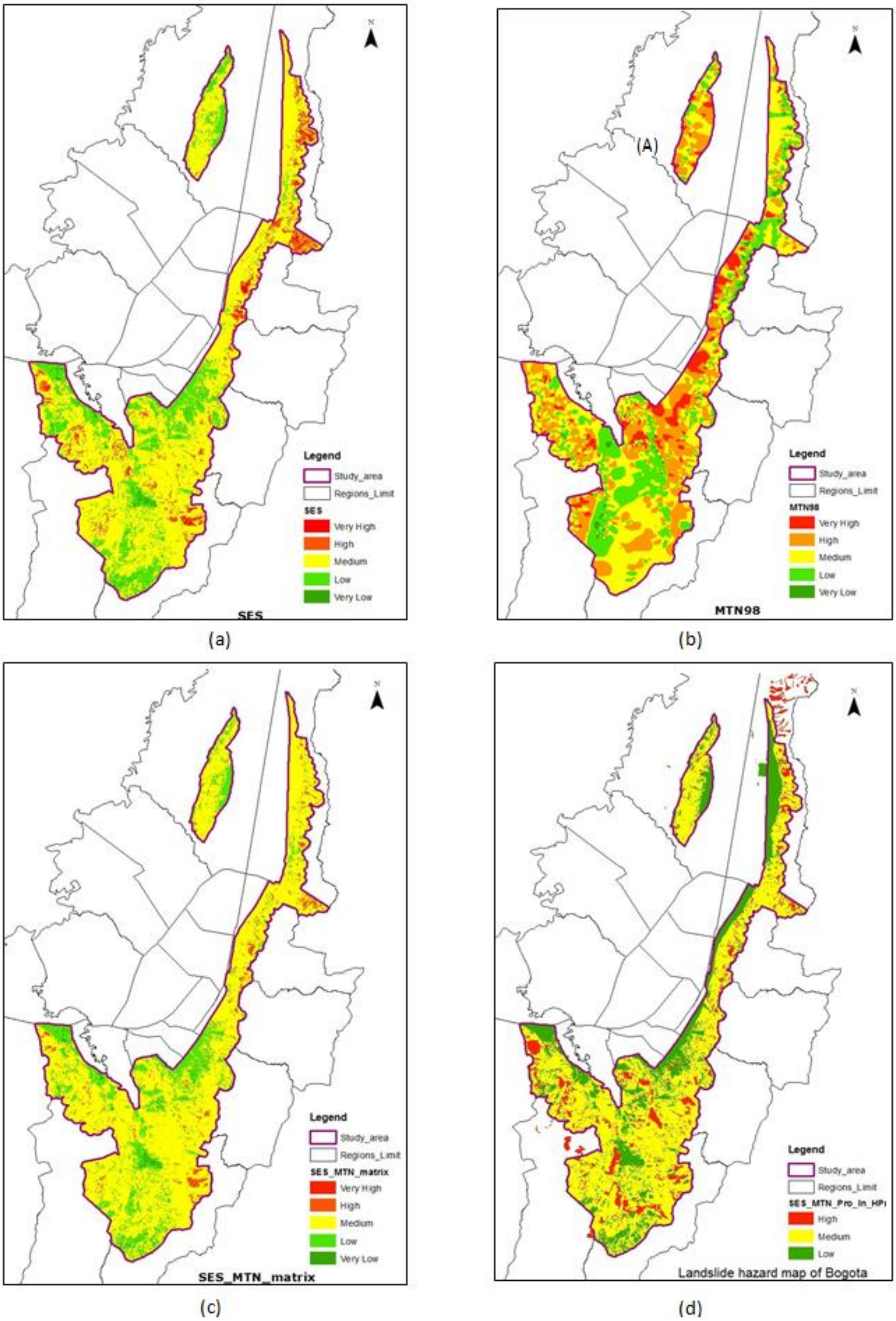

Figure 11: Results (A) SES Methodology, (B) MTN Methodology, (C) SES_MTN combination using matrix 2, (D) Final approach after combining SES, MTN, Processes, Instruments and verifying high threat processes

6 Conclusions

The SES approach has inherent subjectivity criteria because of weighting assignation. To compensate this flaw the probabilistic approach MTN was used, retrieving quite acceptable results when both approaches are combined. Validation of the results was based on the morphodynamic processes whose hazard has been studied in detail and were known beforehand. The landslide hazard map helps to have in a quick and easy way a glimpse about the level of hazard in a location according to the map scale production 1:5000. Conversely, specific and detailed studies should been developed when a finding is detected in monitoring process. Moreover, such studies should be conducted when a construction project will be executed.

In processing of large volumes of geographical information other alternatives different from commercial software should be explored since in many cases they offer a better performance e.g. GRASS GIS. Although GRASS GIS is arcane its power makes it worth to be used.

It cannot be expected that the resulting location of the different hazard zones retrieved in a model is infallible. It should be taken into account that a model means a simplification of the reality and in this process, it is possible that some variables cannot be modelled. In addition, special attention should be paid to the scale 1:5000 which means that the minimal unit to be included in cartography was 400 m thus features smaller that this value are discarded.

References

Alcaldía Mayor de Bogotá D.C. (2010). Decreto 523 de 2010. Microzonificación Sísmica de Bogota D.C.

Comunidad Andina. (2009). Prevención y reducción de riesgos a través de los instrumentos de planificación territorial en Bogotá – Colombia. Serie Experiencias significativas de desarrollo local frente a los riesgos de desastres. Lima.

Cruden, D. M., & Varnes, D. J. (1996). Landslide types and processes. In K. Turner & R. L. Schuster (Eds.), Landslides investigation and mitigation: Washington D. C, National Academy Press, Transportation Research Board Special Report 247 (pp. 36–75).

Dirección de Prevención y Atención de Emergencias - DPAE. (2006). Documento Técnico de Soporte – Plan Distrital de de Prevención y Atención de Emergencias – PDPAE. Bogotá, D.C.

Dirección de Prevención y Atención de Emergencias - DPAE. (2008). Instrumentos para la gestión del riesgo en Bogotá. Bogotá, D.C.

Hungr, O. (2016). A review of landslide hazard and risk assessment methodology. In S. Aversa, L. Cascini, L. Picarelli, & C. Scavia (Eds.), Landslides and Engineered Slopes. Experience, Theory and Practice Proceedings of the 12th International Symposium on Landslides (pp. 3–27). Napoli, Italy.

IDIGER. (2016). Diagnóstico para Fase Preliminar - Proyecto de Actualización del Componente de Gestión del Riesgo para la Revisión Ordinaria del Plan de Ordenamiento Territorial de Bogotá D.C. Bogotá D.C.

IDIGER. (2016). Amenaza por movimientos en masa documento técnico de soporte. Actualización del POT

INGEOCIM. (1998). Zonificación por inestabilidad de laderas para varios sectores de Bogotá. Bogotá D.C.

Shuk E., T. (1990). La Evolución y el Estado Actual de la Metodología Basada en Taludes Naturales para Análisis de Estabilidad en Masas de Materiales Geológicos. In Parte I-III – CSMR—SVMSIF. Caracas.

Soeters, R., & Van Westen, C. J. (1996). Slope instability recognition, analysis and zoning landslides Investigation and Mitigation. In K. Turner & R. L. Schuster (Eds.), Landslides Investigation and Mitigation; Transportation Research Board, Special Report 247 (pp. 129–177). Washington D. C.: National Academy Press.

Varnes, D. J. (1978). Slope movements types and processes. In S. R. & Krizek R. (Eds.), Landslides analysis and control - Transportation Research Board Special Report 176 (pp. 9–33). Washington D. C.: National Academy Press.

Exploring the Potentials of UAV Based Geo-Spatial Data Acquisition in Urban Environment: A Case study in Dhaka City, Bangladesh.

Labib S M[a,*], Md. Z. H. Siddiquee[b], Md. Shafiqul Islam Khondoker[c], Md. Sayfullah[d]

[a] SEED, University of Manchester, United Kingdom, labib.sm@postgrad.manchester.ac.uk;

[b] Institute of Water Modelling, New DOHS, Mohakhali, Dhaka-1206, Bangladesh, zhs@iwmbd.org;

[c] Institute of Water Modelling, New DOHS, Mohakhali, Dhaka-1206, Bangladesh, sik@iwmbd.org;

[d] AplombTech BD, Bangladesh., md.sayfullah@aplombtechbd.com

KEY WORDS: UAV, Geo-spatial data, Urban Planning, DTM, Remote Sensing

ABSTRACT:

The usage of Unmanned Arial Vehicle (UAV) is undoubtedly very potential as well as very rapidly growing geospatial data acquisition method with disruptive role in the domain. The main focus of this research is to utilize an indigenous Quad-Copter to acquire spatial data in complex urban environment with a view to illustrating the potential using UAV data in urban planning and management activities including utility services. The study was conducted in a dense area of Dhaka city, the capital of Bangladesh. The process started with using an indigenous quad-copter; in this case, Mission-planner has been utilized to prepare a flight path for the UAV. After conducting the flight, extensive image processing has been operated, through synchronization of images, registration of the images, bundle block adjustment. For image processing and further extraction of data, Pix4DMapper and Correlator3D have been utilized. Moving forward, the processed images are used to prepare DTM, DSM, Orthographic images, and 3D point clouds. The process provided the data that are essential for several urban planning operations; such as Land Use planning, extracting urban volumetric data, extraction of vegetation structure, and common uses of DTM and DSM. The unique features of the UAV data for Dhaka is highly accurate, as Dhaka is mostly built us unplanned city, the urban fabric is very complex to extract data from medium or semi-high resolution optical satellite images. The UAV data used in this case study has provided 5cm resolution for orthophoto, planimetric accuracy of 2 cm and height accuracy of 5 cm. This study seems to be very effective with special regards to time and cost saving with a significant improvement in data quality. This effort also helps us to overcome the limitations of cloud cover, spatial and temporal resolution of optical satellite images.

1 Introduction

Unmanned Aerial Vehicles or UAVs are fast becoming an immensely important medium of data collection for GIS and remote sensing works. Mainly originated for military purpose, now UAVs have been widely used for many multidisciplinary activities. In particular, for acquiring geo-spatial information in complex environment, UAVs play a vital role by ensuring accuracy, fast processing, smooth operation and personalized data acquiring method (Siebert & Teizer, 2014; Lari & El-Sheimy, 2015). In the era of digital revolution, UAVs are frequently used to acquire high resolution aerial photographs, different sensor imagery (i.e. hyper-spectral), real-time spatial data (i.e. traffic movement) and much more (Samad et al., 2013). In some areas of geo-spatial research UAV data are replacing satellite images, and conventional data collection methods, such as physical survey; due to their flexibility (Zongjian, 2008).

In Bangladesh, planning and engineering related data are collected using traditional survey methods. Implementation and potentials of UAV in urban planning and engineering remain unexplored in Bangladesh.

[*] Corresponding author.

From literature, it has been explored that use of UAV based data collection can not only save time, but can also improve the capacity of the planners and engineers with frequent and realizable data accessibility. Therefore, in this study, using an indigenously developed UAV, within complex urban fabric of Dhaka city, Bangladesh; several spatial data essential for urban planning and management have been acquired. The research targets in explaining the ways of working with UAV in low cost, and timely manner. Additionally, the paper aims to discuss the process of the data collection and processing of images, and extraction of spatial information from UAV images. Additionally, this study also elaborates the possible use of these data in urban planning and their benefits over traditional method of data collection in urban environment.

2 Methods and Materials

2.1 Research flow and working process

The research is carried out on six sequential steps (Figure 1); first the study area has been selected based on the requirements of an existing urban management project (Study area: Kalshi, Mipur, Dhaka City). In the second step, selection of UAV and the corresponding sensor carrier has been conducted. After selecting the carrier and its sensor, a flight path has been planned to operate the UAV on the desired line over the study area. This enables the operation of the carrier easier and effective considering the coverage, and time required by the carrier to cover the study area. In the next step (Step 3), the carrier was actually operated according to the flight path in order to capture raw images. This step is executed as a major task in the whole process, named as image acquisition. In the next step (Step 4) the raw collected images were processed to further generate project outcomes. In the final steps, the process images were used to generate project deliverables, orhto-mosaic photos, The Digital Terrain Model (DTM), the Digital Elevation Models (DEM), 3D point cloud, and others.

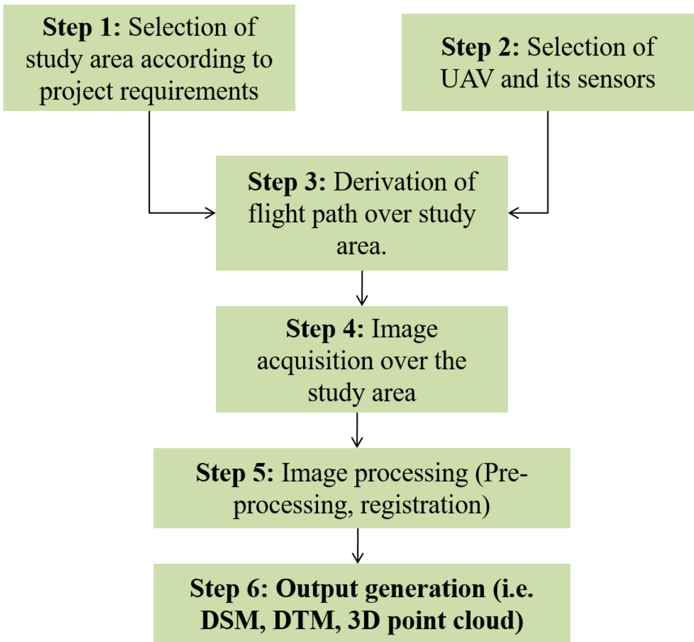

Figure 1: Research flow diagram, indicating the working procedure to use UAV methods in this study.

2.2 Technical specifications and flight path

In this research, an indigenously developed UAV (drone) utilized. The drone was developed by AplombTechBD, a technological Start-Up firm in Bangladesh and they are working as off-shore development center for companies such as Infineon Technologies AG, and SinePulse GmbH. In this study, a multirotor type of UAV (Quadcopter) has been used (Figure 2).

Figure 2: AplombTechBD developed Quad-copter with action camera (GoPro Hero 3+)

Use of Action Cameras (i.e. GoPro Hero 3) for Photogrammetry is a recent approach (Balletti et al., 2014). However, the advanced sensor of action cameras becoming popular for photogrammetry and in this case study, has been utilized to capture high resolution still images. Despite action cameras lack actual sensor attributes the proper calibration of the acquired images can result in highly accurate images with very high resolutions to ensure meaningful data extraction (Khanna et al., 2015; Balletti et al., 2014). The calibrated images of this action camera provide orhto images with 5 cm spatial resolution on the defined height of the drone.

In order to operate the drone over an specific area, and a targeted object, a flight path plan was required, and here for dense urban conditions of the study area, a careful design of flight path was taken into action. Using ArduPilot Mission Planner 2, with MATLAB customization for specific path (Kochersberger et al., 2014), a complete flight path has been designed to operate the UAV (Figure 3). The reasons for using Mission Planner are quite clear; it is an open source autopilot project, that is highly customizable, which can work as a dynamic control operation module for autonomous UAVs. In this study, the flight path was planned following the road ways of the area of interest (as in dense urban setting it was difficult to operate in any direction, and also has altitude restrictions). The overall flight was timed for twenty minutes, and it covered approximately a corridor of two kilometers.

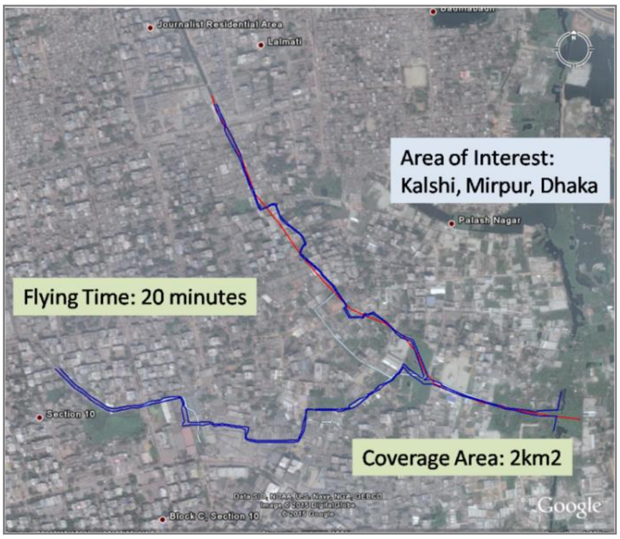

Figure 3: flight path, area, flight time, and study area coverage.

2.3 Image processing and information extraction

The acquired automatic geo-referenced individual images require detail processing before extraction of information. In the process, synchronization of images, registration of the images, bundle block adjustment have been taken into action to prepare the ortho-image for further photogammetric information extraction (Figure 4). In this case, Pix4DMapper software has been utilized extensively to obtain Orthomosaics, Digital surface model (DSM), Digital terrain models (DTM), 3D point clouds (Unger et al., 2014). However, in addition to Pix4DMapper, Correlator3D software also been utilized for 3D model and point generation to ensure cross-validation of resulting outputs. Both software packages work on aerial triangulation process, and automate the process of creating feature points (Unger et al., 2014; Madani, 2012).

Figure 4: Image processing and output generation stages.

Before generating the final DSM, DTM and 3D point cloud from Orthomosaics bundle block adjustments for different blocks of images have been applied. This correction enabled proper positing of the image tiles and helps generate small ground sample distance (GSD), and this operation has also been conducted in Pix4D (Gini et al., 2013). Finally, after all processing and corrections, geo-corrected Orthomosaics, DSM, DTM and 3D points have been generated for the study area.

3 Results and discussion

During the operation of UAV (13 January, 2015 at 11:30 am) along the fight path (Figure 5), the camera captured 544 tiles of images along the flight path. The captured images were then processed and geo-corrected to develop the Orthomosaics. Figure 6 shows one of the images captured by the UAV in the study area. This clearly indicates the richness of details have on each image. Additionally, it is due to the flight height below the atmosphere, thus cloud coverage was not any issue for this kind of images. In this case, after producing the ortho image blocks, the team moves forward to produce DSM, DTM, and 3D point clouds. From all the images, we have produced 7 cm grid based DSM (Figure 7a), DTM (Figure 7b), corresponding hill-shade (Figure 7c) and drape original image on hill-shade image (Figure 7d). Mostly DSM and DTM were the requirements for the project we were working; they required high resolution DSM and DTM for analysis of structure volume, population estimation and understanding slop of the study area.

Figure 5: 3D flight path of the UAV operation in kalshi area, Dhaka city.

Figure 6: Actual Image of a section in Kalshi Area.

Another major result of this study was production of 3D map for the study area in order to understand the volumetric condition of building bulk and structure types. In the aspect, use of UAV was an effective idea, as for Dhaka city, no such data has been produced from 3D mapping. Additionally there were no state of art in case of Dhaka city, to explain the extent of use of ortho photos in extracting building footprint information and understanding building density (Nex and Remondino, 2014). The output from Pix4DMapper, and Correlator3D provided dense points cloud of the study area (Figure 8a), and corresponding 3D model and map has been produced (Figure 8b).

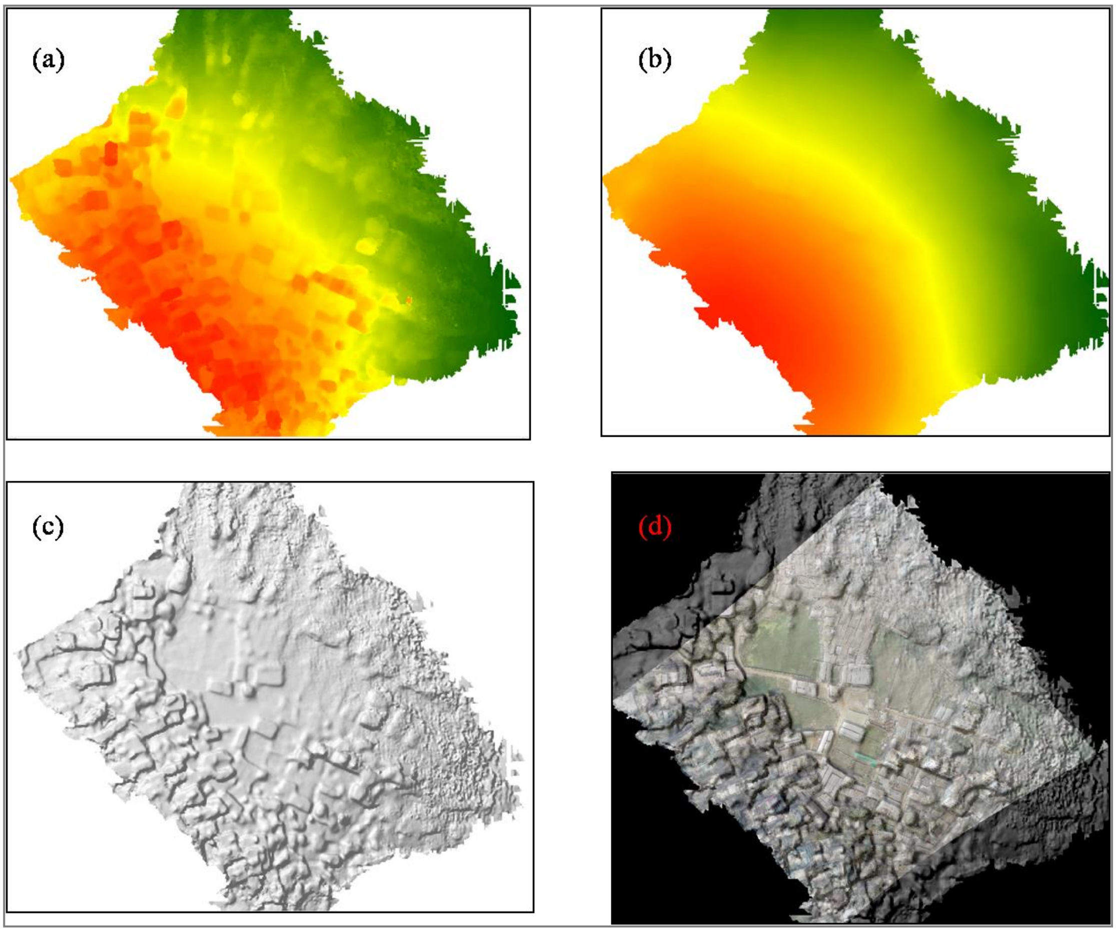

Figure 7: (a) 7 cm DSM of a section in the study area (b) DTM produced from the ortho-images (c) Hill-shade of the DSM produced (d) Draped original image over the hill-shade layer.

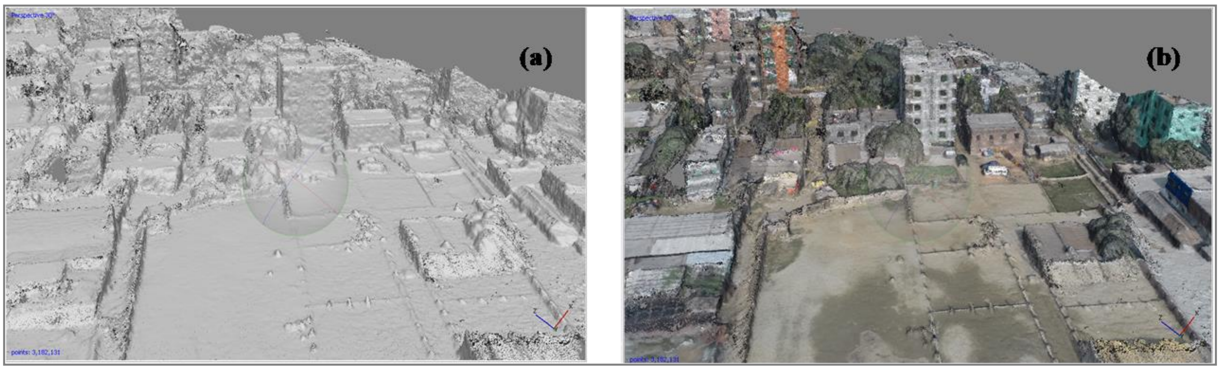

Figure 8: (a) 3D point cloud generated for the study area (b) 3D model generated for study area.

Providing details on how to use UAV for urban environment like Dhaka city is only one section of this paper. The study also focuses on exploring the potentials of UAV in more details. As for Dhaka city or in general in Bangladesh the practice of UAV in geo-spatial data collection is yet not been established, thus the authors move forward to evaluate UAV methods with the existing satellite image output and conventional survey outputs to illustrate clearly the advantages of UAV in these environment. To begin with, we have compared possible satellite imagery methods outputs in general, and not only considered the quality of outcome, but also the potential cost and resources.The spatial resolution of the satellite images (high resolution) varies usually from 40 cm to 69 cm (Table 1) which means that in the ground an object less than 1.5 m in size cannot be figured out; besides there are problems of cloud coverage and the canopy coverage underneath, in such case no feature can be identified without the help of direct filed visit.

Table 1: GSD Comparison between UAV and satellite image methods

Item Name	Resolution	Cloud Coverage	Remarks
Satellite Data	40 -69 cm	Creates Trouble	Workable
UAV Data	Up to 2 cm (out used)	Not Dependent	20x Better

All these three issues GSD, cloud coverage and canopy coverage can be well handled with the UAV systems ensuring better quality of spatial data. In particular (from expert discussion at Dhaka) as much as 20 times better quality can be achieved in GSD if a carefully chosen UAV system is used. In addition, the usual cost of satellite image data is estimated 20 to 50 USD per square kilometer which is recurrent for any specific time frame while with UAV system multiple time frame data can be provided with same capital investment with no additional costs. The satellite image data collection has another significance hindrance of lead time requirement such as in some cases we have to wait for a couple of months for a fresh acquisition. Furthermore, there is a minimum order quantity for new (100 square kilometer) satellite image acquisition while with the UAV system there are no such limitations. It can be utilized for small to medium sized project area with no time delay (Zongjian, 2008).

The authors also have made detailed discussion with physical surveyors and asked them about the potential time and resources they need for 100 km^2 survey in an urban setting like the case study area. The discussion outcome shows, It takes about 4 months to do topographic survey using 10 different stuff members for an Area of Interest (AOI) of 100 km^2. This survey can provide an average quality of spatial data with a necessity of frequent filed visits. In addition, when compared with satellite imagery data extraction, for 100 km^2, the time is found to be approximately 3 months, with slightly better quality than physical survey. However, both of them are highly limited in producing 3D maps, with the quality provided by UAV outcome. In contrast to traditional survey and costly satellite images, we found that it would probably take 4 weeks to cover the same 100 km^2 with UAV, and the outcome images, extracted features, and models of UAV would have better quality compared to physical survey and satellite images.

4 Conclusion

This paper illustrated the methodological process of UAV data extraction case study in a dense urban setting (Dhaka city). The study carefully describes the process of using UAV, elaborates the methods and provided use case scenario for UAV applications in planning and engineering activities in urban areas. Details on low cost

UAV, its path of operation and ways to process and extract valuable geo-spatial information added meaningful insight in the body of knowledge in the area of UAV applications. Additionally, it opens a wide range of options that industries and agencies (e.g. construction, urban planning) in Bangladesh can look for to make their data acquisition more accurate and efficient.

References

Balletti, C., Guerra, F., Tsioukas, V., & Vernier, P. 2014. Calibration of action cameras for photogrammetric purposes. Sensors, 14(9), 17471-17490.

Gini, R., Pagliari, D., Passoni, D., Pinto, L., Sona, G., &Dosso, P. 2013. UAV photogrammetry: Block triangulation comparisons. Int. Arch. Photogram. Remote Sens. Spat. Inf. Sci.

Khanna, R., Möller, M., Pfeifer, J., Liebisch, F., Walter, A., &Siegwart, R. 2015, September. Beyond point clouds-3D mapping and field parameter measurements using UAVs. In Emerging Technologies & Factory Automation (ETFA), 2015 IEEE 20th Conference on (pp. 1-4). IEEE.

Kochersberger, K., Kroeger, K., Krawiec, B., Brewer, E., & Weber, T. 2014. Post- disaster remote sensing and sampling via an autonomous helicopter. Journal of Field Robotics, 31(4), 510-521.

Lari, Z., & El-Sheimy, N. 2015. System Considerations and Challendes in 3d Mapping and Modeling Using Low-Cost Uav Systems. The International Archives of Photogrammetry, Remote Sensing and Spatial Information Sciences, 40(3), 343.

Madani, M. 2012. Accuracy potential and applications of MIDAS aerial oblique camera system. International Archives of the Photogrammetry, Remote Sensing and Spatial Information Sciences, 39, 127-132.

Nex, F. and Remondino, F., 2014. UAV for 3D mapping applications: a review. *Applied Geomatics*, *6*(1), pp.1-15.

Samad, A. M., Kamarulzaman, N., Hamdani, M. A., Mastor, T. A., &Hashim, K. A. 2013. The potential of Unmanned Aerial Vehicle (UAV) for civilian and mapping application. In System Engineering and Technology (ICSET), 2013 IEEE 3rd International Conference on (pp. 313-318). IEEE.

Siebert, S., &Teizer, J. 2014. Mobile 3D mapping for surveying earthwork projects using an Unmanned Aerial Vehicle (UAV) system. Automation in Construction, 41, 1-14.

Unger, J., Reich, M., &Heipke, C. 2014. UAV-based photogrammetry: monitoring of a building zone. The International Archives of Photogrammetry, Remote Sensing and Spatial Information Sciences, 40(5), 601.

Zongjian, L.I.N., 2008. UAV for mapping—low altitude photogrammetric survey. *International Archives of Photogrammetry and Remote Sensing, Beijing, China*, *37*, pp.1183-1186.

Assessment of Earthquake Risk:
A contribution to Smart City's Urban Infrastructure Management

Shams Uddin Al Azad, Swarna Bintay Kadir, Nadia Afrin Noor, Franz-Josef Behr

Stuttgart University of Applied Sciences

KEYWORDS: *Earthquake preparedness, database generation, mobile application, building damage scenario identification.*

ABSTRACT

Earthquake is one of the major problems worldwide. Every year more than one countries of the world are affecting by this devastating disaster. The best way to tackle this catastrophic disaster is to increase preparedness. Many organizations are working worldwide to make a community better prepare to face an earthquake. However, the major problem faced by these organizations is the shortage of building information in the locality. Due to this scarcity, they spend a lot of resources to collect data. Sometimes their projects do not succeed due to this shortage. On the other hand, people who are living in an earthquake prone zone always stay anxious about their safety. They want to if their building is strong enough to tackle possible earthquakes. The motive of this research is to create a mobile application which will be used by the residents of the households and will be applicable worldwide. They will use this application enthusiastically to find the damage scenario of their own building after the hit of a possible earthquake of their place. Moreover, their usage of the application will generate data of their own building and ultimately a database of building information will be created. This paper will describe the algorithms and working process of the mobile application and the process of data visualization.

1 Introduction

The most terrifying disaster on earth is earthquake. We cannot predict when it will occur. It causes immense loss of human life, wild life and economy. Many other disasters are the aftermath of an earthquake like landslides or Tsunamies. Even if we cannot predict earthquake, we can increase our preparedness for it. Many planning or research organizations are working in order to increase preparedness for earthquakes. They are doing a lot of research on earthquake and making a contingency plan for a locality. But for doing any earthquake research the big constraint is the limitation of building data of the locality. In many earthquake-prone developing countries, a lot of organizations are working to make the locality prepare to fight against earthquake. But all of the organizations are suffering much for the scarcity of required data. This research will give a solution for generating required building data in cooperation of building residents.

People living in earthquake prone area want to know whether their building can withstand in most probable earthquakes. So, it is easy to incorporate general people in data generation process through a mobile application, if the application can predict the condition of user's building after the hit of an earthquake and provide some recommendation to the user to minimize earthquake risk. While using the application user will provide some data regarding their building which are required to the research organizations to make a plan. So, this application will benefit both the general people and the research organizations.

2 Algorithms behind the application

Earthquake risk varies from place to place. One of the main factors for this difference is geological characteristics of an area. Federal Emergency Management Agency (FEMA) has divided areas into three risk level: high seismicity, moderate seismicity and low seismicity (FEMA, 2002). One way to estimate earthquake risk of a place is spectral acceleration. Spectral acceleration, with a value related to the natural frequency of vibration of the building, is used in earthquake engineering and gives a closer approximation to the motion of a building or other structure in an earthquake than the peak ground acceleration value. Spectral acceleration value for a period of 0.2 seconds and 1 second is measured for estimating earthquake risk of an area. An area can be categorized into low, moderate or high seismicity by spectral acceleration using the following process.

Table 1: seismic classification with spectral acceleration

Region of seismicity	spectral acceleration response, SA (short period, or 0.2 sec	spectral acceleration response, SA (long period or 1.0 sec
Low	< 0.167 g (in horizontal direction)	< 0.067g (in horizontal direction)
Moderate	≥ 0.167g to < 0.500g (in horizontal direction)	≥0.067g to < 0.200g (in horizontal direction)
High	≥0.500g (in horizontal direction)	≥0.200g (in horizontal direction)

Source: FEMA 2002

In order to assess a building visually, FEMA has developed the Rapid Visual Screening (RVS) method. This method provides three different data collection forms for the three different seismic zones. Through this method, the strength of a building in order to tackle earthquake can be assessed quite easily. The severity of the impact on structural performance varies with the type of lateral-force-resisting system; thus, the assigned score modifiers depend on building type. Score modifiers associated with each performance attribute are indicated in the scoring matrix in table 2 (FEMA 2002).

Table 2: Scoring matrix in RVS algorithm for moderate seismic zones

Building type	W1	W2	S1	S2	S3	S4	S5	C1	C2	PC1	PC2	RM1	RM2	URM
Basic score	5.2	4.8	3.6	3.6	3.8	3.6	3.6	3	3.6	3.2	3.2	3.6	3.4	3.4
Mid Rise (4-7)	N/A	N/A	0.4	0.4	N/A	0.4	0.4	0	0.4	N/A	0.4	0.4	0.4	-0.4
High Rise (>7)	N/A	N/A	1.4	1.4	N/A	1.4	0.8	1	0.8	N/A	0.6	N/A	0.6	N/A
Vertical Irrigularity	-3.5	-3	-2	-2	N/A	-2	-2	-2	-2	N/A	-1.5	-2	-1.5	-1.5
Plan Irrigularity	-0.5	-0.5	-0.5	-0.5	-0.5	-0.5	-0.5	-1	-0.5	-0.5	-0.5	-0.5	-0.5	-0.5
Pre-code	0	-0.2	-0.4	-0.4	-0.4	-0.4	-0.2	-1	-4	-0.2	-0.4	-0.4	-0.4	-0.4
Post-Benchmark	1.6	1.6	1.4	1.4	N/A	1.2	N/A	1	1.6	1.8	N/A	2	1.8	N/A
Soil-Type C	-0.2	-0.8	-0.6	-0.8	-0.6	-0.8	-0.8	-1	-0.8	-0.6	-0.6	-0.8	-0.6	-0.4
Soil-Type D	-0.6	-1.2	-1	-1.2	-1	-1.2	-1.2	-1	-1.2	-1	-1.2	-1.2	-1.2	-0.8
Soil-Type E	-1.2	-1.8	-1.6	-1.6	-1.6	-1.6	-1.6	-2	-1.6	-1.6	-1.6	-1.6	-1.6	-1.6

Source: FEMA 2002

In RVS, fifteen types of residential buildings are considered and a basic score is given in each type of building. Every type of building has different resistance level in tackling earthquake that reflects on the basic score. The types of buildings are shown in table 3. (FEMA, 2002; FEMA, 2015)

Table 3: Different types of building in RVS algorithm

Building code	Building type
W1	Light wood frame residential and commercial buildings equal to or smaller than 5,000 square feet
W2	Light wood frame buildings greater than 5,000 square feet
S1	Steel moment- resisting frame

S2	Braced steel frame
S3	Light metal building
S4	Steel frames with cast-in-place concrete shear walls
S5	Steel frames with unreinforced masonry infill walls
C1	Concrete moment-resisting frames
C2	Concrete shear wall buildings
C3	Concrete frames with unreinforced masonry infill walls
PC1	Tilt-up buildings
PC2	Precast concrete frame buildings
RM1	Reinforced masonry buildings with flexible diaphragms
RM2	Reinforced masonry buildings with rigid diaphragms
URM	Unreinforced masonry buildings

Source FEMA 2002, 2015

One of the score modifiers of rapid visual screening is vertical irregularity. If the building is irregularly shaped in elevation, or if some walls are not vertical, or if located on a steep hill, or if it has soft storey then the modifier will be applied. Plan irregularity can affect all building types. Examples of plan irregularity include buildings with re-entrant corners, where damage is likely to occur; buildings with good lateral-load resistance in one direction but not in the other; and buildings with major stiffness eccentricities in the lateral force-resisting system, which may cause twisting (torsion) around a vertical axis. The post modifier Score Modifier is applicable if the building being screened was designed and constructed after significantly improved seismic codes applicable for that building type (e.g., concrete moment frame, C1) were adopted and enforced by the local jurisdiction. Final score modifier is soil type. Three types of soils are incorporated with the survey, e.g. Hard rock, moderate and landfill (FEMA, 2002; FEMA, 2015). After calculating all these factors of a building, a building is classified as vulnerable to the probable earthquake if the final score is less than 3 (Sucuoglu. H. et al).

If the building is found vulnerable in Rapid Visual Screening then it will be assessed in another algorithm called Turkish Simple Survey. This algorithm describes the possible damage condition of the building after an earthquake. Like RVS, Turkish simple survey basic score is set by building story and is varies according to different seismic zones. In this method, the score modifier are soft story, heavy overhang, apparent quality, short column, pounding effect and topographic effect (Sucuoglu, H. et al 2003). The scoring matrix in Turkish simple survey is shown in table 4. The score predictor of Turkish simple survey is shown in table 5.

Table 4: Score matrix of Turkish simple survey

Story #	Initial score			Vulnerability score					
	High Seismic Zone	Moderate Seismic Zone	Low Seismic Zone	Soft Story	Heavy Overhang	Apparent Quality	Short Column	Pounding	Topographic Effects
1,2	90	125	160	0	-5	-5	-5	0	0
3	90	125	160	-10	-10	-10	-5	-2	0
4	80	100	130	-15	-10	-10	-5	-3	-2
5	80	90	115	-15	-15	-15	-5	-3	-2
6,7	70	80	95	-20	-15	-15	-5	-3	-2
Performance Score, PS = (Initial Score) - Σ (Vulnerability parameter) x (Vulnerability Score)									

Source: (Albayrak. U. et al 2016)

Table 5: Score predictor of Turkish simple survey (Albayrak. U. et al 2016)

Damage State	**Structural Elements**	**Non-structural Elements**	**Score**
None	No visual sign of damage	No visual sign of damage	>=100
Light	Hairline inclined or flexural cracks	Hairline cracks in wall. Flaking of plaster	80-100
Moderate	Concrete sealing	Cracking in walls and joints between panels	50-80
Severe	Local structural failure	Wide and through cracks in wall	0-50
Collapse	Local or total collapse	Crushing of walls or out of plane toppling of walls	

Source: (Albayrak. U. et al 2016)

In the mobile application both Rapid Visual Screening (RVS) and Turkish simple survey algorithm is used. The algorithm of the mobile app is shown in diagram 1.

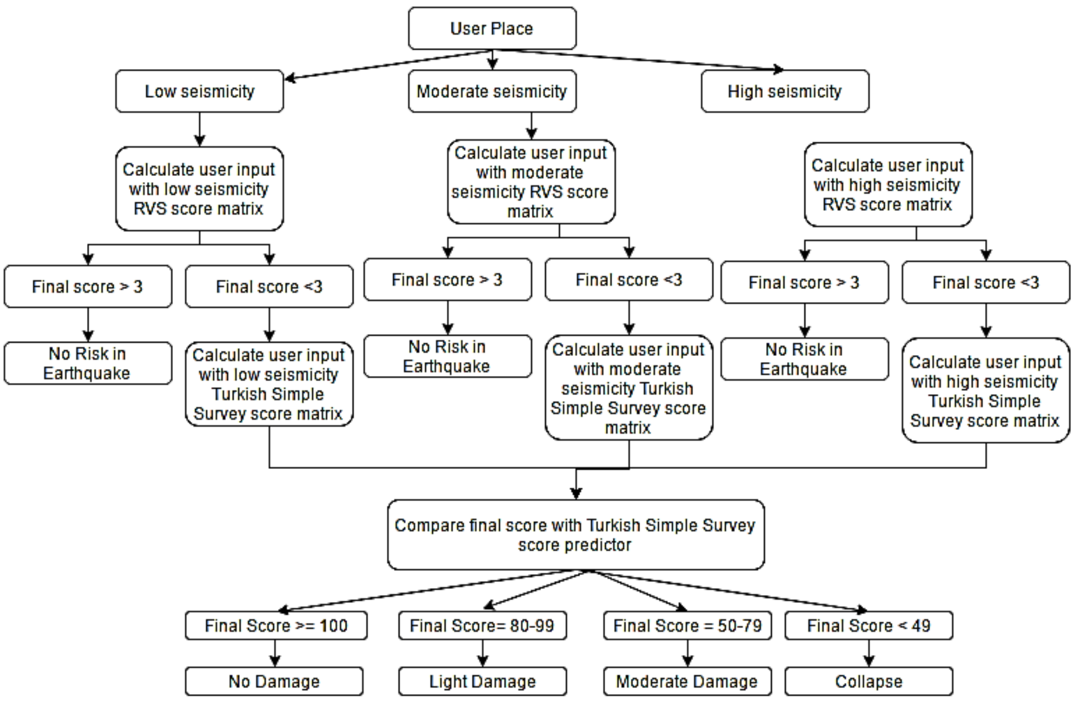

Diagram 1: algorithm of mobile application

3 Methodology

At first City wise spectral acceleration for short period (0.2 second) and long period (1 second) database was created and kept in the server. While using the application at first user has to enter the address of his building. Based on his postal address, the application will fetch the spectral acceleration value of his city from the server and compare this value with table 1. This will determine the seismic zone user lives in. The application will set all the base score and score modifier values according to the seismic zone. According to the survey algorithm used, there is different base score and score modifier value for low, moderate and high seismic zones. The address will be geocoded by the application and in the server, the longitude and latitude value of the building will be saved.

In the next step, user has to give some information about his building such as, number of storeys, total number of inhabitats, presence of soft story, presence of heavy overhang, presence of short column, presence of pounding effect, visual quality of the building, type of the building, presence of vertical irregularity, presence of plan irregularity and soil type of the building. Some of these technical terminologies may be difficult for the user to understand. So, in the UI of the application "help" button was included. If the user taps on the help button then the descriptions and some pictures illustrating the specific terminology will pop up (figure 1).

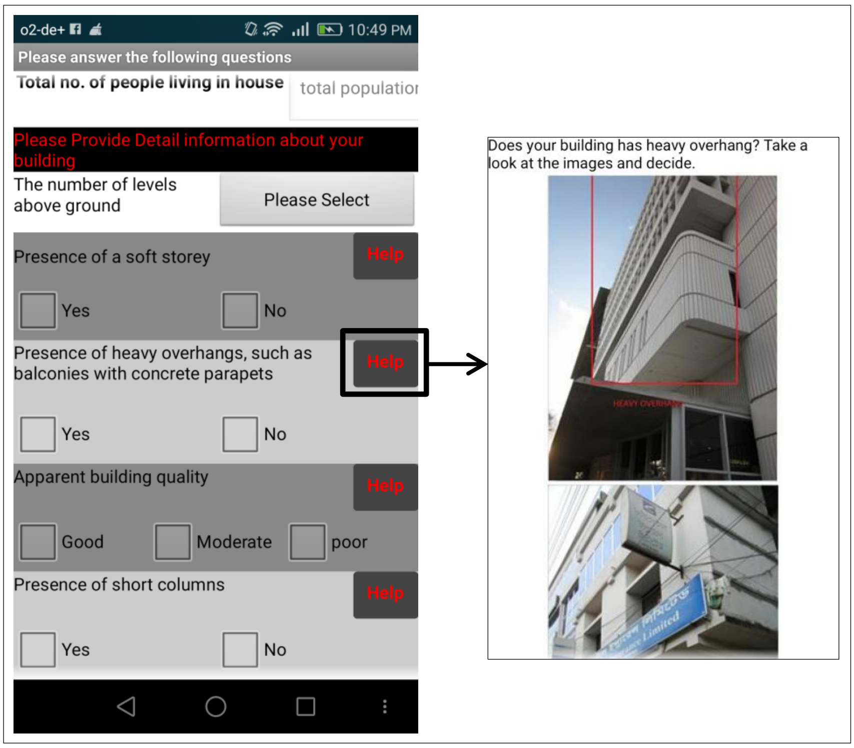

Figure 1: User interface of the application

After giving all the information, the application will show the result to the user. The result window is divided into four sections.

1. In the first section, the app will describe the risk regarding the geological location of the building. It will tell the user whether he is living in low, moderate or high seismic zone.
2. In the second part, it will describe the risk associated wirh the building. The app will calculate the user input with RVS and Turkish simple survey algorithm. The final score of this algorithm will decide the condition of the building after the hit of the earthquake. It will tell the user the week points of their building structure and predicted damage.
3. In this part the app will suggest some recommendation for the user. It will tell the user the reason for his building risk and how to overcome the risk.
4. In the fourth part it will advise user what to do next in order to increase preparedness for the earthquake.

User inferface of the result page of the app is shown in figure 2.

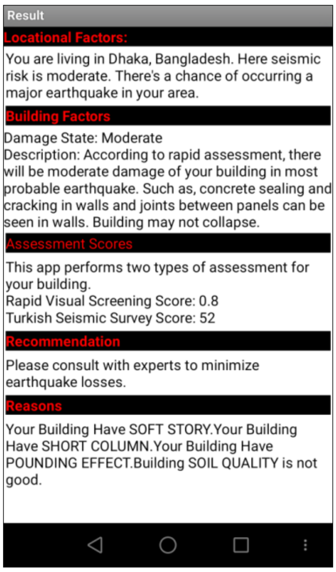

Figure 2: User interface of the application

All of the data entered by the user are saved in a database server including latitude and longitude values the building. All the data will be displaced in Open Layer API webpage. Longitude and latitude of the building data will be used to identify building in API (Figure 3).

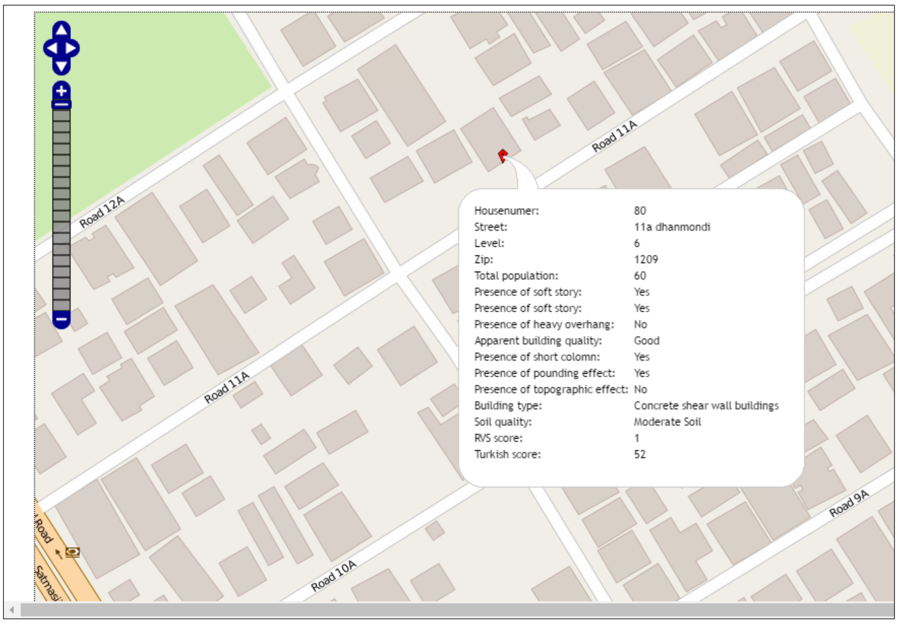

Figure 315: Data visualization through website

4 Application

The mobile application can play a vital role to increase the awareness of general people about the earthquake. Through this app, they will come to know the earthquake risk of the place he is living in. Users also become conscious about the factors which are important to maximize the strength of building to tackle earthquake. The application is also a great source of learning material for the users because within the app, all the critical terminologies are explained in a user-friendly way. Finally, the users will come to know the weak points of their buildings that they can fix to increase preparedness for earthquake.

The greatest beneficiaries of the application are the research organizations or individual researchers who are doing research on earthquake preparedness of a locality. If more and more people use this app then ultimately a huge database of building information will be generated automatically and everyone can access this data through the website.

The architecture of the whole process is shown in figure 4. In the mobile application, there are four levels of tiers, i.e. presentation tier, business logic tier, common tier and data tier. Presentation tier is consisting of the user interface and presentation logics. All the calculations inside the application will be done inside business logic tier. Data tier will hold the internal application data by tiny database. The connection between mobile device and the web server is both ways. All the user input in the application will be transferred to the web server and from the web server, spectral acceleration data of an area will be transferred back to application. The connection between the web server and website is one way. All the building data will be transferred from the server to the website. Each building data will be shown with the open layer website by a marker. The data will be open for all. Architecture of the total system is shown in figure 4.

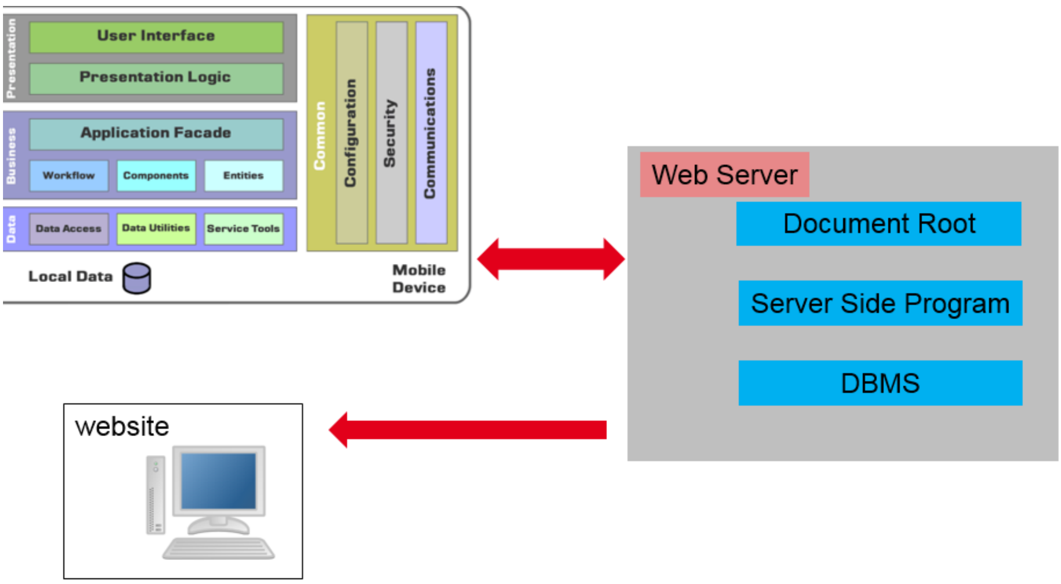

Figure 4: Architecture of the system

5 Conclusion

The scarcity of data is a great problem especially in the developing country or under-developed countries. Due to this shortage, research organizations put a lot of money and time for data collection. If the general people use this mobile application then this scarcity of building data can be solved. The mobile application will satisfy the demand of both residents of the building and earthquake researchers. This whole system will create a platform for data generation with user interaction. People will use this mobile app to know the probable behaviour of his building after an earthquake. While using this app they will provide some information about their building. Their provided information will be used by the organizations to do research and to make the contingency plan for a locality to face the earthquake disaster.

References

Albayrak, U., Canbaz, M., & Albayrak, G. (2016). A Rapid Seismic Risk Assessment Method for Existing Building Stock in Urban Areas. Procedia Engineering.

FEMA (2002), Rapid Visual Screening of Buildings for Potential Seismic Hazards: A Handbook, Third Edition. Prepared by the Applied Technology Council for the Federal Emergency Management Agency, Washington D.C., FEMA 154 Report, in development.

FEMA (2015), Rapid Visual Screening of Buildings for Potential Seismic Hazards: Supporting Documentation, Third Edition. Prepared by the Applied Technology Council for the Federal Emergency Management Agency: Washington, D.C., FEMA 155 Report, in development

Lizundia, B., Durphy, S., Griffin, M., Hortacsu, A., Kehoe, B., Porter, K., & Welliver, B. (2015). Rapid Visual Screening of Buildings for Potential Seismic Hazards: FEMA 154 and FEMA 155 Updates. Tenth U.S. National Conference on Earthquake Engineering.

Sucuoglu, H., & Yazgan, U. (2003). Simple Survey Procedures for Seismic Risk Assessment in Urban Building Stocks. Seismic Assessment and Rehabilitation of Existing Buildings, p 97-118.

Planning of Post-Earthquake Evacuation Route in Ward No. 13 of Dhaka North City Corporation, Bangladesh

[a] Shams Uddin Al Azad, [b] Uttama Barua

[a] Stuttgart University of Applied Science, [b] Bangladesh University of Engineering and Technology

Keywords: *Earthquake Evacuation Route, Disaster Ambulance Route, Earthquake Preparedness*

ABSTRACT:

Bangladesh is an earthquake vulnerable country but the preparedness level is not sufficient to tackle a major earthquake. In some areas post disaster shelters have been determined. But how people will reach in those shelters and hospitals after an earthquake has not yet been analyzed. This research will act as an effective methodology to find safer evacuation routes to reach disaster shelters and emergency health facilities. Thus, the decision makers may integrate the methodology of this research in the plan to increase earthquake preparedness in other earthquake vulnerable areas of Bangladesh; and thereby reduce the after-quake loss to minimum.

1 Introduction

Due to itsgeographic position Bangladesh is considered to be highly vulnerable to earthquake hazards. The increased rate of earthquake events over the last thirty years' time periods suggests reviving tectonic activities in and around the country and indicates the onset of a major one in the very future. Thus, if any major earthquake hits Bangladesh, damage in terms of human casualty, building and other property loss, damage of transportation, utility and other critical facility will be rigorous. But the risk of damage from an earthquake in Dhaka city is very high. According to a study Dhaka city is found among the twenty most vulnerable cities of the world (Davidson, & Shah, 1997). Due to the poor construction of buildings by violation of building codes and safety standards, unplanned, haphazard development and least preparedness among people, a huge number of people would become homeless and another large number of people would become moderate to severely injure.

The northern part of Dhaka city is comparatively vulnerable due to its closer proximity to the Madhupur fault line where PGA (Peak Ground Acceleration) will be very high. But Ward no. 13 of Dhaka North City Corporation (DNCC) is found most vulnerable due to its high population and building density, unplanned growth of building structures constructed by violating building construction codes, narrow roads and the presence of older buildings. Due to unplanned urbanization, there are insufficient open spaces and health facilities in this area, and those are not incapable of meeting all the demands that would emerged after the hazard. Thus, in case of a moderate to high magnitude earthquake, this part of the city would be severely affected.

After the hit of earthquake, how injured people can be moved to hospitals, how homeless people can reach the disaster shelters, how relief can be transported to the disaster shelters and hospitals, are some basic questions. The aim of this research is to create a methodology which can answer the above questions. The most vulnerable area, ward 13 of DNCC, Dhaka, Bangladesh, has been selected as the study area for this research.

2 Demand for Health Facilities

The potential damages and losses due to scenario earthquake of Mw 7.5 (moment magnitude scale) earthquake from Madhupur fault at 2:00 AM morning have been taken as the basis for this planning. CDMP (Comprehensive Disaster Management Program) has already done risk and vulnerability assessment of Dhaka city for the most probable earthquake scenario and prepared a contingency plan. According to the assessment, the injured people after an earthquake event have been segmented into four severity levels along with estimation of the number of injured people according to severity level for each ward of Dhaka city. For Ward no. 13 of DNCC, the number of injured people according to the severity level in case of the most probable earthquake scenario is shown in table 1.

Table 1: Number of injured with respect to severity level in Ward no. 13 of DNCC

Source: CDMP, 2009b

Injury Level	Treatment level required	Number of injuries
Severity level 1	First aid, e.g. bandages or observation.	7,182
Severity level 2	A greater degree of medical care and use of medical technology such as x-rays or surgery, but not expected to progress to a life threatening status.	1,250
Severity level 3	Pose an immediate life threatening condition if not treated adequately and expeditiously.	323
Severity level 4	Instantaneously killed	5,684

There is no need for ambulance facility for the victims who have severity 1 injuries. Ambulance facility are only required for the victims having severity 2 and 3. Total number of assumed victims in these levels is 1573.

3 Types of Evacuation Routes

Serviceability of transportation system is closely connected with the functionality of the community (Pitilakis, & Kakderi, 2011). In the emergency situation after an earthquake, the importance becomes more crucial for: immediate transfer of victims to safer places and shelters, take the injured to health facilities and to transfer relief to the shelters and health facilities (Argyroudis, Pitilakis, & Anastasiadis, 2005). The after quake, loss may be increased for the inability to reach critical locations due to blockage situations of roads and for absence of pre-disaster route planning (Caiado, Oliveira, Ferreira, & Sá, 2012).

The planning of health facilities and disaster shelters have been done for Ward No. 13 of DNCC, where the after quake scenario has been described. According to Comprehensive Disaster Management Plan (CDMP 2009a, 2009b, 2009c, 2013) after the occurrence of an earthquake a number of people will be dead, another number of people will be injured and a number of people will be physically safe but will be homeless. Another part of homeless people may go to their relative’s residence (which are unaffected by earthquake) to take shelter and other will go to the nearest emergency shelter within the ward. So, after the hit of an earthquake there will be major three types of movements that will take place inside the ward:

1. Movement of injured people to health facilities
2. Movement of homeless people to emergency shelters
3. Transport of reliefs from Community Relief Center to emergency shelters and health facilities

Thus, in this research, evacuation routes have been planned to serve the above-mentioned movements in Ward No. 13 of DNCC.

4 Evacuation Route to Reach the Selected Facilities

Direct damage of the routes due to an earthquake event could not be estimated in this study. So, indirect damage of the routes due to an earthquake event has been considered to find out evacuation routes. The main reason for inaccessibility in urban areas after an earthquake event is indirect damage by fallen obstacles such as debris from collapsed buildings or other structures such as overpasses, or / and damages caused by other lifelines (e.g.: gas or water distribution network) (Caiado, Oliveira, Ferreira, & Sá, 2012).

Thus, road blockage depends on width of roads and width of debris generated from buildings adjacent to the roads. There is a correlation between building’s height (i.e. number of storeys) adjacent to a route and the width of the induced debris by the building (Argyroudis, Pitilakis, & Anastasiadis, 2005), which has been utilized for calculating the width of debris produced by a building.

For expertise and information constraint, vulnerability assessment of all buildings could not be done. So, an additional road blockage scenario has been developed to understand the whole scenario. The structures in Ward no. 13 of DNCC are not fit enough to respond well on an earthquake event. In most probable earthquake scenario, among total 12,114 buildings, 256 will be collapsed and 2560 buildings will be completely damaged, which are 23.25 percent of the total number of buildings. (CDMP, 2009b)

Again, 86% of total buildings stock is within the range of three storey buildings. Thus only 14% of the buildings are above three storeys and they comprise a very small portion of the total building stock (DMDP, 2010). Width of debris has been calculated for buildings greater than three storey buildings, assuming that buildings up to three storeys do not produce significant debris (Jahan, 2010).

For the purpose of evacuation route planning, the width of all routes was collected from secondary source and the debris width was calculated for different height of buildings in order to show a scenario of road blockage in the study area:

N=0.06Wd2 + 0.35Wd

Where,

N=Number of storey

Wd =Width of debris (Argyroudis et al, 2005)

Table 2 shows the calculation of width of debris produced from buildings with respect to building height.

Table 2: Width of debris according to the building height

No. of storey	Width of debris (in meter)
4	5.75
5	6.67
6	7.5
7	8.3
8	9
9	9.6

It can be observed that, the road network of Ward no. 13 of DNCC is not in good condition. It is found that majority of the internal roads are very narrow without any footpath. Thus, 98% of the roads of the study area have road width within four meters, where 46% of total road are of three-meter-wide and 10% are of four-meter wide. Again, a given road may experience closure states if at least one of the buildings on its border provides necessary debris for such closure (Zolfaghari, & Mogheisi, 2012). It is observed from field survey that, almost all the road segment has a building which is more than four storeys. Thus, most of the routes will be blocked due to debris produced from buildings. Considering this scenario, evacuation routes to reach the selected health facilities and disaster shelters in Ward no. 13 of DNCC have been planned.

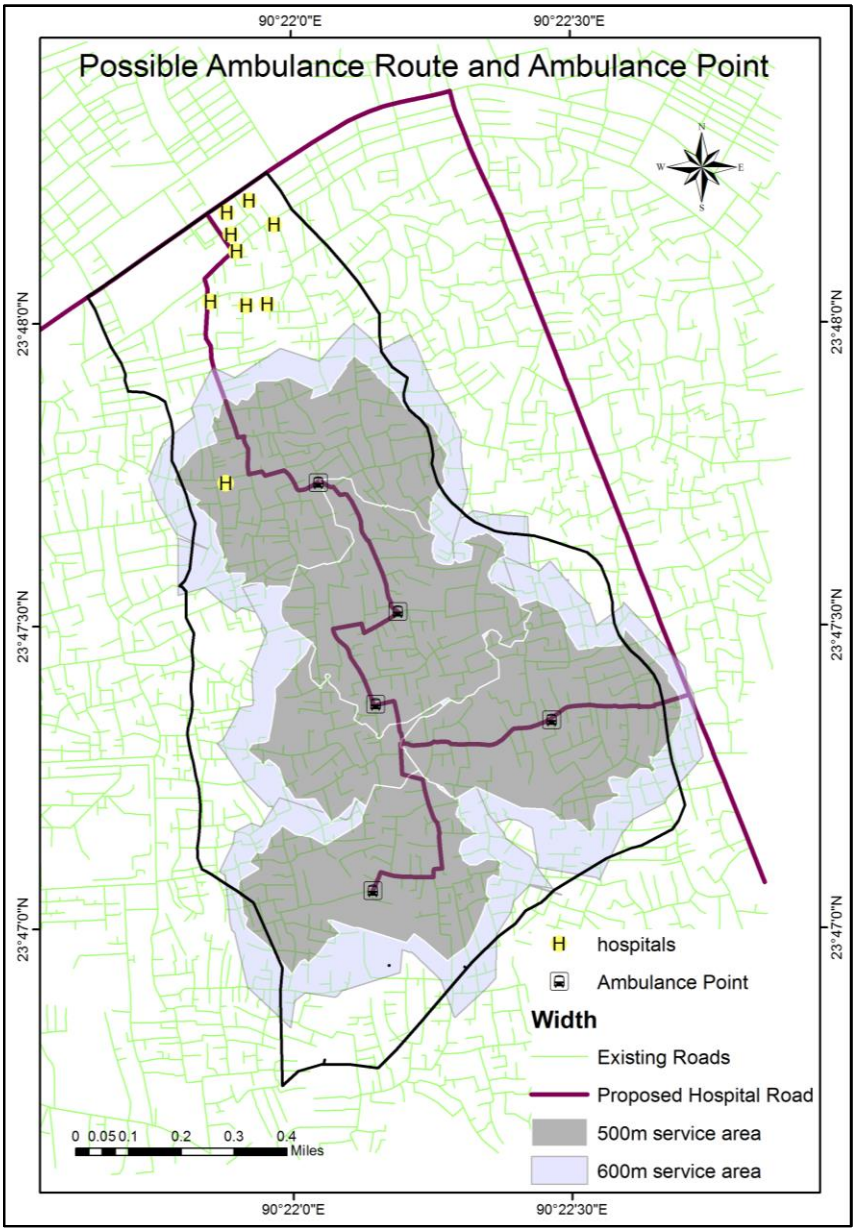

Figure 1: Proposed ambulance point and hospital route to reach the health facilities

It is observed that, most of the routes will be blocked at the event of the most probable earthquake scenario (M 7.5). But, to take injured people to the health facilities, at least one major ambulance route needs to be provided in the Ward which will remain free from debris. According to the interview of key personnel from health facilities, an ambulance needs at least three-meter road width to move freely on the road. So, for selecting evacuation route to reach the health facilities, four facts have been considered. i) Minimum road width three meters, ii) Continuous roads, iii) Minimum number of vulnerable buildings beside the road, and iv) Connectivity with the health facilities and main road.

Firstly, the road segments with greater than three-meter width have been identified. Then continuous road segments have been selected. Road connectivity is provided in a way that the number of high rise building on the both side of the road is lowest. In Figure 1, hospital route is shown. There are two options given in order to transfer patients to the hospital. One option is to use road inside ward boundary and the other option is to use collector road that is outside the ward. But there are a lot of high raised buildings standing along with the collector road. The nature of this road after earthquake is very hard to predict. This road will also be used by civil defense authority in order to perform rescue service and relief facilities. So, the collector road for ambulance is one option but not the best option, the road inside ward is highly preferable for hospital route.

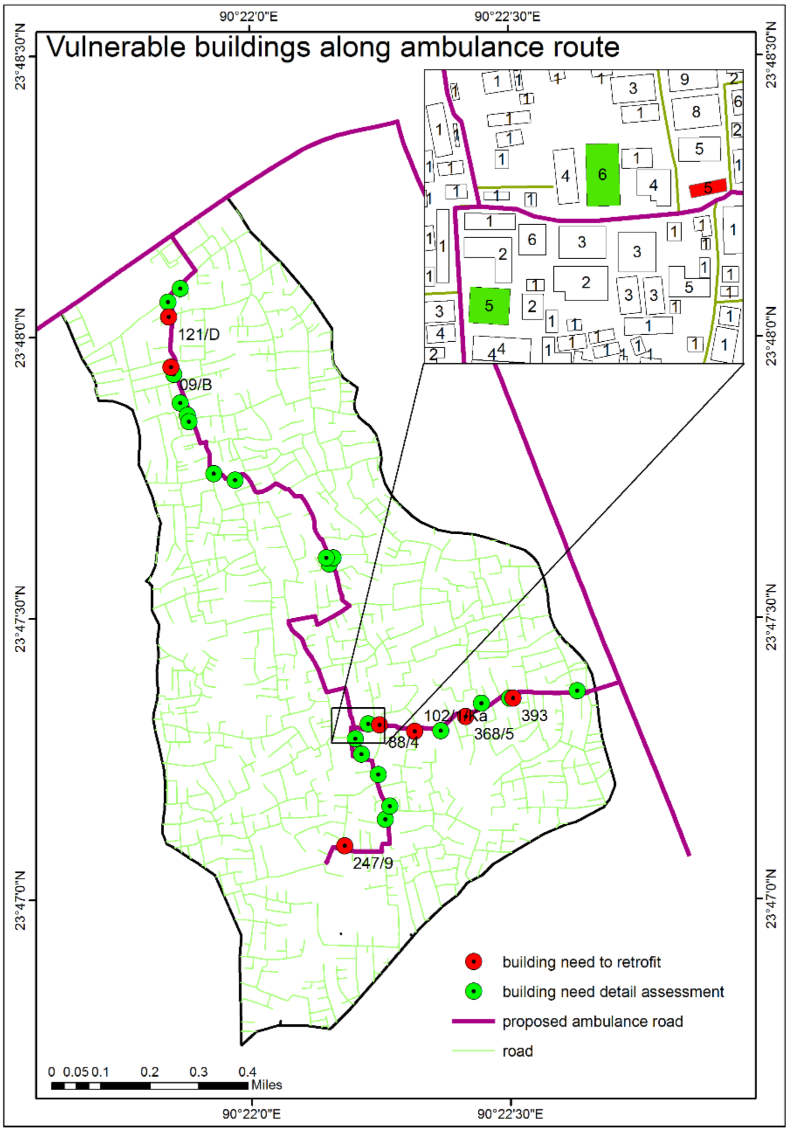

Figure 2: Vulnerable buildings along ambulance route to reach the health facilities in Ward no. 13 of DNCC

In the next step, buildings greater than three storeys along the proposed hospital route have been identified. From the field survey, it is found that along the proposed ambulance route there are twenty-eight buildings with number of storey above three. The, vulnerability assessment of the identified buildings have been done by RVS and Turkish Simple Survey methods. Among the twenty-eight buildings, seven buildings have been found vulnerable which requires to be retrofitted to keep the ambulance route free from debris. In figure 2, the vulnerable buildings are displayed that requires to be retrofitted to keep the hospital route free from debris.

It is not possible for the ambulance to enter in every road after earthquake due to width limitations. So, ambulance should stand in checkpoints and volunteers should bring the patients from the farthest corner of the ward to the checkpoints. In order to locate the position of the ambulance checkpoints two facts have been considered. i) Volunteers should not take more than ten minutes to bring patients to the checkpoints, ii) Checkpoints should be near the intersection of roads.

It is assumed that volunteers can transport patients by trolley or rickshaw van. If they use a trolley then they can cover 500 meters in ten minutes and for rickshaw van they can cover 600 meters. So, every ambulance checkpoint has 500 and 600-meter service area. The location of ambulance points is shown in figure 1.

5 Evacuation Route to Reach the Selected Disaster Shelters

From the road blockage scenario, it is observed that, most of the routes may become blocked on the event of the most probable earthquake scenario. Thus, evacuation to shelters by vehicle would not be possible immediately after an earthquake event. Again, evacuation on foot is the general rule. Thus, victims capable of walking can walk over the debris to reach the nearby emergency shelters. As the similar approach describe before, vulnerability assessment of all buildings and the catchment area for the shelters could be done. It is assumed in this research that victims will use the wider roads to reach the shelters. It is possible that some roads will be will be completely blocked and the victims will not be able the pass through the blockage. In that case the civil defense authority will take quick action so that victims can pass through the blockage on foot. The locations of emergency shelters along with the roads according to width have been shown in figure 3, which can be used by the victims to reach the nearest disaster shelter.

6 Routes Connecting the Selected Health Facilities and Disaster Shelters with the Community Relief Center

The community relief center is a place where the total relief of the ward will be stored and from here relief will be distributed to every disaster shelter. The relief (i.e. foods, cloths) from Government or other donor agency will come to the relief center by trucks using the collector road. The Community relief center for ward 13 is located at the northern boundary which is easily accessible by collector road.

It is required to connect the selected health facilities and disaster shelters with the Community Relief Center to ensure uninterrupted movement of reliefs to the facilities. Immediately after an earthquake event before removal of debris from roads, the reliefs can be transported to the facilities by van, pushcart, wheel barrow and even on foot by volunteers. But, the roads with greater width should be given priority for the purpose. Considering the fact, the routes connecting the selected health facilities and disaster shelters with the Community Relief Center have been identified (Figure 3).

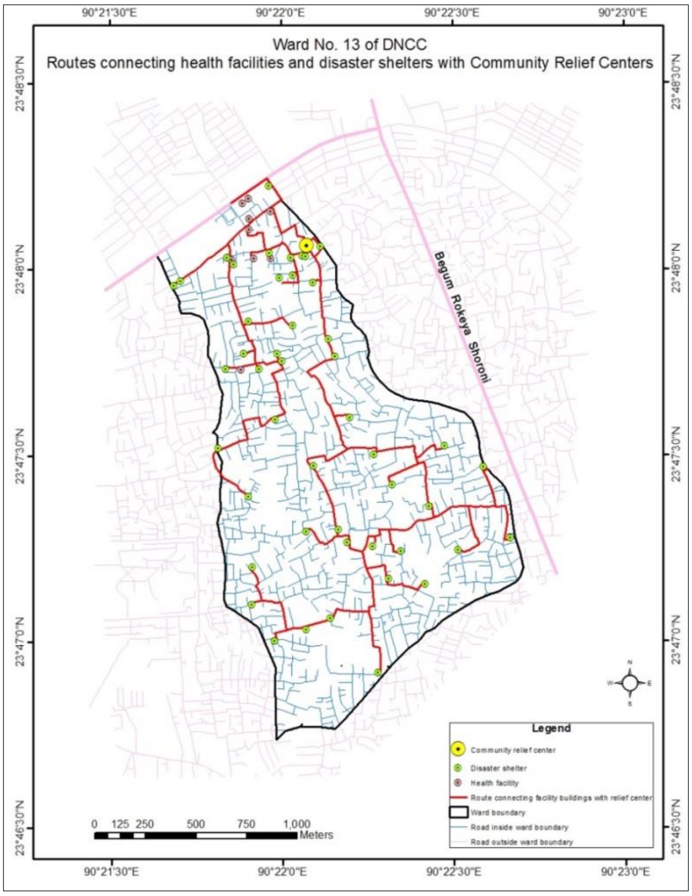

Figure 3: Routes connecting health facilities and disaster shelters with Community Relief Center in Ward no. 13 of DNCC

7 Conclusion

Planning evacuation route is very important for the ward 13 as most of the streets would be blocked after most possible earthquake event. So it is essential to identify at least one road so that ambulance can take the injured victims to the hospitals and community relief can be transported to the hospitals and disaster shelter. This research has also indicates the way to keep the road free from blockage after earthquake. Some vulnerable buildings are selected around the roads and recommended for retrofitting.

References:

Argyroudis, S., Pitilakis, K., & Anastasiadis, A. (2005, May 23-25). Roadway Network Seismic Risk Analysis in Urban Areas: The case of Thessaloniki-Greece. Proc. International Symposium of GEOLINE, Lyon. Retrieved December 22, 2013, from:

http://www.geotech-fr.org/sites/default/files/congres/geoline/GEOLINE2005%20S13%20pp%201-9%20Argyroudis.pdf

Caiado, G., Oliveira, C., Ferreira, M. A., & Sá, F. (2012, September 24-28). Assessing Urban Road Network Seismic Vulnerability: An Integrated Approach. Paper presented at the 15th World Conference on Earthquake Engineering (15 WCEE), Lisbon, Portugal. Retrieved December 22, 2013, from:

http://www.iitk.ac.in/nicee/wcee/article/WCEE2012_1105.pdf

CDMP. (2009a). Risk Assessment of Dhaka, Chittagong and Sylhet City Corporation Area. Dhaka: Comprehensive Disaster Management Programme (CDMP), Ministry of Food and Disaster Management, Government of the People's Republic of Bangladesh, Phase 1.

CDMP. (2009b). Earthquake Contingency Plan for Dhaka City. Dhaka: Comprehensive Disaster Management Programme (CDMP), Ministry of Food and Disaster Management, Government of the People's Republic of Bangladesh, Phase 1.

CDMP. (2009c). Vulnerability Assessment of Dhaka, Chittagong and Sylhet City Corporation Area. Dhaka: Comprehensive Disaster Management Programme (CDMP), Ministry of Food and Disaster Management, Government of the People's Republic of Bangladesh, Phase 1.

CDMP. (2013). Spatial Contingency Plan for Ward No. 13 Dhaka North City Corporation (DNCC). Dhaka: Comprehensive Disaster Management Programme (CDMP), Ministry of Food and Disaster Management, Government of the People's Republic of Bangladesh.

DMDP. (2011). Final Report: Preparation of Detailed Area Plan (DAP) for DMDP Area: Group-C. Rajdhani Unnayan Kartripakha (RAJUK), Dhaka. Retrieved June 10, 2014, from:

http://www.rajukdhaka.gov.bd/rajuk/image/dap/groupC_Report/Chapters_c.pdf

Davidson, R.A., & Shah, H.C. (1997). An Urban Earthquake Disaster Risk Index. The John A. Blume Earthquake Engineering Center, Stanford University, California, Report no. 121. Retrieved Octobor 27, 2013, from: https://blume.stanford.edu/sites/default/files/TR121_Davidson.pdf

Jahan, I. (2010). Earthquake Vulnerability and Evacuation Plan for Old Dhaka. MURP thesis, Bangladesh University of Information and Technology (BUET).

Pitilakis, K. D., & Kakderi, G. K. (2011, January 10-13). Seismic Risk Assessment and Management of Lifelines, Utilities and Infrastructures. Paper presented at the 5th International Conference on Earthquake Geotechnical Engineering, Santiago, Chile. Retrieved December 22, 2013, from:

www.vce.at/SYNER-G/pdf/publications/5ICEGE-Pitilakis%20-%20theme%20lecture.pdf

Zolfaghari, M. R., & Mogheisi, M. (2012, September 24-28). Probabilistic Seismic Damage Assessment for Urban Transportation Network. Paper presented at the 15th World Conference on Earthquake Engineering (15 WCEE), Lisbon, Portugal. Retrieved December 22, 2013, from:

http://www.iitk.ac.in/nicee/wcee/article/WCEE2012_1498.pdf

Big Data Analytics: Data management in Document-oriented data store and Hadoop Framework

Shams Uddin Al Azad, Franz-Josef Behr

Stuttgart University of Applied Sciences

KEYWORDS: *Big data, Hadoop, NoSQL databases,*

ABSTRACT

With the advancement of science and technology data is growing faster than ever and with a great variety. Big data management and analysis is a huge challenge in present days. Due to the inefficiency of handling big data, many organizations throw away a large amount of data which seem unnecessary for that particular time being. However, data is a great resource. Some extraordinary research can be done from the data that seems useless. For managing big data, document-oriented databases and Hadoop ecosystem have been developed. There are also many variety of document-oriented databases are available in the market. This variety of options in data management leads to confusion among the users to figure out the best solution for their specific problem. In this research the inbuilt features of MongoDB, the most popular document-oriented database and Hadoop ecosystem are discussed and analyzed.

1 Introduction

Organizations have been generating data since way back. But as time goes on more and more data is being generated. The researchers of UC Berkeley have analyzed the growth of data a few years ago. “The Berkeley researchers estimated that the world had produced about 1.5 billion gigabytes of information in 1999 and in a 2003 replication of the study found out that amount to have doubled in three years” (Press, 2014). More recent research has been done by IBM. It estimates that 90% of world’s data was created in last two years alone. (Graham et al, 2016)

“This data comes from everywhere: sensors used to gather climate information, posts to social media sites, digital pictures and videos, purchase transaction records, and cell phone GPS signals to name a few” (IBM, 2016). The increase in the amount of data we are generating every day opens up huge possibilities. But there are some problems too. We need to store this huge amount of data and also we need to process it.

In the past, data was only generated by employees. Data volume of data was little and could be pre-anticipated. Today data is not only created by the employees but also the general people. This generates unpredictable amount of data. For example, a few years back, only GIS experts could produce spatial data. But now people are generating spatial data through Open Street Map. So, the volume of data is increasing day by day. Moreover, nowadays machines started generating data. Where machines are involved, gigabytes of data are producing in minutes. For example, Hundreds of millions of smart phones send a variety of information to the network infrastructure. This data did not exist a few years ago. However, In order to handle this huge amount of data, the traditional process of data management systems have become obsolete. In order to process big data Hadoop framework was developed. Apart from the most accepted and widely used relational databases, a new type of database was created, that is called document-oriented database or NoSQL database. But there is a strong confusion among the users when to use a relational database and when to use a document-oriented database.

2 Big data

The term “big data” was first used by the NASA researchers Michael Cox and David Ellsworth (Friedman, 2012). The term big data is very subjective and there are a lot of definitions of big data. But the most acceptable definition among the data scientists is: Big data is the amount of data which is too big to process in a single machine. Such data is created very fast and it comes from different sources with different formats.

Gartner analyst Doug Laney introduced the 3Vs concept of big data (Laney, 2001): Volume, Variety and Velocity. Volume refers to the size of the data. Variety refers to the data which comes from different sources with different formats. Velocity refers to the speed of data it is being generated and the speed at which it needs to be made available for processing. Apart from the 3Vs concept, some data solution companies add two more dimensions for big data. They are variability and complexity. Variability refers to the data flow that can be highly inconsistent with periodic peaks. This is common case for social media. Complexity refers to the difficulty to link, match, cleanse and transformation of data. (SAS)

3 Tabular data store

In tabular databases data are stored or organized in table. Foreign keys link one table to another table. So, the data is spread across multiple tables. Here we cannot delete a column or table at our free will because if a table contains foreign keys and we delete it then the relationship of the dataset might break down. So it has low flexibility in manipulating data. Tabular data sources are very structured. Before feeding data into the tables, the format of each column is defined. Relational database is an example of a tabular data store and typically SQL is used as a controlling language.

For a long time, people have used databases such as SQL server or MySQL or big data warehouses from companies like Oracle or IBM to store their data. The problem in this system is the data structure should be able to fit with the predefined tables. And a lot of the data we deal nowadays tends to be unstructured or semi-structured data.

4 Document-oriented data store

In document-oriented data stores there is no table and relation among tables. Data are kept in a document. It gives us the flexibility to manipulate data and it is a good option for storing big data. As there is no joining among tables while querying, it gives much faster query results. NoSQL databases are document-oriented data stores. There are different kinds of NoSQL data bases, such as key value store, wide column, document store, graph databases. Redis, Amazon's Dynamo and Voldemort are some of key/Value stores database. HBase, Cassandra, Google's big table are some of the wide column databases. MongoDB, CouchDB are document store databases. Neo4j is a graph database. Among the different systems CouchDB, MongoDB and Neo4j have spatial extension. As there are so many NoSQL databases, it is a hoax for the users to select one from so many. (Gálicz, 2014)

5 Comparative analysis among popular document-oriented databases

There are a lot of NoSQL databases available in the market. There exists some basic difference among these databases. According to DB-ranking (DB-engines, 2017 e) the top four popular NoSQL databases are compared in table 1.

Table 1: comparison among popular NoSQL databases

Name / parameters	AmazonDynamoDB	Couchbase	CouchDB	MongoDB
APIs and other access methods	RESTful HTTP API	Memcached protocol RESTful HTTP API	APIs and other access methods	RESTful HTTP API
Server-side scripts	No	View functions in JavaScript	View functions in JavaScript	JavaScript
Triggers	yes	yes	yes	no
Partitioning methods	Sharding	Sharding	Sharding	Sharding
Replication methods	Yes	Master-master replication and Master-slave replication	Master-master replication and Master-slave replication	Master-slave replication
MapReduce	no	yes	yes	yes

Name / parameters	AmazonDynamoDB	Couchbase	CouchDB	MongoDB
Consistency concepts	Eventual Consistency and Immediate Consistency	Eventual Consistency and Immediate Consistency	Eventual Consistency	Eventual Consistency and Immediate Consistency
Description	Hosted, scalable database service by Amazon with the data stored in Amazons cloud	JSON-based document store derived from CouchDB with a Memcached-compatible interface	A native JSON - document store inspired by Lotus Notes, scalable from globally distributed server-clusters down to mobile phones.	One of the most popular document stores
User concepts	Access rights for users and roles can be defined via the AWS Identity and Access Management (IAM)	User and Administrator separation with password-based and LDAP integrated Authentication	Access rights for users can be defined per database	Access rights for users and roles
Developer	Amazon	Couchbase, Inc.	Apache Software Foundation	MongoDB, Inc
Initial release	2012	2011	2005	2009
Current release		4.5, June 2016	2.0.0, September 2016	3.4.2, February 2017
License	commercial	Open Source	Open Source	Open Source
Cloud-based	Yes	no	no	No
Implementation language		C, C++, Go and Erlang	Erlang	C++
Server operating systems	Hosted	Linux, OS X, Windows	Android, BSD, Linux, OS X, Solaris, Windows,	Linux, OS X, Windows, Solaris
Data scheme	schema-free	schema-free	schema-free	schema-free
Typing	Yes	yes	no	yes
Secondary indexes	Yes	yes	yes	Yes
SQL	No	no	no	No

Sources: (DB-engines, 2017 a) (DB-engines, 2017 b) (DB-engines, 2017 c) (DB-engines, 2017 d)

6 Choosing an appropriate data store

There are a lot of NoSQL databases exists in the market today. Users sometimes get confused to choose a system for their application. Computer scientist Eric Brewer in his CAP theorem provided a perfect solution for this problem. The choice of the database selection depends on the characteristics of the application. The CAP theorem states that, it is impossible for a distributed computer system to simultaneously provide more than two out of three guarantees. The guarantees are: Availability, Consistency and Partition tolerance. (Gilbert & Lynch, 2002)

- Availability: Every request receives a (non-error) response – without guarantee that it contains the most recent write. So, each client can always read and write.
- Consistency: Every read receives the most recent write or an error. All clients always have the same view of the data.

- Partition tolerance: The system continues to operate despite an arbitrary number of messages being dropped (or delayed) by the network between nodes.

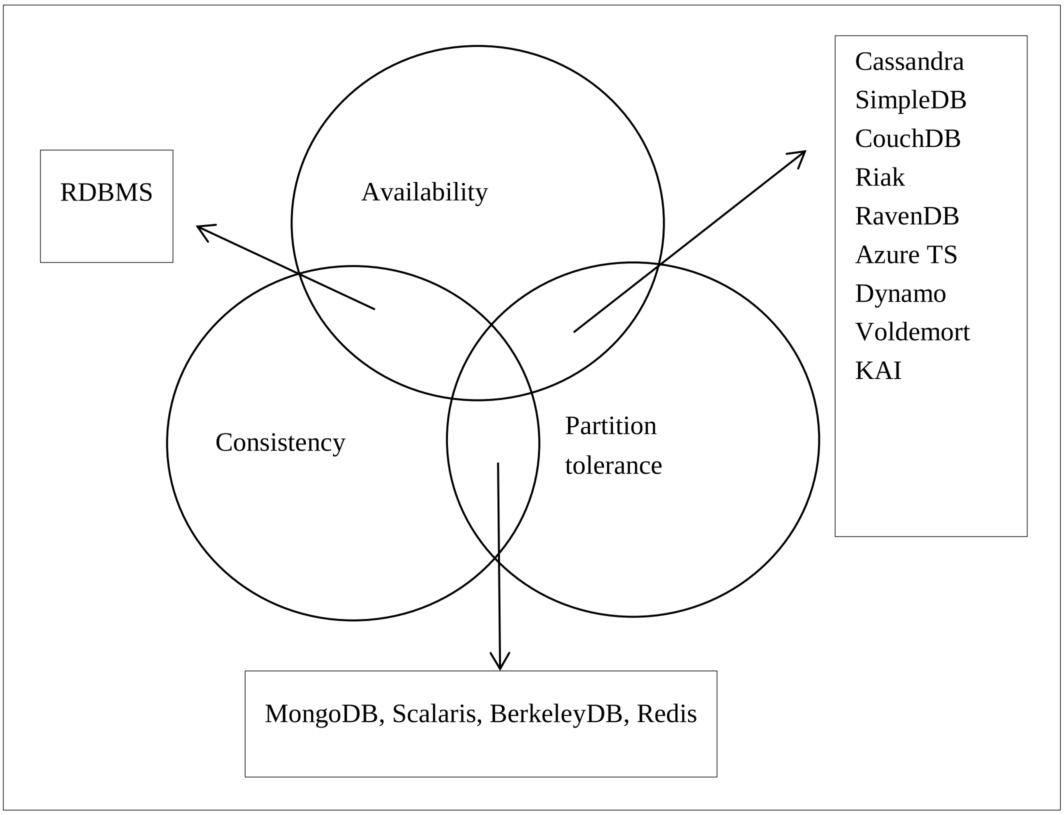

Figure 16 : Selecting an appropriate solution

Source: (Hurst, 2010)

From figure 1, it can be seen that if a system needs availability and consistency then it should use relational databases. NoSQL databases like MongoDB, Scalaris, BerkeleyDB and Redis confirm consistency and partition tolerance. On the other hand, Cassandra, CouchDB, Dynamo etc. provide availability and partition tolerance.

7 MongoDB feature: replication and sharding

For higher availability, data safety and recovery it is possible to apply the replication of data in MongoDB. A replica set in MongoDB is a group of mongod processes that maintain the same data set. Replica sets provide redundancy and high availability and are the basis for all production deployments. With multiple copies of data on different database servers, replication provides a level of fault tolerance against the loss of a single database server. (MongoDB, 2017 a)

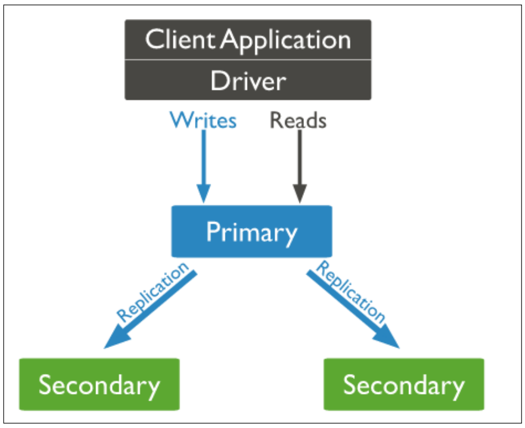

Figure 2: MongoDB replication

Source: (MongoDB, 2017 a)

Replication can also increase the read capacity. In a replicated environment, a client can send request to different servers. For distributed applications data locality and availability can be increased by maintaining copies of data in different data centers. Additional copies of data can be maintained for disaster recovery, reporting or backup. (MongoDB, 2017 a)

The process of replication in MongoDB is shown in Figure 2. Here applications communicate with the primary Mongod, and this primary machine can communicate with secondaries of replicated machines. If the primary machine has a network failure or faces any problem so that it cannot communicate with other members, then a new primary will be selected from the secondary mongod processes. This new member will be selected through an election. So, it is better to have at least three replicated members in the replicated environment.

Sharding is method to distribute data across multiple machines. Through sharding MongoDB promotes horizontal scalability of data. That means we can handle a huge amount of data through multiple machines. MongoDB has three components in a sharded cluster. MongoDB documentation described these components. (MongoDB, 2017 b)

- shard: Each shard contains a subset of the sharded data. Each shard can be deployed as a replica set.
- mongos: The mongos acts as a query router, providing an interface between client applications and the sharded cluster.
- config servers: Config servers store metadata and configuration settings for the cluster. As of MongoDB 3.4, config servers must be deployed as a replica set (CSRS).

In a sharded environment applications communicate with mongos router. Mongos router communicates with the config servers and also the shard. Each shard can have different replica sets. Figure 3 is showing the environment of a sharded cluster.

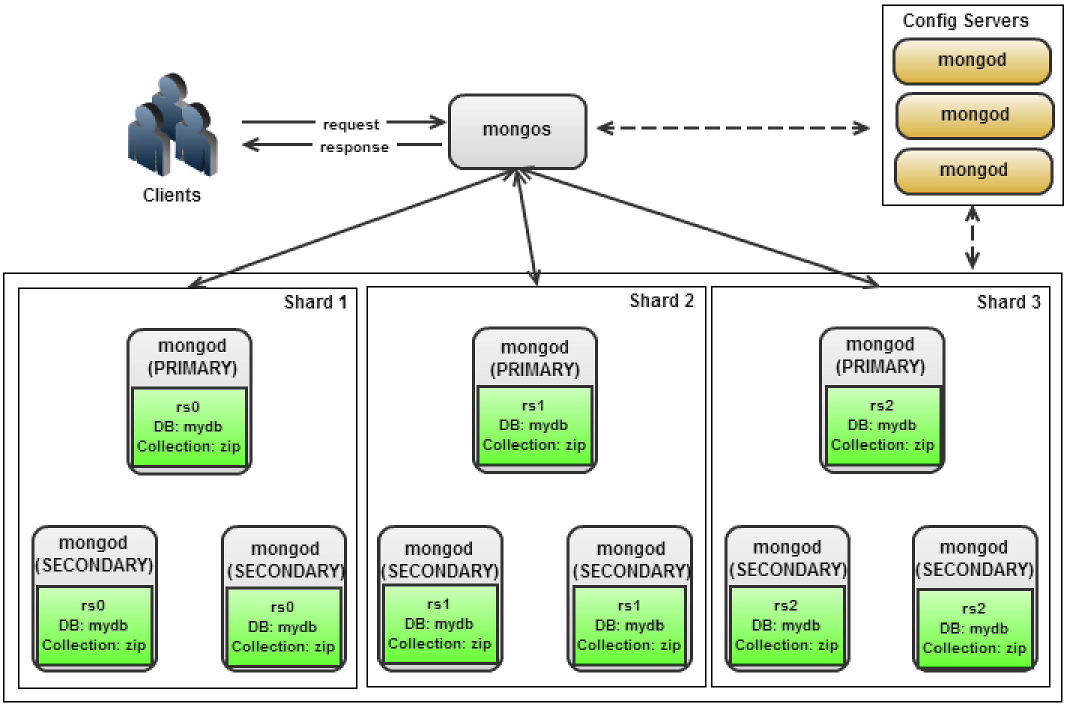

Figure 3: MongoDB sharding architecture

Source: (Severalnines, 2013)

8 MongoDB feature: aggregation framework

Aggregations operations process data records and return computed results. Aggregation operations group values from multiple documents together and can perform a variety of operations on the grouped data to return a single result. MongoDB provides three ways to perform aggregation: the aggregation pipeline, the map-reduce function, and single purpose aggregation methods. (MongoDB, 2017 c)

MongoDB's aggregation framework is modeled on the concept of data processing pipelines. Documents enter a multi-stage pipeline that transforms the documents into an aggregated result. The most basic pipeline stages provide filters that operate like queries and document transformations that modify the form of the output document. Other pipeline operations provide tools for grouping and sorting documents by specific field or fields as well as tools for aggregating the contents of arrays, including arrays of documents. In addition, pipeline stages can use operators for tasks such as calculating the average or concatenating a string. The pipeline provides efficient data aggregation using native operations within MongoDB, and is the preferred method for data aggregation in MongoDB. (MongoDB, 2017 c)

9 MongoDB feature: indexing

Indexes support the efficient execution of queries in MongoDB. Without indexes, MongoDB has to perform a collection scan that means it has to examine the entire document in the collection. If an appropriate index exists for a query, MongoDB can use the index to limit the number of documents it must inspect. MongoDB indexes use a B-tree data structure. Indexes are special data structures that store a small portion of the collection's data set in an easy to traverse form. The index stores the value of a specific field or set of fields, ordered by the value of the field. The ordering of the index entries supports efficient equality matches and range-based query operations. In addition, MongoDB can return sorted results by using the ordering in the index. (MongoDB, 2017 d)

In order to identify the power of indexing one simple query in MongoDB has been performed. In the database there were over 15 million tweet documents. The goal of the query is to get all the tweets from the databases that are retweeted over 100 times.

The query code in mongodb shell would be:

```
db.tweets.explain(“executionStats”).find({“retweet_count”: 100})
```

Table 2: power of Indexing

	With indexing	Without indexing
Execution time	108 seconds	56.38 minutes
Scan type	Index Scan	Full Column Scan
Result returns	13154	13154
Total Key Examined	13154	0
Total Document Examined	13154	15,498,769
Remarks	The number of documents and examined keys is equal to the document returned. That means the query process did not examined unnecessary documents.	Without indexing the system has to look all the documents. It takes excessively large amount of time for the query

Table 2 is showing the power of indexing. When the dataset was indexed, it takes less time to get the result compared to a dataset without indexes. When the dataset was efficiently indexed, the system only scanned the documents that matched with the query condition. On the other hand, without indexing, the system had to scan each and every document, wasting a lot time and making the system inefficient. For example shown above, the query returned 13154 documents, i.e., 13154 tweets in the database were retweeted exactly one hundred times. With indexing in the 'retweet_count' field, it took only 108 seconds to get the result where without indexing it took almost an hour. However, creating indexing for over fifteen million data took some time, on average almost thirty minutes to create an index for a particular field. Before running the query all the necessary fields were indexed first for saving considerable query time.

10 Hadoop

Hadoop is not a database but a whole system to store and process data. Here we can keep huge amount of data and also can process it. "Hadoop is a software technology designed for storing and processing large volumes of data distributed across a cluster of commodity servers and commodity storage. Hadoop was initially inspired by papers published by Google outlining its approach to handling large volumes of data as it indexed the Web. With growing adoption across industry and government, Hadoop has rapidly evolved to become an adjunct to – and in some cases a replacement of – the traditional Enterprise Data Warehouse." (MongoDB, 2016)

In computing world, we have computing resources and data to process. As data grow we have the option to increase our computing capacity as well. But with time data become so huge and grow very fast then it is not a good option to compute this huge amount of data over a single machine because of hardware cost, software cost and high risk of failure. Further computing resources have an upper limit of the amount of data that these can process. But data is growing continuously. Due to this problem, the concept of Hadoop came to light. In Hadoop, Instead of concentrating on one large machine the task is distributed over a cluster of machines. It has several advantages such as, low cost of hardware, reduced risk of failure, data processing time became shorter. Typical scenario now-a-days is 1 TB memory with transfer speed 100 MB/s. So time will take to read the whole drive is (memory/transfer speed) 2.8 hours. If we distribute 1 TB of data over 50 nodes then to read 1TB of data we need only 3.5 minutes. So, it is easily realizable that, in distributed environment huge amount of data can be processed in a faster rate. This is the core concept of Hadoop. It is designed to scale up from single servers to thousands of machines, each offering local computation and storage. The system does not rely on hardware for availability of data. This library was designed in a way, so that it can detect and handle failure at the application layer. (Apache, 2014)

The Hadoop platform consists of two key services. They are HDFS and MapReduce. Beside these, it includes other tools to address particular needs. The component of Hadoop ecosystem is shown in. figure 4.

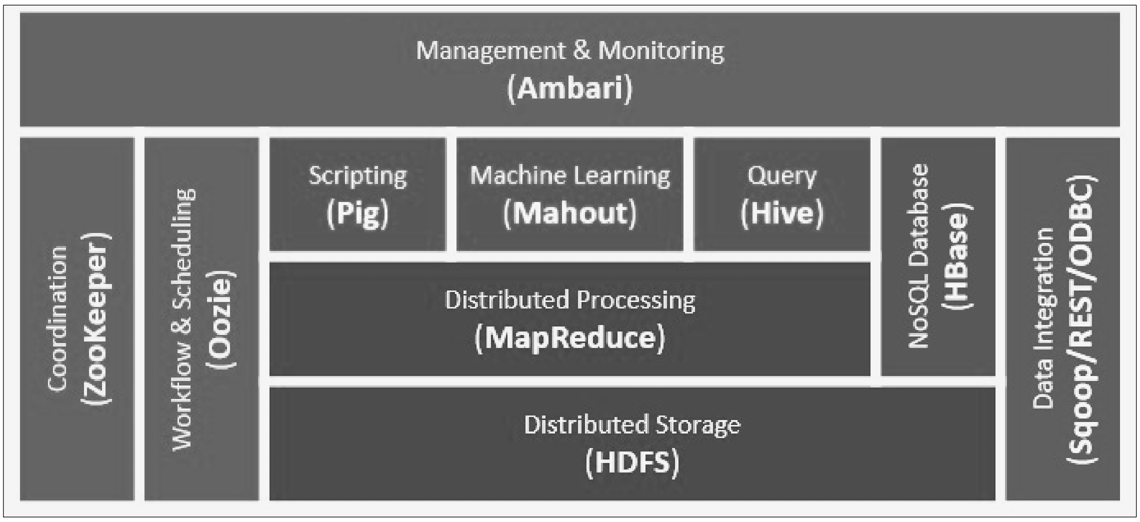

Figure 4: Components of Hadoop

Source: (Dezyre, 2015)

Apache Hadoop's documentation provides brief information about these components. Some information about Hadoop's components is given below.

- HDFS: Hadoop Distributed File System is designed to handle large amount of files (terabyte/petabytes) with sequential read/write operation. (Apache, 2014)
- MapReduce: it is the high performance parallel data processing engine. (Apache, 2014)
- HBASE: this is the NoSQL database that sits atop of HDFS. (pal, 2014)
- Zookeeper: This is basically a centralized system that maintains configuration, naming, synchronization. It is utilized by HBASE database and MapReduce jobs. (pal, 2014)
- Solr/Lucene: These are the search engines. The library was developed by Apache for over ten years. (pal, 2014)
- PIG: This is a high level data flow language. For parallel computation it provides execution framework. (Apache, 2014)
- Hive: Hive was developed by Facebook. It is a data warehouse built on top of Hadoop and provides a simple language known as HiveQL similar to SQL for querying, data summarization and analysis. Hive makes querying faster through indexing. (Dezyre, 2015)
- Sqoop: Sqoop component is used for importing data into Hadoop from external sources. It is also used for exporting data from Hadoop or other external structured data stores. Sqoop parallelized data transfer, mitigates excessive loads, allows data imports, efficient data analysis and copies data quickly. (Dezyre, 2015)
- Mahout: It is a scalable machine learning and data mining library. (Apache, 2014)
- Ambari: Ambari is a RESTful API which provides easy to use web user interface for Hadoop management. Ambari provides step-by-step wizard for installing Hadoop ecosystem services. (Dezyre, 2015)

In this research all components of Hadoop are not explored. Data is analyzed using Hadoop's two core components HDFS and Map Reduce.

11 HDFS architecture

HDFS is a place where data are kept. HDFS has three main components, they are, name node, data node and secondary name node. The name node is the master node and it keeps track of the storage cluster. It manages the file system namespace, regulates client's access and also operates system operations such as renaming, closing, and opening files and dictionaries. Data note is the slave node. It performs read-write operation on the file system. According to instruction of name nodes performs block creation, deletion and replication (Hadoop, 2013). In Hadoop, each file is broken into chunks; these chunks are then replicated on a minimum of three different servers, so that they can be used as an alternative to unforeseen circumstances. These chunks are also called blocks. Block size can be 64 megabytes or 128 megabytes. In some clusters block size can also be 256 megabytes.

Ricky Ho, 2008, described the way HDFS performs read and write operations. Based on the offset of the file pointer, the client API will calculate the chunk index and make a request to the name node. The name node will reply which data nodes has a copy of that chunk. Then the client contacts the data node directly without going through the name node. The architecture of Hadoop HDFS is shown in figure 5.

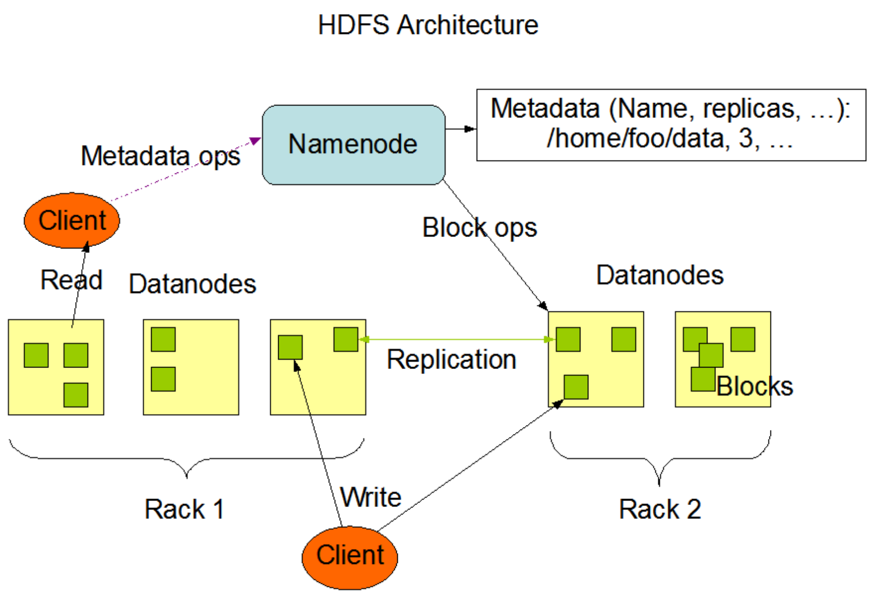

Figure 5: Hadoop HDFS architecture

Source: (Hadoop, 2013)

12 Hadoop Map Reduce

Ricky Ho, 2008, describes the process of MapReduce jobs in Hadoop. To initiate job execution client program needs to submit a job configuration to the job tracker. This configuration specifies the map and reduce functions as well as input and output path of the data. The job tracker will determine the number of splits from the input path. Based on network proximity they select some task tracker. Finally job tracker send task request to task trackers.

After that task tracker start the map phase processing by extracting the input data from the splits. It uses the user provided map function and parses the data and emits a number of key-value pair. When all the task trackers are done, the job tracker will notify the selected task trackers for the reduce phase. Each task tracker will read the region files remotely. It performs shuffle and sort of the key-value pairs that came from map phase. After that the reducer phase starts. In this reducer phase the input data will be the output of shuffle and sort phase. The output of reducer phase will also be key-value pairs.

In the case for big data, map reduce job can take long time to complete. In this long period of time any job tracker or task tracker can be crashed. In a map phase, if task tracker crashes then job tracker will reassign the map task to a different task tracker node, that will rerun the assigned splits. If the in reduce phase task tracker crashes, the job tracker will rerun the reduce program at a different task tracker.

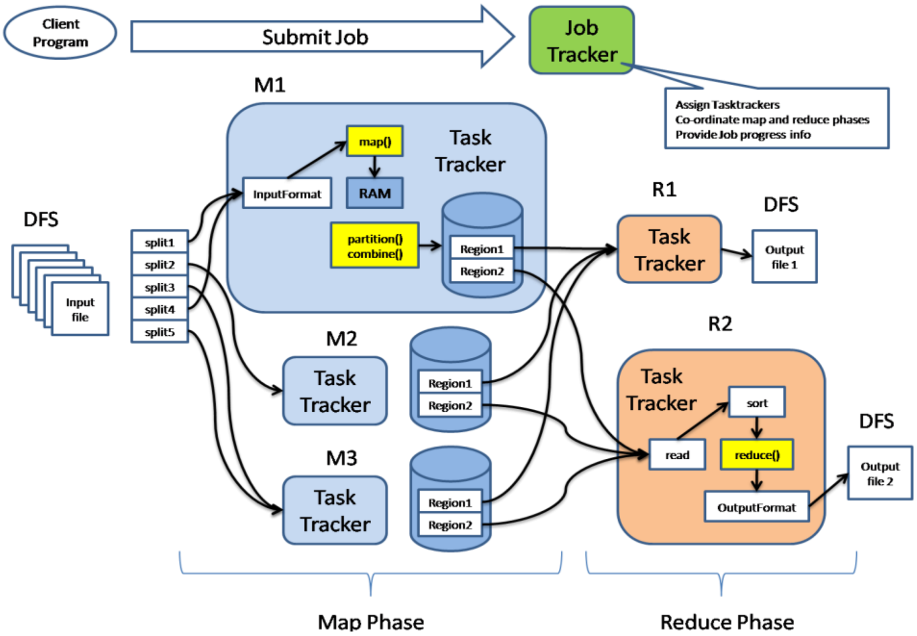

Figure 6: Hadoop Map reduce work procedure

Source: (Ho, 2008)

13 Conclusion

Handling, Managing and analyzing big data in the production environment are a huge challenge today. To deal with this huge data volume, variety and velocity, the performance of tabular databases is not up to the mark. Document-oriented databases are built for storing big data. The performance of these databases for managing a large set of data is way much better than tabular databases. They also provide handful number of useful operators and analysis pipeline for analyzing data. As there are a lot of options available for a data store, this creates confusion in selecting a particular option for an application. This research identified a solution for choosing a proper database for an application. In this research, MongoDB was used as a NoSQL database because it holds the top position in DB ranking among document-oriented databases. The inbuilt features of MongoDB are deeply analyzed and the environment for optimal performance was determined. On the other hand, Hadoop is a complete ecosystem for managing big data. It is not only a data store. It is possible to do more or less everything with big data by Hadoop. This research discussed two core Hadoop components: HDFS and MapReduce. The biggest advantage for both MongoDB and Hadoop is the capacity to work in a distributed environment. They scale out the data and put the data in a distributed system. So it is possible to work with big data efficiently using simple and low-cost machines. They also create replication of data that ensure the safety and availability of data during hardware or connection failure. In the end it can be said that through document oriented databases and Hadoop framework big data can be handled and managed efficiently.

References

Apache. (2014). Welcome to Apache™ Hadoop. The Apache Software Foundation.

DB-engines. (2017 a, March). MongoDB System Properties. Retrieved March 1, 2017, from DB-engines: http://db-engines.com/en/ranking

DB-engines. (2017 b, March). Amazon DynamoDB System Properties. Retrieved March 1, 2017, from DB-engines: http://db-engines.com/en/system/Amazon+DynamoDB

DB-engines. (2017 c, Match). Couchbase System Properties. Retrieved March 1, 2017, from DB-engines: http://db-engines.com/en/system/Couchbase

DB-engines. (2017 d, March). CouchDB System Properties. Retrieved March 1, 2017, from DB-engines: http://db-engines.com/en/system/CouchDB

DB-engines. (2017 e, March). DB-Engines Ranking - Trend of Document Stores Popularity. Retrieved March 1, 2017, from DB-engines: http://db-engines.com/en/ranking_trend/document+store

Dezyre. (2015, june). Hadoop Components and Architecture:Big Data and Hadoop Training. Retrieved Janyary 14, 2017, from https://www.dezyre.com/article/hadoop-components-and-architecture-big-data-and-hadoop-training/114

Gilbert, S., & Lynch, N. (2002, June). Conjecture and the Feasibility of Consistent, Available, Partition-Tolerant Web Services. ACM SIGACT, 33(2), 51-59.

Hadoop. (2013, A August). HDFS Architecture Guide. Retrieved December 14, 2016, from Haddop 1.2.1 Documentation: https://hadoop.apache.org/docs/r1.2.1/hdfs_design.html

Ho, R. (2008, December). How Hadoop Map/Reduce works. Retrieved October 21, 2016, from https://dzone.com/articles/how-hadoop-mapreduce-works

Hurst, N. (2010, March 15). Visual Guide to NoSQL Systems. Retrieved November 27, 2016, from http://blog.nahurst.com/visual-guide-to-nosql-systems

IBM. (2016). Bringing big data to enterprise. Retrieved November 22, 2016, from https://www-01.ibm.com/software/data/bigdata/what-is-big-data.html

MongoDB. (2016). What is Hadoop? Retrieved December 12, 2016, from https://www.mongodb.com/hadoop-and-mongodb

pal, k. (2014, October). Apache Hadoop and its Components. Retrieved October 26, 2016, from http://www.tutorialspoint.com/articles/apache-hadoop-and-its-components

SAS. (kein Datum). Big data history and current considerations. Abgerufen am 15. 1 2017 von https://www.sas.com/en_us/insights/big-data/what-is-big-data.html

Open Geodata for rapid just-in-time and task-adequate Data Provision for Disaster Management

S. Fleischhauer, F.-J. Behr

Stuttgart University of Applied Sciences, Germany – steven9490@gmail.com, franz-josef.behr@hft-stuttgart.de

KEYWORDS: *Disaster management, rapid mapping, geodata, OpenStreetMap, remote sensing, free software, free data*

ABSTRACT:

Statistics prove that the number of disasters, especially weather-related, increased during the last decades. This leads to high demands on participants in disaster management processes where the information base is an essential part in these processes. Geodata, as a part of this information base, play a key role.

This report shows an approach using geodata to support decision makers and helpers in disaster situations. In a preliminary theoretical consideration the potential of geodata in disaster management is explained by the results of the VALID study. The economic value is illustrated by the estimated cost savings within a case study. Evaluations by participants in disaster management illustrate the strategic and operational benefits for the use of significant geodata products. This background research delivers as well the requirement specification for geodata provision and related products. These requirements are based on the use of general information structures in disaster scenarios. Specific aspects for the application of geospatial information are accentuated.

To illustrate the state of the art this work gives an overview of existing concepts using geodata. The rapid mapping approach with remote sensing data illustrates the coordinated mapping process in consequence of a disaster event. The focus lies on the collaborative data acquisition based on the International Charter "Space and Major Disasters". Flood risk maps are an exemplary approach that shows the possible area-wide realization of a precautionary measure. The attention is focused on the mapping process and the position of politics as a driving force behind this realization. The geoinformation system SARONTAR is an approach of an operations control system for alpine regions. This concept combines real time communication features with satellite-based real time positioning. The system architecture and functionality are the main points of the explanation.

As an alternative, this work introduces a new concept of immediate geodata provision for disaster management based on the usage of free data and free software components. The data storage is partitioned into a file-based system and a database system. The functionality of every single system component and the process of implementation are explained. The two data sources, remote sensing data from the United States Geological Survey (USGS) and vector data from the OpenStreetMap (OSM) project, are examined in detail regarding data structure and the form of data provision. In the examination of the remote sensing data there is a comparison between USGS's offers and the Copernicus Programme of the European Union in relation to the data provision.

In the implementation of the system takes batch script controls every software component and data flow. During this workflow the user specifies interactively the OpenStreetMap data for this area are downloaded using regional data extracts or automatically using the Extended OpenStreetMap Application Programming Interface. Osm2pgsql stores this data as geospatial objects in a PostGIS database. By processing incremental update information the vector data of the disaster area are kept up-to-date. The satellite images are converted by the Sentinel Applications Platform to a RGB raster image. A sub-programme of the Geospatial Data Abstraction Library re-projects this raster image to the consistent target spatial reference system World Geodetic System 84/Pseudo Mercator.

The render software Mapnik uses both data sources to create mapping tiles of the affected area. The style sheet is optimized for visualization of disaster related information. The image tiles are suited for immediate use by end-users in disaster management and can be provided on a web-server

The presented system makes it possible to provide geodata for disaster management purposes within minutes.

1 INTRODUCTION

Disasters are an omnipresent phenomenon. Statistics of the Munich Re (Munich Re, 2015) and of the United Nations Office for Disaster Risk Reduction (UNISDR, 2012) show an increasing number of disaster situations during the last three decades. The devastating effects are evidenced by the total extent of damage. From 2000 to 2012 material damages in the amount of US$ 1.7 trillion and a loss of 1.2 million human lives worldwide were recorded (UNISDR, 2013).

These numbers show the importance of efficient disaster management. One fundamental element in the disaster management process is the basis of information and in particular geospatial information, as the Spatial Data Infrastructure Germany (GDI-DE) committee, an initiative of public authorities in Germany, states (Ostrau et al., 2013): „The Management […] of disasters require static geodata (for certain areas) as well dynamic geodata (i.e. flooded areas)." The general benefits of the use of geoinformation in disaster scenarios are discussed in the VALID study by the United Nations. Its results regarding the economic and strategic value of geodata are presented in the following section.

From a variety of solutions using geoinformation to support the disaster management this work will present some existing concepts to point out the state of the art.

A requirements specification will show criteria taken into consideration during the conception phase of the approach presented here.

Some definitions will be helpful for the further sections. IFRC (2011) describes a disaster as "a serious disruption of the functioning of society, which poses a significant, widespread threat to human life, health, property, infrastructure or the environment, whether arising from accident, nature or human activity, whether developing suddenly or as the result of long-term processes, but excluding armed conflict."

According to the Copernicus website (European Commission, 2017) rapid mapping "consists of the […] provision (within hours or days) of geospatial information in support of emergency management activities immediately following an emergency event. The products are standardized." *Reference Maps* show the boundaries, names and unique identifiers of standard geographic areas, as well as major cultural and physical features, such as roads, railroads, coastlines, rivers and lakes, i.e. topography, *delineation maps* the extents of the area affected by the disaster and *grading maps* present the assessment of the damage grade and its spatial distribution.

The main part of this paper describes an alternative concept of a geoinformation system (GIS) for disaster management support. The description of the process and its architecture depicts the functionality of the system with all its components. We will show that a mapping solution can provide reference maps and delineation maps rapidly within minutes or a few hours. The reference map will be created based on the worldwide data coverage of the OpenStreetMap database, complemented by remote sensing imagery. Assessment of the damage grade could be done additionally afterwards based on remote sensing products.

2 THEORETICAL CONSIDERATION

Before going into details regarding the technical implementations of geoinformation systems in disaster scenarios it has to be determined which status geoinformation has in the field of disaster management. These theoretical considerations provide the basis for subsequent sections.

2.1 Benefit assessment of geodata in disaster management

One basic question is to what amount users benefit from the usage of geoinformation in disaster situations. The United Nations Platform for Space-based Information for Disaster Management and Emergency Response (UNSPIDER) in cooperation with the Joint Board of Geospatial Information Societies (JB GIS) and scientists from the University of Amsterdam created the VALID study to evaluate the economic value and the strategic and operational benefits (Altan et al., 2013)

The 2009 flood catastrophe in Namibia served as case study for the monetary evaluation. Stakeholders had to estimate the potential cost savings for the use of a flood early warning system in this scenario, yielding a final result of 40% of cost savings.

The strategic and operational benefits were determined by two online surveys. In the first survey participants had to choose the most important geoinformation items for disaster management. Out of the responses the ten most frequently mentioned (regarding floods, earthquakes and drought) were used again in a second survey (Altan et al., 2013:23). The participants had to estimate the strategic and operational benefits of these ten geoinformation products. The responses showed appreciation for risk and vulnerability maps. For all strategic and operational aspects of every single product the benefits were valued medium to high. Benefits for preventions measures, economic loss reduction and for the usage in both disaster prevention and management were estimated high.

2.2 Requirements specification

In the conception of geoinformation processing systems it is important to incorporate the conditions and requirements of the field of application, i.e., disaster management. The Open Geospatial Consortium (OGC) has published a discussion paper with theoretical aspects for the conception of information structures in disaster management (Penman et al., 2015). Out of these considerations the following points can be adapted for the conception and usage of geospatial information structures for rapid mapping:

- Reliable data basis,
- Data of different sources,
- Predefined formats and interfaces,
- Possibility to integrate optional new data sources,
- Application of data under supervision of experts,
- Access control by user authentication,
- Comprehension and transparency of information,
- Predefined symbology.

Other aspects mentioned by Penman et al. (2015), like alert messages and independent network, are not part of the solution presented here. Further design considerations however were:

- Rapid provision of geodata,
- Availability for everyone instead of a limited group of people, especially for local actors (IFRC, 2011:9), and accordingly,
- Usage of free/respectively open source software and data.

3 STATE OF THE ART

After the evaluation of the benefits of geodata and the delineation of the requirements some existing approaches in the field of disaster mapping are described.

3.1 Collaborative remote sensing data acquisition

In 2000 the International Charter "Space and Major Disasters" was created to allow an immediate data acquisition for disaster situations. The approx. 16 members of this charter include inter alia the French and the European Space Agency, the National Oceanic and Atmospheric Administration (NOAA) and the Indian Space Research Organization (ISRO) (https://www.disasterscharter.org/web/guest/about-the-charter). To activate the charter an access point is established. Authorized institutions can start a data acquisition cycle in case of a disaster situation through request to this access point. Under the administration of a project manager appropriate satellite data from a wide range of sensors are requested from archives as well as active satellites are programmed to record new images of the disaster area. The acquired data can be processed in the affected country to create maps via interpretation algorithms and analysis. For example radar images are suitable for the identification of flood areas whereas optical images are appropriate for fire disasters or visual damage mapping after earthquakes (Danzeglocke, 2014).

As charter member the DLR Center for Satellite Based Crisis Information (ZKI) provides a permanent service for the rapid provision, processing and analysis of satellite imagery (Voigt, 2013). The focus of this approach is the current provision of processed imagery and its analysis and interpretation, not of reference maps. However, as DLR (2017) points out, the “Charter has committed resources to support [only] some specified authorised users such as relief organisations as well as civil protection and defence organisations with free of charge satellite data in order to help mitigating the effects of disasters”.

3.2 Volunteered Geographic Information (VGI)

If a disaster strikes often the OSM community like the Humanitarian OpenStreetMap Team (HOT, http://hotosm.org/) is activated to collect additional data for the affected area. Following the crowd sourced approach of OpenStreetMap the data are contributed on a voluntary basis. The contribution for the mitigation of the Haiti earthquake disaster is one of most prominent examples (Neis et al., 2010, Neis & Zielstra, 2014).

According to the Annual report there were five activations of HOT in 2015 due to disaster situations. In the course of the earthquake in Nepal in April 2015 over 8000 people contributed more than 13 million edits (HOT, 2015).

3.3 Flood hazard maps

Altan et al. (2013) have shown that flood related geoinformation items have a high impact in disaster management. *Flood hazard maps* visualize information about potential flood hazards from a relatively common to an extreme scenario and probability (Müller et al., 2009). Like *flood risk maps* they are defined in the EU Floods Directive 2007/60/EG. This policy instructed the member countries of the European Union to create both type of maps for significantly vulnerable areas until 22 December 2013. According to article 10 of the policy these maps have to be available for the public. German states provide them web-based by administrative authorities.

Based on a risk analysis for every area in accordance with the determinations in article 5 of the EU Floods Directive 2007/60/EG data has been collected by terrestrial surveying. The flood hazard maps can be derived from this data blended with a digital terrain model and hydraulic models. Starting 22 December 2019 the update frequency will be six years.

3.4 SARONTAR

The system SARONTAR results from a cooperation between the University of Technology Graz, the alpine police and the telecommunications company TeleConsult Austria. In two implementation phases they created an operation control system for accidents and disasters in the Alpine region. The system architecture consists of mobile terminals, a mission control centre and a central server component (Prüller et al., 2015). The purpose of this approach is to coordinate the rescue forces on site to supply affected people efficiently. The rescue workers navigate with the mobile terminals in the destination area via satellite-based DGPS (Hofmann-Wellenhof, 2010). On these mobile devices runs the SARONTAR application that visualizes the current position on a map and allow communication with the operation control centre. On the other side the movement of the rescue teams can be monitored and corrected through instructions if necessary. The used maps are official topographic maps provided through a map service. In a pilot stage in 2015 the system was tested under real conditions (Prüller et al, 2015). The core aspects of this approach are real-time communication and positioning in dynamically changing rescue missions.

4 CONCEPT

This work provides an alternative concept of a geoinformation system for the use in disaster scenarios. The main task is to provide geodata in separate data storage and visualize it as reference map delineating the extents of the affected area. The concept is extents the work of Hellal (2012). It is based on the usage of free software and free data combined in a multi-tier architecture as depicted in Fig. 1 comprising

- Data import tier
- Data tier
- Application and styling tier
- Presentation and export tier

The user defines the extent of the disaster area. This area is used as a region of interest for data acquisition in the data import segment. OpenStreetMap (OSM) data can be exported in different ways using the Extended OSM API or regional extracts. The export results are imported into a PostgreSQL database with osm2pgsql. Afterwards the user chooses a suitable satellite image based on the defined polygon. The system uses the Sentinel Application Platform (SNAP) to convert the remote sensing product into a geocoded RGB raster image. *Gdalwarp*, part of the *Geospatial Data Abstraction Library* (GDAL), serves to re-project the converted satellite image to a uniform target spatial reference system World Geodetic System 84/Pseudo Mercator. The stored data in the data tier can be visualized with the render software *Mapnik* in the application tier. The result of the concept is a map, which can be used in to support the disaster management tasks. There is also an option to update the OSM data in the database. With Osmosis replication files can be exported from OSM and the changes within the affected area imported into the existing database using *osm2pgsql*.

5 WORKFLOW

5.1 Preparation

The conceptualized system was labelled “disasterGIS” and implemented for Windows 10 due to the potentially wider range of users1, according to the experience of the authors especially in public authorities. A central batch script controls the several system components and the data stream during the mapping process. Therefore the interaction with the user primarily takes place in the windows console.

The final version requires PostgreSQL with PostGIS extension, Python 2.7, the Sentinel Application Platform and an executable version of GDAL as prerequisites. In addition the user has to set environment variables for the main executables of these tools. Other system components are directly integrated in the folder structure of the disasterGIS provided as a portable zip archive

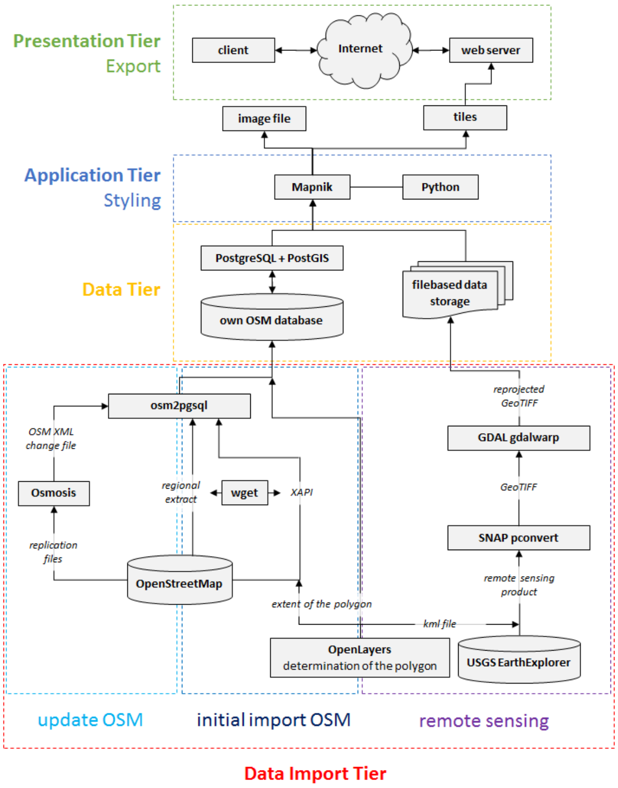

Figure 1. System architecture and components

The archive contains a README file that provides the necessary instructions for the setup of the system.

During the mapping workflow the user is guided by instructions in the console window. Export results are stored inside a separate project folder in disasterGIS.

As first step the script creates a new local PostgreSQL database with PostGIS and hstore extension. For each database operation the user has to authenticate himself by user id and password.

After the preparation of the database a local web browser opens a HTML document referencing the OpenLayers library. In the appearing map window the user navigates to the affected area and delineates its extents. When closing the map window the coordinates of this rectangle (in WGS 84) are transferred to the clipboard. The user can paste the coordinates to the console window to continue the mapping process. After confirming the coordinate input the script creates a KML file used for the satellite image acquisition in later steps of the workflow.

[1] See Desktop Operating System Market Share Worldwide http://gs.statcounter.com/os-market-share/desktop/worldwide/

5.2 Import of OpenStreetMap vector data

There are two options implemented to obtain OSM data for the reference map. On the one hand the disasterGIS processes regional extracts based on administrative boundaries (see https://wiki.openstreetmap.org/wiki/Processed_data_providers and https://wiki.openstreetmap.org/wiki/Planet.osm#Regional_extract_sources). The user is redirected to the website of Geofabrik GmbH, a provider of regional OSM extracts on a daily basis (http://www.geofabrik.de/en/data/-download.html). It is necessary to manually choose a suitable PBF-encoded file and paste the URL in the console window. After confirmation the batch script retrieves the file using wget and saves it to a predefined folder.

On the other hand the OSM Extended API (XAPI, http://wiki.openstreetmap.org/wiki/Xapi) is supported as second option. Based on the disaster extent a bounding box is submitted. Main advantage is the automatic retrieval of OSM data in uncompressed OSM XML format, using again wget.

The standard OSM API was not used because of its limitations in the amount of data; however the Overpass API (http://overpass-api.de/) could be additionally integrated.

The script now parametrizes osm2pgsql to import the downloaded data into the PostGIS database.

As an alternative Osmosis (http://wiki.openstreetmap.org/wiki/Osmosis) was tested. This command line based tool uses database schemas similar to the original OSM data structure. A disadvantage is the lacking support of areal features. Even the manual creation of areal features using SQL queries cannot compete with osm2pgsql's result. Therefore osm2pgsql is the preferred database import tool, but Osmosis is used to synchronize the data with updates of the central OSM server (see section 5.5).

5.3 Import of remote sensing data

Remotely sensed data from satellite-borne or airborne sensors are widely used in disaster mapping (Theilen-Willige & Wenzel, 2011; NASA, 2015; FSD, 2017). In the approach described here satellite-borne remote sensing data are incorporated. The United States Geological Survey (USGS) *Earth Explorer* (https://earthexplorer.usgs.gov/) serves as basis for satellite images. The web portal provides for example Landsat-8 and Sentinel-2 mission images as free data. The data offered by EU's Copernicus platform (https://scihub.copernicus.eu/) could not be integrated into this study due to technical limitations in November 2016.

The rectangular extent of the disaster area is used to create a KML file which is used in Earth Explorer as region of interest. The user still has to download manually suitable datasets completely covering the affected area without cloud coverage.

The Sentinel Application Platform's sub-programme *pconvert* (SNAP, http://step.esa.int/main/toolboxes/snap/), converts each file to GeoTIFF, a format supported by the rendering components. Because of the identical index of the spectral bands for Landsat-8 and Sentinel-2 mission products only these two types of satellite images are allowed in the disasterGIS.

The link between the downloaded satellite image and the batch script is a metadata file in the extracted dataset. Its file path has to be inserted in the console window to continue the conversion process with *pconvert*. After this CPU- and time-intensive process the satellite image is saved. Because the geocoding refers to WGS 84 the image still has to be re-projected by GDAL's *gdalwarp* tool to the uniform target spatial reference system WGS 84/Pseudo Mercator.

5.4 The rendering process

Vector and raster data are now available in the platform's data tier. *Mapnik* (http://mapnik.org/), a well-known render tool for various OSM maps, is used to generate a map image using the Python bindings (with Python 2.7 as additional prerequisite).

The main batch script creates now an additional project-specific script which starts the rendering process after the termination of the main script. Currently rendering is based on a former OSM XML style with some modifications to reduce the density of information and to emphasize the transport infrastructure to support navigation and logistics. Raster tiles and/or a raster image of the affected area are created.

5.5 Updating the local database

To synchronize the local database with the central OSM database, i.e. to retrieve collaboratively collected data from the OSM community, an update mechanism has been implemented. Replication files, also known as replication diffs, contain changes within a specific period of time. In the main batch script the user chooses the period from the options minutely, hourly and daily (see http://wiki.openstreetmap.org/wiki/Planet.osm/diffs). At first the command line based programme Osmosis initializes a working directory while the main batch script creates a configuration file that determines the update rhythm with the chosen option. The main script also generates a project-specific update script similar to the render batch script. After this step the disasterGIS project is completed and ready to be visualized or updated.

Updating the project data is done by *Osmosis*. With the period of time from the configuration file Osmosis compares the timestamp of the local state file with the timestamp of the state file on the OSM servers. If the time difference is greater than the defined time period Osmosis requests all OSM data changes in *osmChange format* up to the last point of update. To transfer the data changes into the database osm2pgsql is used again, however in append mode. Thereby the new data are appended to the existing data instead of overwriting it. By using a bounding box only the relevant information for the disaster area will be stored in the database.

Figure 2. Exported image file of a disasterGIS project

5.6 Results

The final products of the mapping process in disasterGIS are tiles or images of the affected area. A printout of an image (see Figure 2) for example can be used as an overview map and be distributed among the auxiliary staff. In case of the collapse of communication infrastructures in the disaster area these printed maps can provide a current overview.

In comparison to the raster image the tiles have to be provided via webserver. Figure 3 shows a mapping client accessing the disasterGIS server.

Figure 3. Tile-based visualization of flooded areas (flood event in India, 2016, data © OpenStreetMap-Contributors, USGS)

The tile-based map presentation can be retrieved via stationary and mobile devices with internet access.

6 Summary and Conclusions

6.1 Outcomes

Geodata are a key resource in successfully handling disaster situations. The results of the VALID study prove the positive effects of the application of geospatial information in disaster management in both economic and operational regards. Cost savings around 40% illustrate the monetary potential for a specific case study. Experts in disaster management also acknowledge a medium to high additional value in the use of geoinformation in all strategic and operational aspects.

The disasterGIS provides an alternative approach for a geoinformation-based solution of free software components using freely available data to create reference maps for disaster management. In the crisis management cycle, the response phase is the one where immediate access to information and different resources is needed. DisasterGIS can provide geospatial information very rapidly within minutes or a few hours.

Regarding the requirements specification (see chapter 2.2) most of the mentioned criteria are implemented. DisasterGIS provides an automated, rapid workflow to create a reference map. The system is easy to deploy/to install, for small and large public agencies and NGOs, for any nations.

Another particular aspect regarding the relevance of geoinformation is its actuality. The data sources used provide a medium to high topicality: Landsat-8 and Sentinel-2 have a repetition cycle of 10 to 16 days, OSM data can be up-to-the-minute. DisasterGIS can take the advantage of data updates in disaster areas due to crowd mapping events (see chapter 3.2). It offers a continuous synchronisation with the central OpenStreetMap database to retrieve collaboratively collected data from the communities like HOT. This approach enables also local actors to collect and provide geospatial information.

The cartographic presentation is controlled by a style file. Modification can be applied to support local map styles, even using with toponyms in different languages.

The disasterGIS approach distinguishes itself from the approaches mentioned in chapter 3:

Compared to the “Collaborative remote sensing data acquisition” approach the disasterGIS is available for everybody, not only for a limited group of organisations. In addition the mapping process takes less time. A disadvantage however is the smaller number of available satellite missions and the lack of further analysis of the data.

The volunteered geographic information of the OSM community (see chapter 3.2) is essential part of the disasterGIS as OpenStreetMap is a main data source.

Flood hazard maps, as shown for the EU member states, provide full areal coverage of reference data with consistent quality and high reliability whereas the coverage of OSM data in the proposed reference map differs between urban and rural regions and different regions/countries. Both approaches address however different phases of the disaster management cycle (prevention vs. response phase). The flood hazard maps are characterized by long update intervals compared to the reference maps created by disasterGIS.

Regarding the SARONTAR system disasterGIS can be an addition instead of an alternative. It is conceivable that the map tiles generated with disasterGIS can be used as map background for the interactive map services like SARONTAR.

6.2 Limitations and potential extensions

In general there are areas of improvement in disaster management. The lack of interoperability is one aspect. Bartels (2015) cites security and privacy concerns as well as the competitive situation as possible reasons for obstacles to data sharing. Developing interoperable systems for disaster management bears financial risks and the needs-based conception is a precarious point. National and international infrastructures for spatial information, e.g. the European Spatial Data Infrastructure (INSPIRE), can play a decisive role. With disasterGIS the geodata collected in the data tier can be made available using standardized OGC web services (e.g., WMS and WFS).

The current version of disasterGIS is executable under Windows 64 bit because some components are not available as 32 bit versions. Although disasterGIS is currently implemented under Windows it is possible to implement the system architecture under a Linux distribution too. The port to Linux is planned as a next step. The mapping products of disasterGIS – geodata, map images and tiles – can be used however independent of the operating system.

Currently two data sources are integrated in disasterGIS. Due to the plugin architecture of Mapnik to a variety of formats additional data sources could be supported.

Concerning the accuracy both type of data are sufficient for orientation and navigation in disaster management. The ground resolution of the satellite images amounts to minimum 10 m. OSM’s data positional accuracy, usually captured with civil GNSS accuracy, is also around 10 m. However as another potential resource for disaster management UAV-based imagery could be integrated after processing and rectification. The immediate operational readiness and better ground solutions have advantages compared to satellite imagery. In conjunction with the rapid data provision presented here this would be an interesting contribution to the generation of near real-time ground information.

References

Altan O., Backhaus R., Boccardo P., Tonolo F. G., Trinder J., van Manen N., Zlatanova S. (eds.), 2013. The Value of Geoinformation for Disaster and Risk Management (VALID) Benefit Analysis and Stakeholder Assessment . http://www.un-spider.org/sites/default/files/VALIDPublication.pdf [2017-05-22]

Bartels, M., 2015. Warum scheitern interorganisationale Katastrophenmanagementsysteme bisher? In : Akteure verbinden, Lösungen finden - Katastrophenvorsorge im Dialog zwischen Wissenschaft und Praxis. 14. Forum Katastrophenvorsorge. Bonn, Leipzig: Dt. Komitee Katastrophenvorsorge (DKKV-Publikationsreihe), pp. 24–25. http://www.dkkv.org/fileadmin/user_upload/Veroeffentlichungen/Publikationen/DKKV_54_14._Forum_Katastrophenvorsorge.pdf [2017-05-22]

Danzeglocke, J., 2014. Hochwasserkatastrophen – Unterstützung aus dem All. In: Zeitschrift für Vermessungswesen 139 (1/2014), pp.. 50–53

DLR, 2017. International Charter 'Space and Major Disasters'. https://www.zki.dlr.de/services/charter [2017-05-24]

European Commission, 2017. Service Overview. http://emergency.copernicus.eu/mapping/ems/service-overview [2017-05-22]

FSD – Swiss Foundation for Mine Action, 2017: Drones in Humanitarian Action – A guide to the use of airborne systems in humanitarian crises. http://drones.fsd.ch/wp-content/uploads/2016/11/Drones-in-Humanitarian-Action.pdf [2017-05-26]

Hellal, K., 2012. Rapid Mapping to Support Disaster Management based on Open Sources. Unpublished Master’s Thesis, Stuttgart University of Applied Sciences, Germany

Hofmann-Wellenhof, B, 2010: Der Alpenraum und seine Herausforderungen - manchmal ein Wettlauf mit der Zeit. Graz. http://www.tzs.at/fileadmin/TZS/Intra-net/PDF/Hofmann-Wellenhof_geschuetzt_Gmunden_24-11-2010.pdf [2017-01-03].

Humanitarian OpenStreetMap Team (HOT), 2015. 2015 Annual Report - Mapping Our World Together. https://www.hotosm.org/sites/default/files/HOT_2015_Annual_Report.pdf [2017-05-25].

International Federation of Red Cross and Red Crescent Societies (IFRC), 2011. IDRL Guidelines Guidelines for the domestic facilitation and regulation of international disaster relief and initial recovery assistance. http://www.ifrc.org/PageFiles/41203/1205600-IDRL%20Guidelines-EN-LR%20(2).pdf [2017-05-22]

Müller, M.; Panczak-Geörg, M.; Mattes, E.; Ellmenreich, B.; Schillinger, W.; Moser, M. et al. (2009): GIS-Einsatz zur Web-basierten Darstellung von Hochwassergefahrenkarten in Baden-Württemberg. In zfv 134 (6/2009), pp. 333–339

Munich Re, 2015. Loss events worldwide 1980 – 2014. http://www.preventionweb.net/files/44281_19802014paketworldusde4zu3.pdf [2017-05-22]

NASA, 2015. Landsat 8 Reveals Extent of Quake Disaster in Nepal's Langtang Valley. https://www.nasa.gov/jpl/landsat-8-reveals-extent-of-quake-disaster-in-nepal-s-langtang-valley [2017-05-22]

Neis, P., Singler, P., Zipf, A., 2010. Collaborative Mapping and Emergency Routing for Disaster Logistics—Case Studies from the Haiti Earthquake and the UN Portal for Afrika. In Proceedings of the Geoinformatics Forum, Salzburg, Austria, 6–9 July http://koenigstuhl.geog.uni-heidelberg.de/publications/2010/Neis/un-osm-emergency-routing.gi-forum2010.full.pdf [2017-05-26]

Neis, P., Zielstra, D., 2014. Recent developments and future trends in volunteered geographic information research: The case of OpenStreetMap. Future Internet, 6(1), 76-106 2010 http://www.mdpi.com/1999-5903/6/1/76/htm [2017-05-26]

Ostrau, S. et al., 2013. Einsatz von Geoinformationen in den Kommunen. Ergebnisse der Umfrage, Good Practice Beispiele, Handlungsempfehlungen. http://www.geoportal.de/SharedDocs/Downloads/DE/GDI-DE/-KoKoStudie_Einsatz_Geoinfo_Kommunnen.pdf?__blob=publicationFile [2017-05-22]

Penman, J.; Knudson, J.; Luraschi, G. (2015): OGC 15-095 Emergency and Disaster Management Information Framework. Version 0.0.2. Open Geospatial Consortium. https://portal.opengeospatial.org/files/?artifact_id=66868 [2017-05-22]

Prüller, R., Fösleitner, C., Sommer, C., 2015. SARONTAR – ein Einsatzleitsystem für Notfälle in alpinen Regionen. In: Josef Strobl (Hg.): AGIT 1-2015. Journal für Angewandte Geoinformatik. Berlin: Wichmann, S. 252–257. http://gispoint.de/fileadmin/user_up-load/paper_gis_open/AGIT_2015/537557036.pdf [2017-05-22]

Theilen-Willige. B., Wenzel. H., 2011. Remote Sensing And GIS Contribution to Earthquake Disaster Preparedness in Hungary. GeoInformation for Disaster Management Gi4DM, 03/05/2011 - 08/05/2011, Antalya, Turkey. http://www.isprs.org/proceedings/XXXVIII/Gi4DM/CDDATA/sessions.html [2017-05-25]

UNISDR, 2012. Number of Climate-related Disasters Around the World (1980-2011). www.preventionweb.net/files/-20120613_ClimateDisaster1980-2011.pdf [2017-05-22]

UNISDR, 2013. DISASTER IMPACTS / 20002012. http://www.preventionweb.net/files/31737_20130312disaster20002012copy.pdf [2017-05-22]

Voigt, S., 2013. DLR Center for Satellite Based Crisis Information. In: Altan et al. (2013).

Identifying and Development of Wetlands as Flood Retention Areas of the Flood Management System in Galle City

Pubudu Kalinga

Strategic Cities Development Project, Ministry of Megapolis and Western Development, Sri Lanka.

KEYWORDS: *Flood Management, Flood Model, GIS, Drone Survey, Galle City*

ABSTRACT:

In recent decades, the city of Galle experienced number of flooding events. Therefore, rehabilitation of drainage network to reduce the flood risks in the Galle city area has been identified as a prime concern and Galle Municipal Council has been commissioned to carry out its designs. The drainage network of the Galle city mainly consists of three streams: Moragoda ela, Mode ela and Kepu Ela. These streams take the excess storm water from cross-drains, which are fed by outflow from road side drains, into the sea. In design step, MIKE 11 flood model has been utilized to design cannel network. Simultaneously, it was planned to connect the flood retention areas to canal network for controlling flash floods effectively. This study was focused to identify possible wetlands/lowlands to be developed as flood retention areas, demarcate the flood retention areas, improvement of connectivity among wetlands and the canal network, identify green channels development across the wetlands and estimate retention capacities. Available spatial data and drone survey have been utilized for data collection and analysis. The digital elevation model (DEM), available landuse (i.e. wetland characteristics hydrology, retention capacity, effective extent and green channel possibilities) and flood levels which are derived from the MIKE11 model were employed to determine possible wetlands connected to canal network and connectivity improvements. Eight number of retention areas which can be connected to cannel network and single green channel are identified from the study.

Using Digital Terrain Models for the Assessment of Flood Risks

Dietrich Schröder

Stuttgart University of Applied Sciences, Germany – dietrich.schroeder@hft-stuttgart.de

ABSTRACT:

The damage and losses caused by flash floods hazards are an increasing phenomenon worldwide. There are numerous causes for this increase like the ongoing urbanization, the sealing of land, the increase of the population worldwide or the climate change which will result in higher atmospheric energy transportation leading to more strong rain events in many areas. Thus the demand of evaluation of areas according to their flash flood risk is getting more and more important. Digital Terrain Models (DTMs) are the starting points for the analysis and simulations of flood prone areas. Terrain characteristics will, beside the infiltration rate and the evapotranspiration will determine the discharge behavior of a catchment area. Depending on the target scale of the simulations, two main concepts are in use: topographic risk analysis based on the geomorphology of a terrain using GIS and 2D hydraulic analyses using specialized software to solve numerically the differential equations modelling the flow behavior. For both types of analyses DTMs are the most crucial input. For the large scale hydraulic modelling very detailed DTMs are needed, based e.g. on LiDAR data with resolution of one meter or even sub-meter enriched with additional structural information, whereas for a coarse small scale geomorphological analysis worldwide available DTMs like SRTM digital elevation data, ASTER GDEM or AW3D with 30m resolution may be used.

In this presentation both approaches will be discussed and fields of application will be shown. A special focus is set on the characteristics of the DTMs used as input. The hydraulic approach will be discussed first with the Heavy Rain Risk Maps produced for many communities in Germany and secondly by climate change scenario simulations for a river system in the Philippines. The geomorphological approach will be discussed mainly by the example of a project in Sinai Peninsula, extended by some other study areas showing different terrain characteristics.

In addition, a short overview of software tools available for analysis and simulation will be given and a possible workflow implemented in ArcGIS for the geomorphological analysis used for the classification of sub-basins related to flash flood risk will be discussed. The examples used in this presentation will highlight some of the ongoing research projects at HFT Stuttgart, Germany.

Radar Remote Sensing: Basics, Applications and Its Potential in Land Deformation Monitrong

Yasser Maghsoudi Mehrani

Faculty of Geodesy and Geomatics Engineering, Khaje Nasir Toosi University of Technology, Tehran, Iran

ABSTRACT:

The Workshop is split into three main parts. The first part covers the fundamental principles of SAR remote sensing and its applications. RADAR remote sensing is the start of new explorations in the field of satellite remote sensing. In active remote sensing, the antenna uses its own source of energy such as microwave. The antenna transmits the signal toward the objects and collects the reflected or backscattered signal from the target. Synthetic aperture radar (SAR) is a form of radar which is used to create images of objects, these images can be either two or three dimensional representations of the object. SAR can be mounted on a moving platform such as an aircraft or spacecraft, successive pulses of radio waves are transmitted to "illuminate" a target scene, and the echo of each pulse is received and recorded. This workshop will give the theoretical foundations of important aspects of radar remote sensing, and provide the students a sufficient introductory to explore specific applications in more detail. We will also talk about the main influencing parameters on the SAR backscatter including the system and target parameters. The systems parameters comprise frequency, polarization, incident angle and the look angle whereas the target parameters include the geometry, structure, dielectric constant and the local incidence angle. Some applications of the Radar remote sensing will be explained in this workshop. In the second part of this workshop, we will continue with polarimetric SAR data and learn how to visualize polarimetric quantities and to find meaningful representations of polarimetric information. Various ideas and concepts will be addressed such as coherent and incoherent decomposition techniques. The workshop will help to gain a deeper understanding of the subject and bridges the gap between theory and real world applications. The last part of the workshop covers the basic principles of Interferometric Synthetic Aperture Radar (InSAR). InSAR is an imaging technique for measuring the topography of a surface, its changes over time, and other changes in the detailed characteristics of the surface. By exploiting the phase of the coherent radar signal, interferometry has transformed radar remote sensing from a largely interpretive science to a quantitative tool, with applications in cartography, geodesy, land cover characterization, and natural hazards. This part of the workshop reviews the techniques of interferometry and applications in a rapidly growing area of science and engineering. We will introduce some applications of InSAR in measuring Earth surface deformation due to earthquakes, volcanic unrest and ground water migration.

Road Accident Disaster Management in Nigeria: Experiences and Organisational Issue

Emmanuel Dada

Department of Geography and Planning Sciences, Adekunle Ajasin University, Akungba Akoko, Ondo State, Nigeria. – vissitemma@yahoo.com

KEYWORDS: *road traffic accident, reported cases, fatality*

ABSTRACT:

The great advantage of automobile transportation does not overcome its shortcomings. Foremost among these is the road traffic accident noticed to be among the major causes of death since the history of human existence. This study examined and mapped the rate of reported cases of road accidents across the 36 States and the federal capital of Nigeria between 2013 and 2015. Data acquired from Federal Bureau of Statistics was analysed using descriptive method. Bar charts, graphs, dot map and thematic map were prepared to depict the spatial distribution of the occurrence and fatality classification. Results showed that; highest rate of accidents 36.9% occurred in the year 2013 with 5,539 deaths. Ogun State recorded highest number of accidents with 9.7% in 2013, Lagos State with 15.4% in 2014 and Ogun State with 6.1% in 2015 which can be attributed to the strategic position of these two States as the gate ways to Nigeria economy. The study however concludes that reduced death rate in 2014 and 2015 was as a result of the commencement of electronic drivers' license and improvement in the sensitization of the road users and the general public. It therefore recommends that consistent sensitization and establishment of mobile hospitals should be enhanced and sustained.

Determine the Sustainable change detection at Tamirabarani River, Tirunelveli, Tamilnadu using Cartosat-1 satellite data

S. Karuppasamy[a], S. Kaliappan[b]

[a] Department of civil Engineering, Regional office, Anna University, Tirunelveli- 627007, Tamilnadu, India, karuppasamys@yahoo.com

[b] Former professor of Civil Engineering Anna University Chennai-600025, Tamilnadu,India - drkaliappan@gmail.com

KEYWORDS: *Tamirabarani River, River flow, Cartosat-1, DEM, Encroachment*

ABSTRACT:

Tamirabarani River is one of the main sources of drinking water in Tirunelveli and Tuticorin district, Tamilnadu, India. The width of the river is narrowed down by trees, bushes, buildings and anthropogenic activities. In the present study, encroachment change detection between the year 2006 and 2014 over 35km stretch of the river is measured using the Cartosat-1 generated Digital Elevation Model (DEM) and topographical data. Cartosat-1 DEM is inevitable input for Orthorectification of the study area for further measurement of the encroachment changes between the year 2006 and 2014. Though Cartosat-1 DEM generated Orthophoto is in meter accuracy, it accuracies is better than 30 meter spatial resolution satellite data such as Landsat and IRS P6. The study revealed nearly 74 encroachments area due to the trees, bushes, houses and other manmade structures inside and edge of the river bank, reducing the river flow between the year 2006 and 2014. Out of 74, the number of encroachments with area more than 5000 m2 was 21 in the year 2014 whereas it was 11 in the year 2006. The total encroachment area in the year 2006 was 0.475345 km2, but in the year 2014 it has increased to 0.70964282 km2 (approxim. 33 %increase) Due to the encroachments, original river width reduced to 44 m in Taruvai, 58 m in Sutthamalli region and 164m and 78 in Gopalasamuthram region. It reveals that, the original depth and width of the river in many places has reduced substantially over a period of 8 years. This study is essential for Tirunelveli Corporation as removal of natural and human encroachment inside and at the bank of the river is essential to increase the water flow and to reduce the flood threat during the rainy season.

How to set a small API by using NodeJS, PostgreSQL and LeafletJS mapping library

Rafael Ricardo Bastidas Mendez

International Master Degree Programme Photogrammetry and Geoinformatics at the Hochschule für Technik Stuttgart (alumnus), Colombia

ABSTRACT:

The workshop will introduce PostgreSQL a Relational Database Management System, NodeJS as an application server and Leaflet the JavaScript Mapping library. In the workshop, the postgres database is installed and configured to manage geographic data. Once the database is configured, an API that connects with the database will be developed by using NodeJS and the Express framework. A query will be implemented to retrieve data in a GeoJSON format from the database. Finally, the results of the query will be plotted in a webmap by using Leaflet a JavaScript mapping library. The workshop will be conducted in a Linux Ubuntu environment. The instructor will provide a Virtual Machine configured with the Operating System.

Disappearing large lakes: Current ecological status and impact assessment using remote sensing

Sajid Pareeth

Department of Water science and Engineering, IHE Delft Institute for water education, Westvest 7, 2611 AX Delft (The Netherlands) – s.pareeth@un-ihe.org

KEYWORDS: *Remote sensing, satellite imagery, Lakes, climate change, agriculture*

ABSTRACT:

Lakes are sentinels of climate change [1]. Any change in the spatio-temporal pattern in the physical and biological parameters of lakes can be considered as cue towards changes occuring in the adjoining catchment area due to climate change, human induced pressures etc [2]. Large lakes are often key towards economy of the catchment area, being source to irrigation, fishing, tourism, and other ecosystem services which they provide to the local people [3]. However, recent studies show that lakes globally are undergoing changes in its physical and biological properties, like warming, loss of fish species, introduction of new species of planktons, which also has its effects on water level and quality. Many lakes are experiencing higher level of evaporation due to climate change induced warming thereby reducing the quantity of water available for irrigation [4].

Last two decades witnessed disappearance of multiple large area lakes in different geographical regions of the world. Most recent being disappearance of Lake Poopó in Bolivia with a surface area of around 3000 Sq.Km, the lake completely deserted by the end of year 2015. This study will focus on four such large lakes – Lake Poopó, Aral Sea, Lake Chad and Lake Urmia which are either completely disappeared or undergone massive shrinkage. These lakes played key role in local catchment area being important source of water for irrigation, fishing, tourism etc. In this project using the earth observation data available from multiple satellites, the temporal pattern and the major drivers behind this phenomenon, followed by an impact assessment on bio-physical properties of the catchment area will be studied. With the help of high frequency satellite data, seasonal variation in its pattern of shrinkage over last thirty years will be studied, to better understand the pattern of disappearance [5]. The project will give researchers and policy makers an opportunity to understand the cause and impacts of such phenomenon, listing such vulnerable lakes, and take appropriate steps to alleviate the effects and to avoid such extreme events in future.

Being in the first phase of this project, a current assessment of these lakes using latest multi-spectral data obtained from Landsat 8, Sentinel 2A and Synthetic Aperture Radar (SAR) data obtained from Sentinel 1A satellites will be presented. In this phase, the existing water surface area, and the ecological assessment of the catchment area using vegetation indices will be estimated and compared with those from the existing historical data. This will give us an overall picture on the Lake's current ecological status.

References

[1] Adrian, R., O'Reilly, C.M., Zagarese, H., Baines, S.B., Hessen, D.O., Keller, W., Livingstone, D.M.,

Sommaruga, R., Straile, D., Van Donk, E., Weyhenmeyer, G.A., Winder, M., 2009. Lakes as sentinels of climate change. Limnol Oceanogr 54, 2283–2297.

[2] Williamson, C.E., Saros, J.E., Schindler, D.W., 2009. Sentinels of Change. Science 323, 887–888.

doi:10.1126/science.1169443

[3] UNEP (2008), Vital Water Graphics - An Overview of the State of the World's Fresh and Marine Waters. 2nd Edition. UNEP, Nairobi, Kenya. ISBN: 92-807-2236-0

[4] Pareeth, S., Salmaso, N., Adrian, R., Neteler, M., 2016. Homogenized daily lake surface water temperature data generated from multiple satellite sensors: A long-term case study of a large sub-Alpine lake. Scientific Reports. 6, 31251; doi:10.1038/srep31251

[5] Pareeth, S., Delucchi, L., Metz, M., Rocchini, D., Devasthale, A., Raspaud, M., Adrian, R., Salmaso, N.,

Neteler, M., 2016. New Automated Method to Develop Geometrically Corrected Time Series of Brightness Temperatures from Historical AVHRR LAC Data. Remote Sensing 8, 169. doi:10.3390/rs80301

Low cost UAV-based Remote Sensing for Autonomous Wildlife Monitoring

Milad Mirzaie[a], Hossein Arefi[b*], Fatemeh Alidoost[b]

[a] School of Aerospace Engineering, Faculty of New Sciences and Technologies, University of Tehran, Tehran, Iran - milad.mirzaie@ut.ac.ir

[b] School of Surveying and Geospatial Engineering, College of Engineering, University of Tehran, Tehran, Iran – {hossein.arefi, falidoost@ut.ac.ir}

ABSTRACT:

In recent years, developments in Unmanned Aerial Vehicles (UAVs), light weight on-board computers and low cost thermal imaging sensors offer a new opportunity for wildlife monitoring. In contrast with traditional methods, in order to obtain population and location of endangered species, modern surveying techniques based on UAVs has become more cost-effective and least time-consuming. In this paper, a low-cost UAV-based remote sensing platform is introduced to monitor and track animals using the combination of RGB and thermal sensors. The proposed system is a small, low-cost, flexible remote sensing platform, which it is utilized the object detection and classification algorithms and measure the accurate GPS coordinates of animals in wild or agriculture areas.

The paper describes both hardware and software architectures of a UAV such as the thermal camera, an RGB camera, an on-board computer as well as the object detection and recognition algorithms. As the results, the proposed UAV system proved to be capable for detection of animals in vast areas, providing wildlife rehabilitators and rangers with a cost-effective and time-saving resource.

Investigating toxic element contents of soils in mining areas by means of proximal spectroscopy

Vahid Khosravi[a,*], Faramarz Doulati Ardejani[b], Saeed Yousefi[c]

[a*] Faculty of Mining, Petroleum and Geophysics, Shahrood University of Technology, Shahrood, Iran, v.khosravi@shahroodut.ac.ir

[b] School of Mining, College of Engineering, University of Tehran, Tehran, Iran

[c] Nehbandan mining college, University of Birjand, Nehbandan, Iran

KEYWORDS: *Spectroscopy; Arsenic; Mine waste dump; Regression; prediction*

ABSTRACT:

Soil toxic element pollution due to mining activities is a serious environmental problem in many mining areas. Quick identification of the amount and extent of that pollution is an important basis for remediation plans. Visible to shortwave infrared spectroscopy was used in this study to predict the arsenic concentration in 55 soil samples gathered from one of the Sarcheshmeh porphyry copper mine waste dumps. The dry samples were scanned using an ASD FieldSpec3 Spectroradiometer under laboratory condition with a measurement range of 350–2500 nm. Reflectance spectra was transformed to absorbance and then subjected to First Derivative (FD), Second Derivative (SD), Standard Normal Variate (SNV), Multiplicative Scatter Correction (MSC) and Continuum Removal (CR) pre-processesing scenarios. The performance of three regression techniques, namely, Partial Least Squares Regression (PLSR), Random Forest (RF) and Multivariate Adaptive Regression Splines (MARS) were then compared to identify the best method to assess soil arsenic concentration using spectral data. Main mechanism allowing the prediction of arsenic by spectroscopy was also investigated. Key wavebands for predicting arsenic concentration were found to be at spectral features of both Fe and clay minerals, though, regression coefficients of the PLSR model between arsenic and the spectral features of Fe were higher than those of clay minerals. Hence, element-sorption by spectrally active Fe-oxides was the major mechanism by which to predict spectrally featureless arsenic. FD-MARS and FD-RF methods yielded the best prediction accuracies with R2 values of 0.83 and 0.71 respectively. Finally, concentrations of heavy metals in contaminated dumpsite soils could be indirectly assessed by visible to shortwave infrared spectroscopy.

AGSE Publishing
ISBN 978-3-943321-15-9